

Volcanic Ash and Aviation Safety: Proceedings of the First International Symposium on Volcanic Ash and Aviation Safety

Edited by Thomas J. Casadevall

**Property of
DGGG LIBRARY**

U.S. GEOLOGICAL SURVEY BULLETIN 2047

*Proceedings of the First International Symposium on Volcanic Ash
and Aviation Safety held in Seattle, Washington, in July 1991*



Symposium sponsored by
Air Line Pilots Association
Air Transport Association of America
Federal Aviation Administration
National Oceanic and Atmospheric Administration
U.S. Geological Survey

Symposium co-sponsored by
Aerospace Industries Association of America
American Institute of Aeronautics and Astronautics
Flight Safety Foundation
International Association of Volcanology and Chemistry of the Earth's Interior
National Transportation Safety Board

UNITED STATES GOVERNMENT PRINTING OFFICE, WASHINGTON: 1994

U.S. DEPARTMENT OF THE INTERIOR

BRUCE BABBITT, Secretary

U.S. GEOLOGICAL SURVEY

Gordon P. Eaton, Director

For sale by U.S. Geological Survey, Map Distribution
Box 25286, MS 306, Federal Center
Denver, CO 80225

Any use of trade, product, or firm names in this publication is for descriptive purposes only and
does not imply endorsement by the U.S. Government

Library of Congress Cataloging-in-Publication Data

International Symposium on Volcanic Ash and Aviation Safety (1st : 1991 Seattle, Wash.)

Volcanic ash and aviation safety : proceedings of the First International Symposium on Volcanic Ash and Aviation Safety / edited by Thomas J. Casadevall ; symposium sponsored by Air Line Pilots Association ... [et al.], co-sponsored by Aerospace Industries Association of America ... [et al.].

p. cm.—(U.S. Geological Survey bulletin ; 2047)

"Proceedings of the First International Symposium on Volcanic Ash and Aviation Safety held in Seattle, Washington, in July 1991."

Includes bibliographical references.

Supt. of Docs. no.: I 19.3:2047

I. Volcanic ash, tuff, etc.—Congresses. 2. Aeronautics—Safety measures—Congresses. I. Casadevall, Thomas J. II. Air Line Pilots Association. III. Title. IV. Series.

QE75.B9 no. 2047

[QE461]

557.3 s—dc20

[629.13'0289]

94-17789

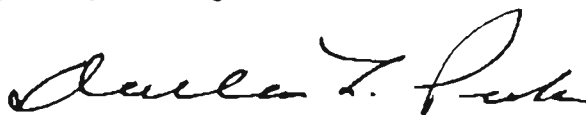
FOREWORD

A Boeing 747 jumbo jet approaching the Anchorage International Airport, Alaska, on December 15, 1989, lost power to all four engines and nearly crashed as a result of flying through volcanic ash erupted from Redoubt Volcano. In separate incidents in 1982, two commercial jumbo jets en route to Australia across Indonesia suffered loss of engine thrust from ingesting volcanic ash from the erupting Galunggung Volcano, Java, and descended more than 20,000 ft before the engines could be restarted. These are not the only incidents of this kind. During the past 15 years, about 80 commercial jet aircraft have suffered damage from inadvertently flying into ash clouds that had drifted tens to hundreds of miles from erupting volcanoes.

The U.S. Geological Survey (USGS) has been involved in research on geologic hazards, such as volcanic eruptions and earthquakes, since its earliest days. With the Disaster Relief Act of 1974, the USGS was given formal responsibility "to provide technical assistance to State and local governments to ensure that timely and effective disaster warning is provided" for all geologic hazards. Addressing the threat of volcanic ash to aircraft safety, however, requires far more than the monitoring of volcanoes and warning of erupting ash clouds by the Survey. The ash must be traced and its likely trajectory must be forecast; aircraft must be alerted, and proper evasive actions must be taken by pilots. Agencies such as the National Weather Service and National Environmental Satellite Data and Information Service (both part of the National Oceanic and Atmospheric Administration), the National Aeronautics and Space Administration, and the Federal Aviation Administration are partners critical to the success of this mission. The International Civil Aviation Organization, various pilots' associations, air carriers, aircraft manufacturers, and many others are important as well.

The Redoubt encounter spurred government and university scientists, pilots, and representatives of the aviation industry to work together to reduce the hazards caused internationally by volcanic ash. As a result of the concern generated by the Redoubt eruptions and associated aircraft encounters, the First International Symposium on Volcanic Ash and Aviation Safety was held in Seattle, Washington, July 8–12, 1991. This volume contains the proceedings from that meeting.

Volcanologists and the subject of volcanic ash clouds are relatively new to discussions of aviation hazards. As a result, the various parties concerned with the hazard have had to set up new communication channels and to bridge substantial differences in organizational culture and professional language. The Seattle symposium in 1991 alerted and educated many about ash hazards to aviation. More importantly, it started a serious dialogue that resulted in a series of follow-up workshops, improvements in the detection and tracking of ash clouds, and revised warning and response procedures. These are the actions that will be needed if the hazard of ash in airways is truly to be mitigated.



Dallas L. Peck
U.S. Geological Survey
Director, 1981–1993

CONTENTS

Foreword	
<i>By Dallas L. Peck</i>	III
Introduction	
<i>By Thomas J. Casadevall</i>	1
Issues and Needs	
Developments Since the Symposium	
International Efforts	
Efforts in the United States	
Future Directions	
Acknowledgments	
References Cited	
Introductory Remarks for the First International Symposium on Volcanic Ash and Aviation Safety, Seattle, Washington, July 1991	
<i>By Donald D. Engen</i>	7
Technical Reports	
Volcanoes and Ash Clouds	
Volcanoes and Aviation Safety in Costa Rica	
<i>By Jorge Barquero</i>	9
A Method for Characterizing Volcanic Ash from the December 15, 1989, Eruption of Redoubt Volcano, Alaska	
<i>By Gregory K. Bayhurst, Kenneth H. Wohletz, and Allen S. Mason</i>	13
The Concentration of Ash in Volcanic Plumes, Inferred from Dispersal Data	
<i>By Marcus I. Bursik, R.S.J. Sparks, Steven N. Carey, and Jennie S. Gilbert</i>	19
Electrical Phenomena in Volcanic Plumes	
<i>By Jennie S. Gilbert and Stephen J. Lane</i>	31
Volcanic Ash: What It Is and How It Forms	
<i>By Grant Heiken</i>	39
Volcanism in the Canadian Cordillera: Canada's Hazard Response Preparedness	
<i>By Catherine J. Hickson</i>	47
Volcanic Ash in Kamchatka as a Source of Potential Hazard to Air Traffic	
<i>By Vladimir Yu. Kirianov</i>	57
Ash Clouds: Characteristics of Eruption Columns	
<i>By Stephen Self and George P.L. Walker</i>	65
Volcanoes: Their Occurrence and Geography	
<i>By Tom Simkin</i>	75

Technical Reports—Continued

Volcanoes and Ash Clouds—Continued

The Controls of Eruption-Column Dynamics on the Injection and Mass Loading of Ash into the Atmosphere <i>By R.S.J. Sparks, Marcus I. Bursik, Steven N. Carey, Andrew W. Woods, and Jennie S. Gilbert</i>	81
Melting Properties of Volcanic Ash <i>By Samuel E. Swanson and James E. Beget</i>	87
Ash-Fall Deposits from Large-Scale Phreatomagmatic Volcanism: Limitations of Available Eruption-Column Models <i>By Colin J.N. Wilson</i>	93
The Injection of Volcanic Ash into the Atmosphere <i>By Andrew W. Woods and Juergen Kienle</i>	101

Damage and Impacts

Influence of Volcanic Ash Clouds on Gas Turbine Engines <i>By Michael G. Dunn and Douglas P. Wade</i>	107
Volcanic Ash—Aircraft Incidents in Alaska Prior to the Redoubt Eruption on 15 December 1989 <i>By Juergen Kienle</i>	119
Mitigation of Volcanic Ash Effects on Aircraft Operating and Support Systems <i>By J.R. Labadie</i>	125
Impact of Volcanic Ash from 15 December 1989 Redoubt Volcano Eruption on GE CF6-80C2 Turbofan Engines <i>By Zygmunt J. Przedpelski and Thomas J. Casadevall</i>	129
Economic Disruptions by Redoubt Volcano: Assessment Methodology and Anecdotal Empirical Evidence <i>By Bradford H. Tuck and Lee Huskey</i>	137
Effects of Volcanic Ash on Aircraft Powerplants and Airframes <i>By Lester M. Zinser</i>	141

Communications and Procedures

AIA Recommendations Aimed at Increased Safety and Reduced Disruption of Aircraft Operations in Regions with Volcanic Activity <i>By AIA Propulsion Committee 334-1, Zygmunt J. Przedpelski, Chairman</i>	147
Recommended Flight-Crew Procedures if Volcanic Ash is Encountered <i>By Ernest E. Campbell</i>	151
Development of a Real-Time ATC Volcanic Ash Advisory System Based on the Future Aviation Weather System <i>By James E. Evans</i>	157
Warning Systems and Pilot Actions <i>By Peter M. Foreman</i>	163

Technical Reports—Continued**Communications and Procedures—Continued**

Volcanic Ash—The International Regulatory Aspects <i>By Tom Fox</i>	169
Seattle Air Route Traffic Control Center Response to Eruptions of Mount St. Helens <i>By Robert F. Hamley and Donald H. Parkinson</i>	175
An Automated Volcanic Ash Warning System <i>By David M. Harris</i>	183
Aviation Safety and Volcanic Ash Clouds in the Indonesia-Australia Region <i>By R. Wally Johnson and Thomas J. Casadevall</i>	191
The Smithsonian's Global Volcanism Network: Facilitating Communication of Volcanic-Eruption Information <i>By Lindsay McClelland</i>	199
Volcanic Ash and Aircraft Operations <i>By Edward Miller</i>	203
Volcanic Event Notification at Mount St. Helens <i>By Bobbie Myers and George J. Theisen</i>	207
Aviation Safety Measures for Ash Clouds in Japan and the System of Japan Air Lines for Monitoring Eruptions at Sakurajima Volcano <i>By Saburo Onodera and Kosuke Kamo</i>	213
Volcanic Ash Warnings in the Australian Region <i>By Rodney J. Potts and Frank Whitby</i>	221
Ash Cloud Aviation Advisories <i>By Thomas J. Sullivan and James S. Ellis</i>	229

Meteorology and Ash-Cloud Monitoring

Alaska Volcano-Debris-Monitoring System: New Technologies to Support Forecasting Volcanic-Plume Movement <i>By Gary L. Hufford</i>	239
A Statistical Approach to the Assessment of Volcanic Hazard for Air Traffic: Application to Vesuvius, Italy <i>By Giovanni Macedonio, P. Papale, M. Teresa Pareschi, Mauro Rosi, and Roberto Santacroce</i>	245
Using a Personal Computer to Obtain Predicted Plume Trajectories During the 1989–90 Eruption of Redoubt Volcano, Alaska <i>By Thomas L. Murray, Craig I. Bauer, and John F. Paskievitch</i>	253
Volcanic Eruptions and Atmospheric Temperature <i>By Reginald E. Newell and Zhong Xiang Wu</i>	257
A Mesoscale Data Assimilation System Adapted for Trajectory Calculations Over Alaska <i>By Thomas W. Schlatter and Stanley G. Benjamin</i>	269

Technical Reports—Continued**Meteorology and Ash-Cloud Monitoring—Continued**

Modeling Volcanic Ash Transport and Dispersion By Barbara J.B. Stunder and Jerome L. Heffter	277
Development of a Prediction Scheme for Volcanic Ash Fall from Redoubt Volcano, Alaska By Hiroshi L. Tanaka	283
The Aeronautical Volcanic Ash Problem By Jerald Uecker	293
Defining a Keep-Out Region for Aircraft After a Volcanic Eruption By Peter L. Versteegen, Douglas D. D'Autrechy, Michael C. Monteith, and Charles R. Gallaway	297

Detection and Tracking

Detection and Discrimination of Volcanic Ash Clouds by Infrared Radiometry—I: Theory By Alfred J. Prata and Ian J. Barton	305
Detection and Discrimination of Volcanic Ash Clouds by Infrared Radiometry—II: Experimental By Ian J. Barton and Alfred J. Prata	313
Satellite Monitoring of Volcanoes Using Argos By J.P. Cauzac, Christian Ortega, and Laurel Muehlhausen	319
Current and Future Capabilities in Forecasting the Trajectories, Transport, and Dispersion of Volcanic Ash Clouds at the Canadian Meteorological Centre By Real D'Amours	325
An Aircraft Encounter with a Redoubt Ash Cloud (A Satellite View) By Kenneson G. Dean, Lawrence Whiting, and Haitao Jiao	333
GEO-TOMS: Total-Ozone Mapping Spectrometer for Ozone and Sulfur-Dioxide Monitoring from a Geostationary Satellite By Ulli G. Hartmann, Robert H. Hertel, Herbert A. Roeder, and J. Owen Maloy	341
Passive, Two-Channel, Thermal-Infrared Imaging Systems for Discrimination of Volcanic Ash Clouds By Frank R. Honey	347
Seismic Identification of Gas-and-Ash Explosions at Mount St. Helens— Capabilities, Limitations, and Regional Application By Chris Jonientz-Trisler, Bobbie Myers, and John A. Power	351
Infrasonic and Seismic Detection of Explosive Eruptions at Sakurajima Volcano, Japan, and the PEGASAS-VE Early-Warning System By Kosuke Kamo, Kazuhiro Ishihara, and Makoto Tahira	357
Volcanic Hazard Detection with the Total Ozone Mapping Spectrometer (TOMS) By Arlin J. Krueger, Scott R. Doiron, Gregg S.J. Bluth, Louis S. Walter, and Charles C. Schnetzler	367

Technical Reports—Continued**Detection and Tracking—Continued**

Monitoring Volcanic Eruptions Using NOAA Satellites By Michael Matson, James S. Lynch, and George Stephens	373
Volcanic Tremor Amplitude Correlated with Eruption Explosivity and its Potential Use in Determining Ash Hazards to Aviation By Steven R. McNutt.....	377
Airborne Radar Detection of Volcanic Ash By Mark E. Musolf.....	387
Radar Remote Sensing of Volcanic Clouds By William I. Rose and Alexander B. Kostinski.....	391
Tracking of Regional Volcanic Ash Clouds by Geostationary Meteorological Satellite (GMS) By Yoshihiro Sawada	397
Observations of the 1989–90 Redoubt Volcano Eruption Clouds Using AVHRR Satellite Imagery By David J. Schneider and William I. Rose.....	405
Application of Contemporary Ground-Based and Airborne Radar for the Observation of Volcanic Ash By Melvin L. Stone	419
The Potential for Using GPS for Volcano Monitoring By Frank H. Webb and Marcus I. Bursik	429
Selected Glossary of Volcanology and Meteorology	437
List of Selected Acronyms	439
Authors' Address List	443

INTRODUCTION

By Thomas J. Casadevall

Volcanic ash from the 1989-90 eruptions of Redoubt Volcano disrupted aviation operations in south-central Alaska and damaged five jet passenger aircraft, including a new Boeing 747-400, which cost in excess of \$80 million to repair (Steenblik, 1990). The Redoubt eruptions served to increase interest by the aviation community in volcanic hazards and made it clear that mitigating the hazards of volcanic ash to aviation safety would require the cooperation and efforts of volcanologists, meteorologists, air traffic managers, engine and airframe manufacturers, and pilots.

Soon after the December 1989 eruptions of Redoubt, Senator Ted Stevens of Alaska requested that Federal agencies form an interdepartmental task force to develop and coordinate both an immediate and a long-term response to the Redoubt eruptions. In March 1990, in response to this request, the U.S. Geological Survey, the Federal Aviation Administration (FAA), and the National Oceanic and Atmospheric Administration (NOAA) formed an interagency task group and began planning for an international technical symposium to review the available information about volcanic ash clouds and to assess what was being done to address the ash hazard, both domestically and internationally. This interagency group received strong support from the aviation community, and the Federal agencies were soon joined by the Air Line Pilots Association (ALPA), the Aerospace Industries Association (AIA), the Air Transport Association (ATA), the Flight Safety Foundation (FSF), and the American Institute of Aeronautics and Astronautics (AIAA). An important early result from this cooperation was the "First International Symposium on Volcanic Ash and Aviation Safety," to address the effects of volcanic activity on aviation safety in a multidisciplinary way and at a global scale. The aims of the symposium were: to bring together individuals who were interested in the volcanic ash problem but who may have been unaware of other scientists, engineers, pilots, and aviation authorities with similar interests; to encourage and define needed improvements in the detection, tracking, and warning of volcanic ash hazard so that aircraft may avoid ash clouds; and to review the effects of volcanic ash on aircraft so that pilots who encounter ash can respond appropriately. The symposium was held in Seattle, Wash., from July 8-12, 1991.

The symposium was attended by more than 200 participants from 28 countries, representing the major air carriers, airplane and engine manufacturers, pilots and aviation safety organizations, air traffic managers, meteorologists, and volcanologists. More than 100 technical presentations were made during the symposium, including a special session on the effects on aviation operations of the June 15, 1991, eruption of Mt. Pinatubo in the Philippines (Casadevall, 1991). Field trips to the Federal Aviation Administration air traffic control facility in Auburn, Wash., to the Boeing 737 assembly plant in Renton, Wash., and to the Mount St. Helens National Volcanic Monument gave participants the opportunity to view the volcanic hazard-aviation problem from several perspectives. Such broad participation demonstrated a clear need and wide support for a meeting of this type.

In the past 15 years, more than 80 jet airplanes have been damaged owing to unplanned encounters with drifting clouds of volcanic ash in air routes and at airports. Seven of these encounters caused in-flight loss of jet engine power, which nearly resulted in the crash of the airplane. The repair and replacement costs associated with airplane-ash cloud encounters are high and, to date (May 1994), have exceeded \$200 million. In addition to the high economic costs of these encounters, more than 1,500 passengers aboard the seven airliners that temporarily lost engine power were put at severe risk.

The hazard is compounded by the fact that volcanic ash clouds are not detectable by the present generation of radar instrumentation carried aboard aircraft and are not likely to be detectable in the foreseeable future. Complete avoidance of volcanic ash clouds is the only procedure that guarantees flight safety, and this avoidance requires communication between the pilot and observers outside the aircraft.

Since the Seattle meeting, eruptions at Pinatubo, Sakurajima Volcano (Japan), Pacaya Volcano (Guatemala), Galeras Volcano (Colombia), Hudson and Lascar Volcanoes (Chile), Mt. Spurr (Alaska), Nyamuragira Volcano (Zaire), Sheveluch Volcano (Russia), and Manam Volcano (Papua New Guinea) have further disrupted air traffic, damaged aircraft in flight, and delayed flights and curtailed operations at a number of airports. The issue of volcanic hazards and aviation safety continues to be timely and in need of more effort

if we are to improve the margin of flight safety in the presence of volcanic ash.

ISSUES AND NEEDS

During the symposium, discussions focused on the following technical areas: the 1989–90 Redoubt eruptions and their impacts on aviation operations, the nature of volcanoes and their ash clouds, the effects of volcanic ash on aircraft, methods and procedures of communicating the ash-cloud hazard to pilots, the role of meteorology and the use of atmospheric models to forecast cloud movement, and detection and tracking of ash clouds. This volume contains reports for 60 of the 108 technical presentations made during the symposium. The papers presented about the Redoubt eruptions have been published elsewhere (Miller and Chouet, 1994).

In addition to the technical presentations, symposium discussions identified a number of key issues and needs that participants felt must be addressed in order to mitigate the volcanic threat to aviation safety. These included:

1. Improved communications among volcano observers, meteorologists, air traffic controllers, flight dispatchers, and pilots about drifting ash clouds, including immediate notification of volcanic eruptions to pilots.
2. Improved education of pilots, flight managers, and manufacturers about the ash-cloud hazard, including specific recommendations for avoiding ash clouds.
3. Improved detection and tracking of ash-cloud movement using remote-sensing techniques and atmospheric-transport models.
4. Improved monitoring of the Earth's active volcanoes, especially in the remote Aleutian-Kamchatka-Kurile volcanic region.
5. New methods for eruption identification and ash-cloud detection.
6. Development of instruments that will enable pilots to detect ash clouds while in flight, especially useful when flying over remote, unmonitored regions of the Earth.
7. Development of better methods to remove and clean ash from airplanes and airports.
8. Determination of minimum levels of ash concentration that are capable of damaging aircraft and engines.
9. Development of a worldwide notification system and clearinghouse for information about active volcanoes, including planning charts to show the location of volcanoes relative to air routes.

DEVELOPMENTS SINCE THE SYMPOSIUM

A number of ad hoc working groups were formed following the symposium to examine these topics and have produced significant progress on many of these technical issues. Accomplishments include:

1. A training video for pilots entitled "Volcanic Ash Avoidance," produced by the Boeing Company in cooperation with the Air Line Pilots Association and the U.S. Geological Survey (Boeing Company, 1992).
2. An international workshop on communications among volcanologists, meteorologists, air traffic managers, and pilots was held in Washington, D.C., in September 1992.
3. An FAA review on aviation safety as affected by volcanic ash (FAA, 1993a).
4. A workshop on the dynamics and characteristics of the ash clouds from the 1992 eruptions of Mt. Spurr was held in Washington, D.C., in April 1993 (FAA, 1993b).
5. An international workshop on volcanic ash and airports was held in Seattle, Wash. (Casadevall, 1993).
6. New communications links with Russians for warnings and information about Kamchatkan volcanoes, which underlie the increasingly busy air routes of the north Pacific region, were established in 1993 (Miller and Kirianov, 1993).
7. An interagency plan for volcanic ash episodes in Alaska was put into effect by the FAA, NWS, USGS, Department of Defense, and the State of Alaska in 1993 (Alaska Interagency Operating Plan, 1993).
8. A global planning chart showing the position of active volcanoes relative to air routes and air navigation aids was published (Casadevall and Thompson, 1994).

INTERNATIONAL EFFORTS

Since 1982, the International Civil Aviation Organization (ICAO) has worked to address the volcanic threat to aviation safety worldwide (Fox, 1988, this volume). This threat came to wide public attention in 1982 when two 747 passenger jets encountered ash at night from separate eruptions of Galunggung Volcano in Indonesia. In these incidents, volcanic ash extensively damaged exterior surfaces, instruments, and engines, resulting in the loss of thrust and powerless descents of nearly 25,000 feet before the pilots of both aircraft restarted their engines and landed safely at Jakarta (Smith, 1983). The Galunggung encounters occurred for two main reasons. First, the pilots were unable to see the ash or to otherwise detect it using on-board instruments, and sec-

ond, no warnings about the activity of the volcano were contained in the aeronautical information generally available to pilots, such as notices of significant meteorological events—SIGMET's—or in notices to airmen—NOTAM's. These incidents led in 1982 to the formation of a volcanic ash warning group under leadership of the ICAO.

Eruptions and aircraft encounters with ash clouds during the past 15 years have prompted several other important international efforts to mitigate the volcanic hazard to aviation safety. Because volcanic ash clouds are carried by upper-level winds and often cross national boundaries as well as boundaries separating flight-information regions, efficient and prompt communications between regions are essential to avoiding encounters. The May 1985 encounter between a jumbo jet and an ash cloud from an eruption of Soputan Volcano in Indonesia prompted the Indonesian and Australian governments to form a bilateral volcanological/airspace liaison committee to improve communications about volcanic eruptions in the Indonesian region (Johnson and Casadevall, this volume). In North America, drifting ash clouds from the 1989–90 eruptions of Redoubt Volcano, and the 1992 eruptions of Mt. Spurr, sent ash clouds over Canada and disrupted operations in Canadian airspace. These incidents prompted establishment of closer bilateral communications between Canadian and U.S. agencies including volcanologists, meteorologists, and air traffic controllers (Hickson, this volume).

In 1988, ICAO member states adopted regulations to provide alerts to pilots about eruptive activity worldwide. These efforts included a special volcanic activity report form (VAR), which requires that pilots make a number of critical observations about the location, timing, and nature of an ash cloud. This information is communicated directly to the nearest area control center and is introduced into the communication network so that other aircraft may avoid airspace contaminated by volcanic ash (Fox, 1988, this volume).

Also in 1988, the World Organization of Volcano Observatories (WOVO), in cooperation with ICAO and with the International Association of Volcanology and Chemistry of the Earth's Interior (IAVCEI), requested WOVO member institutions to establish contacts with civil aviation authorities to improve communications between ground-based observatories and air traffic in order to minimize the volcanic hazards to aircraft. Currently, WOVO is examining ways to improve the exchange of information between observatories and agencies concerned with aviation operations, including the use of electronic mail (Riehle and Fink, 1993).

Following the 1991 Seattle symposium, ICAO addressed the volcanic threat to aviation safety at regional meetings in Bangkok (September 1992) and Mexico City (October 1992). In November 1992, changes to the international standards and recommended practices for meteorological services (ICAO, 1992) went into effect. The changes

relate to the types of information about volcanic clouds that are entered into aeronautical communications networks using the SIGMET mechanism. The new regulations require that a volcanic advisory forecast be issued every 4 hours regarding the status of a volcanic cloud, with a 12-hour forecast of ash-cloud behavior.

Information for these advisories could come from many sources, but would most likely come from analysis of satellite images and from analysis of ash-cloud movement using atmospheric-transport models (Stunder and Heffter, this volume; Tanaka, this volume). For example, an important source of information for these volcanic advisories for the Southwest Asia region is the Darwin Regional/Specialized Meteorological Centre, established in 1993 by the Australian Bureau of Meteorology. The Darwin center utilizes satellite imagery to provide outlook advisory information about the occurrence and movement of ash clouds from eruptions in the Indonesian region. The center also serves as a venue for training meteorologists from the Asian region about detection and tracking of volcanic ash clouds so other countries in the region might carry out similar analysis at the local level.

To further assist ICAO member states in meeting the requirements for more detailed advisories, ICAO established a special implementation project to member states with active volcanoes as well as to those states responsible for flight information in regions adjacent to areas with active volcanoes. Through this project, an ICAO team consisting of a volcanologist and an aeronautical meteorologist visited countries in the Asia-Pacific region in 1992–93 (Casadevall and Oliveira, 1993) and the South American region in 1993–94 to advise on methods for meeting the new ICAO regulations. The new regulations should result in more rapid and clearer communications about volcanic ash clouds to the aviation community.

In addition to these bilateral efforts to improve the speed and quality of information, several countries have addressed specific volcanic threats to aviation operations by applying existing technology and by seeking to develop new methods and equipment for ash detection. For example, in 1991, scientists and aviation authorities in Japan installed specialized seismic and infrasonic detectors at Sakurajima Volcano to detect ash-producing eruptions. Results from these sensors are continuously transmitted to nearby Kagoshima Airport to provide real-time notification of explosive eruptions that threaten airport operations (Kamo and others, this volume; Onodera and Kamo, this volume). In another example, scientists in Australia are seeking ways to supplement information that is available to the pilot by developing an ash-detection sensor that can be carried onboard the aircraft to detect the presence of ash in the flight path (Barton and Prata, this volume; Prata and Barton, this volume). Such a sensor would be especially valuable for international flights over regions where volcanoes are poorly

monitored and where ground-based communications are poorly established.

EFFORTS IN THE UNITED STATES

The United States has approximately 56 volcanoes with historical eruptive activity; 44 are located in Alaska. The U.S. Geological Survey (USGS) is the principal Federal agency with responsibility for assessing volcanic hazards and monitoring active volcanoes in the United States (Wright and Pierson, 1992). This work is carried out primarily from volcano observatories in Hawaii, Alaska, California, and Washington. For example, the Alaska Volcano Observatory monitors the activity of volcanoes in the Cook Inlet area, including Redoubt and Spurr. Continuous seismic and other monitoring of these volcanoes, day and night, in all seasons and weather conditions, enables volcanologists to detect eruption precursors as well as eruptions themselves. Early detection of eruptions and prompt communication of this information to the FAA and to the National Weather Service offices in Anchorage are an essential part of the role played by USGS scientists in mitigating the ash hazard to aircraft.

The National Oceanic and Atmospheric Administration (NOAA) and the Federal Aviation Administration (FAA) also have responsibilities for dealing with the hazard of volcanic ash clouds that affect aviation operations in the United States. Cooperation between these two agencies was formalized shortly before the December 1989 eruption of Redoubt, when a memorandum of understanding between the agencies created a volcanic hazard alert team and established procedures to respond to volcanic eruptions affecting air operations in the United States. Since 1989, these procedures have been activated for eight volcanoes in the United States (J. Lynch, NOAA-SAB, written commun., March 1993). In 1993, a letter of agreement between the USGS and NOAA attempted to speed the exchange of information that notifies the aviation community of ash-cloud hazards and formalized the de facto collaboration between these agencies that has existed since the Redoubt eruptions.

The principal tools used by NOAA for assessing volcanic activity are analysis of data from satellites (Krueger and others, this volume; Matson and others, this volume) and wind-field data, which enables the forecast of drifting ash clouds (Murray and others, this volume; Stunder and Heffter, this volume). Since 1990, the National Weather Service office in Anchorage has implemented several new techniques for detecting and tracking volcanic ash clouds from volcanoes in the Cook Inlet and Aleutian regions (Hufford, this volume). These efforts are integrated with the monitoring efforts of the Alaska Volcano Observatory and with the air-traffic-control efforts of the FAA. The FAA, through its

area control centers, has the primary responsibility for communicating with pilots and for providing NOTAM's.

Following the 1989–90 eruptions of Redoubt, the 1992 eruptions of Mt. Spurr also had an important impact on aviation, affecting operations in Alaska, Canada, and the conterminous United States (Alaska Volcano Observatory, 1993). Ashfall from the August 18, 1992, eruption of Mt. Spurr deposited from 1 to 3 mm of ash in Anchorage and caused Anchorage airports to curtail operations for several days (Casadevall, 1993). The cost of airport cleanup alone in Anchorage from the August 18 ashfall was more than \$650,000. The ash cloud from the September 17 eruption disrupted air traffic routing around the volcano—2 days later it disrupted air routes over western Canada and in the congested air corridors of the northeastern United States. Fortunately, there were no encounters between aircraft and the drifting Spurr ash clouds. The lack of damaging encounters following the Spurr eruptions reflects increased awareness about the hazards of ash clouds and improvements made since 1990 in the warning, detection, and tracking of volcanic clouds. These improvements are largely a direct result of the previously mentioned initiatives by Federal and international agencies to reduce the hazards from volcanic ash.

From an operational perspective, experience in the Australia-Indonesia region and in Alaska has indicated that the threat of volcanic ash can be effectively addressed at the regional or local level. For example, the 1989–90 Redoubt eruptions and the 1992 Spurr eruptions prompted Federal and State agencies in Alaska to establish a regional plan for aviation-related volcanic hazards (Alaska Interagency Operating Plan, 1993). The plan outlines the responsibilities of the agencies involved in eruption responses to meet the public's need for information to protect against volcanic ash hazards. The Redoubt and Spurr eruptions also prompted U.S. and Canadian agencies to refine bilateral operational plans for communicating about volcanic hazards (Hickson, this volume).

In addition to the efforts by international and Federal agencies, the major airplane and jet engine manufacturers have also studied the damage to aircraft from ash encounters in efforts to develop mitigation strategies, including practical steps for pilots to minimize damage should an ash cloud be entered accidentally. The manufacturer's principal trade association, the Aerospace Industries Association (AIA), formed a volcanic ash study committee in 1991 to evaluate the volcanic threat to aviation safety (AIA Propulsion Committee, this volume). The findings of this committee are reflected in a number of the reports presented in Seattle (Campbell, this volume; Dunn and Wade, this volume; Przedpelski and Casadevall, this volume).

The Air Line Pilots Association (ALPA), the Air Transport Association (ATA), and the Flight Safety Foundation (FSF), as well as the American Institute of Aeronautics and

Astronautics (AIAA) and the Aerospace Industries Association (AIA) have all taken active roles to communicate about the ash problem with their members and constituents, both nationally and internationally. ALPA and ATA were sponsors of the Seattle Symposium, along with the FAA, NOAA, and the USGS. AIA, AIAA, FSF, LAVCEI, and the National Transportation Safety Board were co-sponsors of the symposium.

FUTURE DIRECTIONS

As we gain understanding about the nature of ash clouds and the hazard of volcanic ash to aviation operations, we constantly improve our abilities to deal with the threat (Casadevall, 1992). Multidisciplinary cooperation and communications were major factors in the success of the Seattle meeting. This cooperation created an excitement among the participants that has been kept alive at later workshops and in cooperative efforts such as the production of the Boeing training video (Boeing Company, 1992). Even though the ash-aviation safety problem is global in scope, the solutions that have worked best have often been on a local or regional scale. The optimal solutions require understanding the location and character of the nearby active volcanoes, the structure of the air routes that cross or pass by these volcanoes, and an understanding and use of all available resources to detect, track, and forecast the movement of ash clouds. At the same time, as new pilots are introduced to new routes, efforts to educate pilots must continue.

The Seattle symposium and the efforts following the symposium indicate that we have much to do to satisfactorily address concerns about the threat of volcanic ash to aviation safety. This requires application of existing technologies, such as methods that enable scientists to detect eruptions from remote, unmonitored volcanoes; early detection of ash clouds; tracking of ash clouds in real time; and development of better and faster ways to get information into the cockpit. Also, despite the recent advances in testing jet engines for their tolerances to volcanic ash (Dunn and Wade, this volume) and advances in using remote-sensing technologies to detect and track ash clouds (Schneider and Rose, this volume; Wen and Rose, 1994), it is essential that ash clouds be sampled directly as they drift from their source volcanoes (Riehle and others, 1994). Only direct sampling will allow us to obtain information with which to corroborate and validate laboratory tests and computational models. The results of the Seattle symposium should be viewed as a start of efforts to address the threat that ash clouds present to aviation safety. Volcanoes will certainly continue to erupt, and air traffic and aircraft sophistication will continue to grow. To successfully coexist with the threat of volcanic ash, we must continue to address the volcanic hazard in a responsible fashion. Open

communications about these efforts are essential to successfully dealing with the volcanic hazard to aviation safety.

ACKNOWLEDGMENTS

The success of the Seattle symposium required the energy and efforts of a large number of colleagues. The symposium was organized under the leadership of Chris Newhall of the USGS and came about through the efforts of an inter-agency task group that was first suggested by Senator Ted Stevens of Alaska. Principal representatives on this task group included Robert Machol of the FAA, Mike Matson of NOAA, Doug Wade of the Department of Defense, Ed Miller of the Air Line Pilots Association, and Don Trombley of the Air Transport Association. Their assistance and support in the production of this report is gratefully acknowledged. The editor of this report served on this task group as program coordinator for the symposium.

Several colleagues provided long-term encouragement for this project, including Grant Heiken (Los Alamos National Laboratory), Tom Fox (ICAO), Mike Dunn (CALSPAN), Tom Simkin (Smithsonian Institution), and Bill Rose (Michigan Technological University). A special thanks goes to Robert Wesson of the USGS, who had the earliest and clearest vision of what the Seattle symposium should be.

The cooperation of those who acted as reviewers is especially appreciated. They include: Robert Anders, Steve Brantley, Marcus Bursik, Dan Dzurisin, David Harris, Grant Heiken, Wally Johnson, Steve Lane, Steve McNutt, C. Dan Miller, Tom Murray, Tina Neal, Chris Newhall, John Power, Jim Riehle, Bill Rose, Dave Schneider, Steve Self, George Stephens, Barbara Stunder, and Bob Tilling.

Deloris Klausner of the Branch of Volcanic and Geothermal Processes (USGS, Denver) was responsible for collating all the manuscripts. Rick Scott, geologist and technical publications editor (USGS, Denver), provided editorial guidance and supervised preparation of illustrations and the final layout of the volume.

REFERENCES CITED

- Alaska Interagency Operating Plan, 1993, Alaska Interagency Operating Plan for Volcanic Ash Episodes: Anchorage, Alaska, Alaska Division of Emergency Services, Alaska Volcano Observatory, Department of Defense, Federal Aviation Administration, and National Weather Service, June 16, 1993, 18 p.
- Alaska Volcano Observatory, 1993, Mt. Spurr's 1992 eruptions: Eos, Transactions, American Geophysical Union, v. 74, p. 217 and 221-222.

- Boeing Company, 1992, Volcanic ash awareness: Seattle, Wash., Boeing Customer Training and Flight Operations Support, video 911202, 33 minutes.
- Casadevall, T.J., ed., 1991, The First International Symposium on Volcanic Ash and Aviation Safety, Program and Abstracts: U.S. Geological Survey Circular 1065, 58 p.
- Casadevall, T.J., 1992, Volcanic hazards and aviation safety—Lessons of the past decade: FAA Aviation Safety Journal, v. 2, no. 3, p. 9–17.
- 1993, Volcanic ash and airports: U.S. Geological Survey Open-File Report 93-518, 53 p.
- Casadevall, T.J., and Oliveira, F.A.L., 1993, Special project in the Asia/Pacific region boosts awareness of danger posed by volcanic ash: ICAO Journal, v. 48, no. 8, p. 16–18.
- Casadevall, T.J., and Thompson, T.B., 1994, Volcanoes and air navigation aides—A global planning chart: U.S. Geological Survey Geophysical Investigations Map GP-1011.
- Federal Aviation Administration, 1993a, Assuring aviation safety after volcanic eruptions: Washington, D.C., Office of the Associate Administrator for Aviation Safety, Special Review, 35 p.
- 1993b, FAA Workshop on old volcanic ash clouds: April 22–23, 1993: Washington D.C., Office of the Chief Scientist, abstract volume, 37 p.
- Fox, T., 1988, Global airways volcano watch is steadily expanding: ICAO Bulletin, April, p. 21–23.
- International Civil Aviation Organization [ICAO], 1992, Meteorological service for international air navigation—International standards and recommended practices: Montreal, International Civil Aviation Organization, Annex III to the Convention for International Civil Aviation, 11th edition, 82 p.
- Miller, T.P., and Chouet, B.A., eds., 1994, The 1989–1990 eruption of Redoubt Volcano, Alaska: Journal of Volcanology and Geothermal Research, v. 62.
- Miller, T.P., and Kirianov, V.Y., 1993, Notification procedures for Kamchatkan volcanic eruptions: A case history of Sheveluch Volcano, April, 1993: U.S. Geological Survey Open-File Report 93-569, 9 p.
- Riehle, J.R., and Fink, J.H., 1993, Some advantages of global electronic communications among volcanologists [abs.]: World Organization of Volcano Observatories workshop (Volcano observatories, surveillance of volcanoes, and prediction of eruptions), Guadeloupe, 13–17 December, 2 p.
- Riehle, J.R., Rose, W.I., Schneider, D.J., Casadevall, T.J., and Langsford, J.S., 1994, Unmanned aerial sampling of a volcanic ash cloud: Eos, Transactions, American Geophysical Union, v. 75, p. 137–138.
- Smith, W.S., 1983, High-altitude conk out: Natural History, v. 92, no. 11, p. 26–34.
- Steenblik, J.W., 1990, Volcanic ash: A rain of terra: Air Line Pilot, June/July 1990, p. 9–15, 56.
- Wen, Shiming, and Rose, W.I., 1994, Retrieval of sizes and total masses of particles in volcanic clouds using AVHRR bands 4 and 5: Journal of Geophysical Research, v. 99, p. 5421–5431.
- Wright, T.L., and Pierson, T.C., 1992, Living with volcanoes: U.S. Geological Survey Circular 1073, 57 p.

A METHOD FOR CHARACTERIZING VOLCANIC ASH FROM THE DECEMBER 15, 1989, ERUPTION OF REDOUBT VOLCANO, ALASKA

By Gregory K. Bayhurst, Kenneth H. Wohletz, and Allen S. Mason

ABSTRACT

The development of an automated program for characterization of particles using a scanning electron microscope (SEM) with an energy dispersive X-ray detector (EDS) has greatly reduced the time required for analysis of particulate samples. The SEM system provides a digital representation of all particles scanned such that further measurement of the size, shape, and area are a product of image processing. The EDS and associated software provides information as to the particles' chemical composition. Data obtained from the SEM by this method are reduced by computer to obtain distribution graphs for size, density, shape, and mineralogy. These SEM results have been tested by comparisons with results obtained by traditional optical microscopy—the results obtained by optical microscopy support the SEM results and provide details concerning crystallinity and glass content.

This method was applied to the ash that damaged the engines from the Boeing 747-400 flight of December 15, 1989 (Brantley, 1990), which flew into the ash cloud from Redoubt Volcano. The sample was collected from the pitot-static system and had not been exposed to any engine parts that might have changed its characteristics. The sample analysis presented here demonstrates the capabilities and information obtainable from our automated SEM technique.

INTRODUCTION

Studies of volcanic ash particles can be used to understand problems associated with volcanic ash clouds such as aircraft engine damage, visibility, atmospheric dispersion, and deposition of ash (Heiken, this volume). By using several analytical techniques, particles can be characterized in terms of size, shape, mass, mineralogy, and chemical composition. These characteristics provide detailed information necessary to understand the nature of volcanic ash clouds.

METHODS OF STUDY

SAMPLE PREPARATION

Loose samples, such as the ash collected from the pitot-static system, can easily be prepared by traditional thin-section techniques. This involves mixing the ash with epoxy on a microscope slide and then polishing flat to a desired thickness. Both the SEM technique and optical microscopy techniques can use the same slide.

If the sample has been collected on filters, it is necessary to remove the particles from the filter medium. For ash collected on cotton or paper filters, the filters can be ashed in a low-temperature radio-frequency oven. The ashing destroys the filter material and leaves the particles unaltered. The particles then can be mixed with epoxy and made into a thin section.

SEM PARTICLE-ANALYSIS PROGRAM

The SEM uses a software program originally developed by L.J. Lee Group, Inc. for identification of airborne asbestos particles. It was modified to analyze volcanic ash particles. For each particle, the size, diameter, area, elemental composition and density are recorded. The location of each particle is also noted for easy return to a particular particle if detailed examination is needed.

TREATMENT OF DATA

The data is first transferred from the SEM into a spreadsheet from which various operations are performed. These operations characterize the particles as to their mineralogy, morphology, densities, and abundances. The spreadsheet and operations are done with BBN Software Products Corporation's RS-1 software program (G. Luedemann and G. Bayhurst, unpub. data, 1989).

Table 1. Mineral definitions used in this report.

(Numbers in definitions column indicate weight percent)

Mineral	Definitions
Quartz	Si \geq 90
Calcite	Ca \geq 90
Magnetite	Fe + Ti \geq 90
Gypsum/anhydrite	Ca + S \geq 90; Ca > 41; S > 29
Mica/clay	Ca + K + Al + Si \geq 80; Fe > 4; K > 4; 23 < Si < 80
Feldspar	Ca + Na + K + Al + Si \geq 80; Fe \leq 4; Al + Si > 59; 30 < Si < 80
Amphibole	Fe + Mg + K + Ca + Al + Si \leq 80; Fe > 5; K \geq 3; 28 > Si > 80

Using the chemical analysis for each particle, the mineralogy is determined based on seven minerals or mineral classes. If the particle does not meet the criteria of the mineral definitions (table 1), it is labeled as "other." Because the SEM gives only chemical composition and not crystal structure, the glass content of the ash is not available by this method. The particles are then plotted according to the frequency of their mineral content.

The mean diameter, which is based on 16 measurements, is used to establish size frequencies. These size frequencies are calculated for both mineral type and overall bulk particles. The longest diameter measurement and the shortest measurement are ratioed without regard to mineralogy to provide an aspect ratio that gives an indication of shape. Digital image representation also allows computation of a shape factor given as the particle perimeter squared divided by the product of its area and 4 π .

By using the results from the chemical analysis, we can determine the mass of each particle by combining densities and diameters. The densities are based on values for oxides for each element in the particle such as SiO₂, Na₂O, and CaO. The masses are used in several ways. The mass for each particle can be plotted on a log cumulative mass versus log diameter to give mass accumulation curves. The mass distribution can also be expressed as a percent total versus phi ($\phi = -\log_2 \times (\text{diameter in mm})$) and analyzed using the sequential fragmentation/transport (SFT) model of Wohletz and others (1989).

The final function of the software is to determine various statistical values for each sample. Our statistics summary contains the mean, standard deviation, minimum, and maximum for several parameters and automatically prints out a summary sheet.

To verify our programs, we prepared chemical-composition standards by grinding well-characterized mineral standards to a fine powder. The powders were then prepared in the exact same manner as the ash particles. To verify our sizing-routine software, we used National Institute of Standards and Technology (NIST) standards for particle size. The software program that identifies minerals from chemical

analysis was also tested by using these composition standards, achieving 95 percent or better correct identification.

PETROGRAPHIC METHODS

Several hundred particles were examined and counted by standard petrographic methods on an optical microscope. This method allows us to determine not only the mineralogy of the particle but also if the particle is noncrystalline or glass. The importance of this is that the glass component of the volcanic cloud has a big influence on melting temperatures (Swanson and Beget, this volume).

RESULTS AND DISCUSSION

The mineralogy of the ash particles determined by chemical composition was about 70 percent feldspar. The other components were quartz, magnetite, mica or clay, calcite, and amphiboles (fig. 1). An occasional particle of gypsum or anhydrite was also observed. By using fairly large ranges for defining the minerals or mineral groups, only about 10 percent of the ash was unidentified. The majority of unidentified particles appear to be mixtures of mineral phases that were probably welded on glass fragments. This result suggests that about 10 percent of the sample is composed of lithic fragments.

The optical analysis gives another perspective of the mineralogy in that the glass component can be readily identified. The results from the optical analysis showed that the particles are mostly plagioclase feldspar (46.7 percent), with many of them being fractured. The glass component was second most abundant at 28.6 percent. The following were

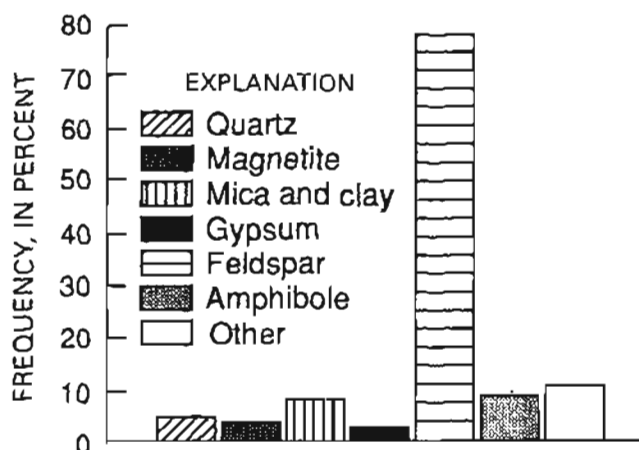


Figure 1. Mineralogy of ash particles from the December 15, 1989, eruption of Redoubt Volcano as determined by scanning electron microscopy.

Table 2. Bulk chemistry of glass from Redoubt volcanic ash from December 15, 1989, eruption.

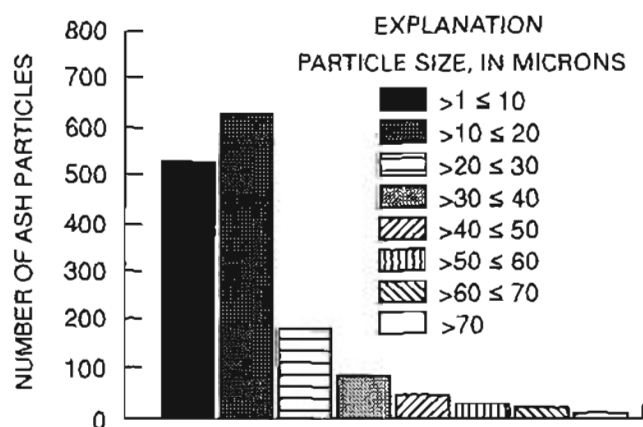
Species	Weight percent
SiO ₂	69.9
Al ₂ O ₃	10.4
FeO.....	5.0
MgO.....	0.5
CaO.....	8.4
Na ₂ O.....	4.3
K ₂ O.....	0.1

minor components: pyroxene 2.8 percent, hornblendes 4.2 percent, opaque minerals 5.6 percent, altered rock 7.0 percent, and magnetite 5.2 percent. The petrographic name of this sample is a hornblende, two-pyroxene andesite.

If we assume that the glass component has nearly the same chemical composition as the crystalline minerals, then the results of the two methods are in good agreement. For example, if approximately 30 percent of the chemically defined feldspar particles are noncrystalline, then the percentage of crystalline feldspar would be approximately 49 percent.

With our method, we are able to obtain bulk-chemistry compositions by simply averaging each chemical component. For example, the average SiO₂ composition from our Redoubt sample was 69.9 percent. Because of the high glass content, the overall bulk chemistry (table 2) showed a higher SiO₂ concentration than the magma erupted during this time (Nye and others, 1990). This result is, however, consistent with other studies of Redoubt volcanic ash (Swanson and Beget, 1991).

Our sizing routine showed that, for this sample, the majority of the particles were 20 μ m or less (fig. 2). The different mineral types can show slight differences in size distribution from the overall distribution, but they still show

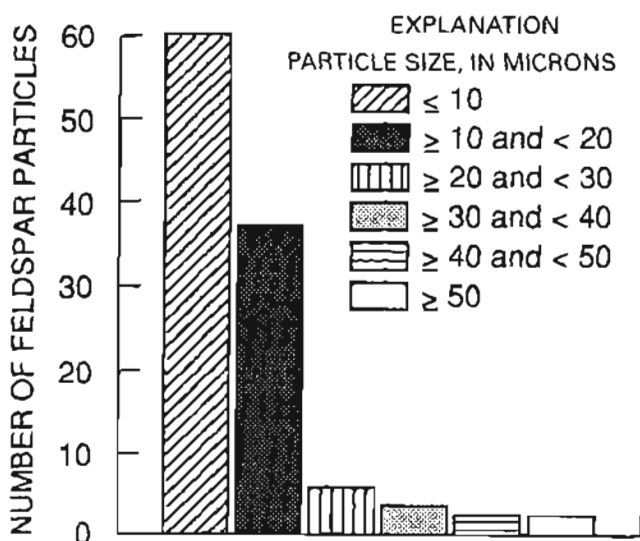
**Figure 2.** Size distribution of all minerals contained in ash from the December 15, 1989, eruption of Redoubt Volcano.

that most of the particles are smaller than 20 μ m (fig. 3). The information obtained from size distributions can provide insight as to the factors controlling the type of damage done to aircraft engines. For example, if the ash encountered had a large percentage of coarse particles, then increased damage from abrasion might be observed. If the ash is fine, it will melt more rapidly and contribute to the material adhering to turbine surfaces.

Aspect ratios can be used for several purposes. The morphology of the particle can be described in this way. Aspect ratios that are close to 1 indicate that the particle is approximately equant in shape. For example, the aspect ratio of the feldspar particles (and glass) showed that about in one-third of them were equant (fig. 4). Also, the average shape factor for the sample is 1.16, which characterizes nearly equidimensional, polygonal cross sections.

The mass distribution curve gives other important information about the nature of the volcanic ash. In our Redoubt sample, even though the small particles were the most numerous, they contributed only a small amount of the mass (fig. 5). Another way of looking at mass distribution is the phi plot (fig. 6). This plot shows that over 60 weight percent of the sample occurs between 62 μ m (4.0 phi) and 125 μ m (3.0 phi). The overall mean diameter is 78 μ m.

SFT analysis shows that the size distribution is poly-modal, which is likely a consequence of the various densities and shapes in crystals, glass, and lithics that determine the mass-to-size ratio. Furthermore, SFT analysis (fig. 7) shows a mean diameter of 3.68 phi (0.078 mm) and a standard deviation of 0.79 phi (+0.57 mm, -0.033 mm) and predicts this distribution by three subpopulations: (1) crystals (mode = 0.210 mm), (2) lithic fragments (mode = 0.099 mm), and (3)

**Figure 3.** Size distribution of feldspar minerals from the December 15, 1989, eruption of Redoubt Volcano.

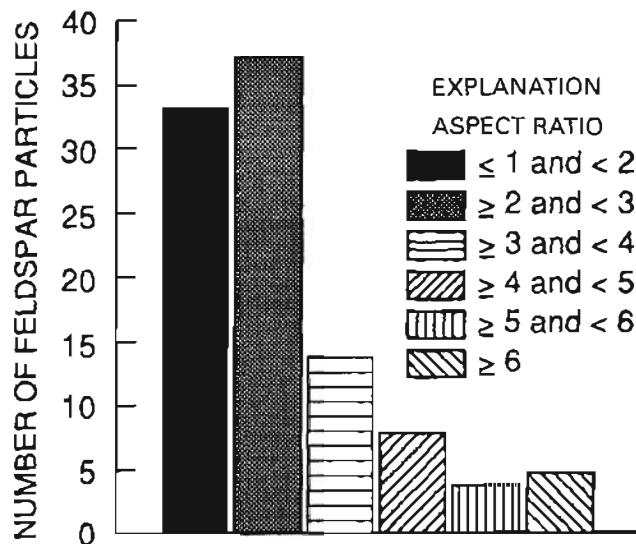


Figure 4. Aspect ratios of feldspar particles from the December 15, 1989, eruption of Redoubt Volcano. Aspect ratio is determined by dividing the longest diameter by the shortest diameter.

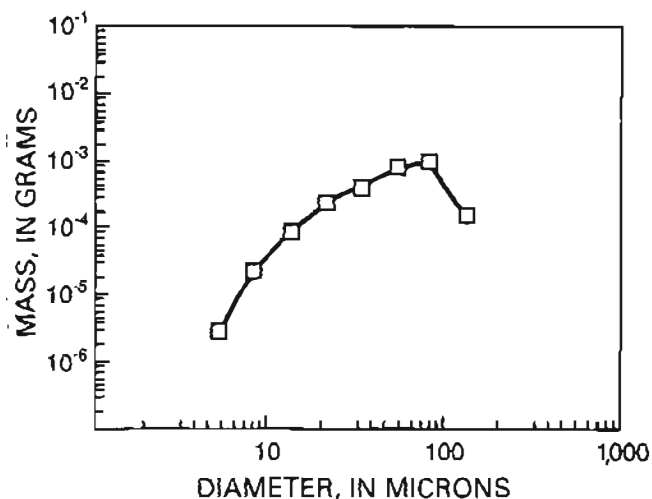


Figure 5. Mass distribution curve of ash particles found in ash from the December 15, 1989, eruption of Redoubt Volcano.

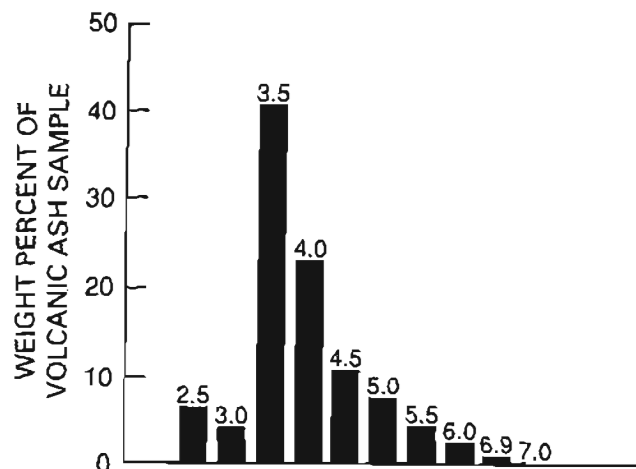


Figure 6. Phi size distribution plot of ash particles from the December 15, 1989, eruption of Redoubt Volcano. $\Phi = -\log_2 \times (\text{diameter in mm})$. Individual bars along x-axis are labeled with size in phi units.

glass (mode = 0.041 mm). The dispersion values of these subpopulations are analogous to standard deviations for log-normal distributions. In addition, the dispersion values have physical significance: with increasing dispersion, subpopulation distributions are generally more peaked, which results from more evolved particle fragmentation and size sorting. The crystal subpopulation (1) has a dispersion value of 0.50, which reflects the tight distribution in size determined by growth kinetics. Positive dispersion values generally come about from particle aggregation or nucleation, whereas negative values arise from fragmentation and attrition. In contrast, the glass subpopulation (3) has a dispersion value of -0.51 , which is a function of its fragmentation and transport history (dispersion values of -0.6 or greater are typical of fragmentation by water-magma interaction). The lithic subpopulation (2) has a dispersion value (0.15) that indicates some aggregation after its fragmentation.

The statistical summary (table 3) gives overall averages for many important parameters of the volcanic ash sample. This summary can be used to study the differences between different ashes or samples of the same ash.

Subpopulation size characteristics analyzed by the sequential fragmentation/transport (SFT) model of Wohletz and others (1989).

[See Wohletz and others (1989) for additional explanation]

Subpopulation	Mode		Dispersion	Fraction
	phi	mm		
Crystals	2.25	(0.210)	0.50	0.08
Lithic fragments	3.34	(0.099)	0.15	0.07
Glass	4.60	(0.041)	-0.51	0.21

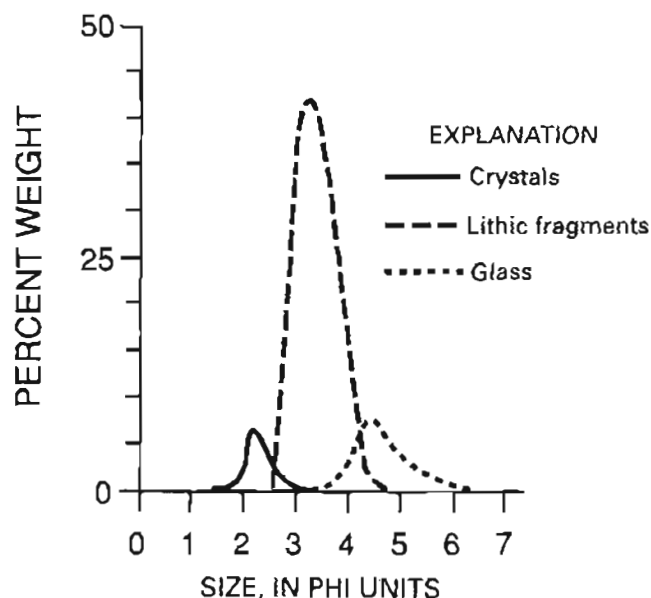


Figure 7. Subpopulation size characteristics of ash from the December 15, 1989, eruption of Redoubt Volcano.

CONCLUSIONS

To understand the nature of volcanic ash clouds, we must understand the nature of the particles that make up the cloud. By combining SEM and optical petrographic techniques with powerful software analysis and theories on particle transport, we obtain detailed information on the

Table 3. Statistical summary for Redoubt volcanic ash from December 15, 1989, eruption.

	Average	Standard deviation	Maximum
Diameter (μm)	13.3	12.9	141.0
Aspect ratio	3.5	3.1	
Area (μm^2)	284.0	889.8	11,989.0
Density (g/cm^3)	2.42	0.79	6.6

characteristics of the particles in volcanic ash clouds. The characteristics of the ash cloud will determine where it goes, how long it will stay in the atmosphere, how much damage it will cause to an aircraft, and its effects on the environment.

The volcanic ash ingested by the Boeing 747-400 that encountered the Redoubt ash cloud on December 15, 1989, has characteristics of material derived from eruption of andesitic magma by rapid release of high-pressure gases, perhaps by a hydrovolcanic mechanism. Optical microscope inspection revealed glass, blocky shards of minerals, and hydrothermally altered andesitic rock fragments. The chemical analysis derived from SEM analysis confirms the andesitic nature of the ash. Size analysis shows fragmentation characteristic of an evolved fragmentation process, such as is expected for a water-magma interaction. The shape analysis revealed dominantly low shape factors, characteristic of hydrovolcanic ash. Knowing the chemical composition and finding that a large fraction of particles have a glass structure, the melting-temperature range can be estimated.

REFERENCES CITED

- Brantley, S.R., ed., 1990, *The eruption of Redoubt Volcano, Alaska, December 14, 1989–August 31, 1990*: U.S. Geological Survey Circular 1061, 33 p.
- Nye, C.J., Swanson, S.E., and Miller, T.P., 1990, The 1989–1990 eruption of Mt. Redoubt—Magma chemistry [abs.]: *Eos, Transactions, American Geophysical Union*, v. 43, p. 1705.
- Wohletz, K.H., Sheridan, M., and Brown, W., 1989, Particle size distributions and the sequential fragmentation/transport theory applied to volcanic ash: *Journal of Geophysical Research*, v. 94, p. 15703–15721.

MELTING PROPERTIES OF VOLCANIC ASH

By Samuel E. Swanson and James E. Beget

ABSTRACT

Volcanic ash from eastern Aleutian volcanoes (typical of circum-Pacific volcanoes) is composed of rhyolitic (silica-rich) glass, minerals (feldspars, pyroxene, hornblende and Fe-Ti oxides), and rock fragments. Melting temperatures of the glasses, estimated from liquidus phase relations in the system $\text{SiO}_2\text{-KAlSi}_3\text{O}_8\text{-NaAlSi}_3\text{O}_8$, ranged from 1,000°C to 1,300°C, whereas minerals begin melting at about 1,100°C.

Volcanic ash that is ingested into operating turbofan engines will partially melt (i.e., all of the glass and some of the minerals). The molten ash is then deposited on high-temperature parts of the turbine—this can result in engine shutdown.

Reduction of engine operating conditions to idle settings lowers the engine temperatures below the melting point of volcanic glass (below 1,000°C), thus preventing the melting of ingested volcanic ash. However, at idle conditions, engines still operate at temperatures in excess of the glass transition temperature (700°–860°C), and annealing of glass particles to hot parts of the turbine may still be a problem.

INTRODUCTION

Volcanic ash is a widespread product of eruptions of volcanoes that are located around rim of the Pacific Ocean. Ash is formed by explosive fragmentation and quenching of magma (crystals + melt + gas) during an eruption. Melt in the magma is quenched to a glass when the temperature is rapidly lowered upon exposure to atmospheric conditions. The explosive character of these volcanoes is caused by the silica-rich melt, which often contains dissolved volatile components, such as H_2O or SO_2 . Crystallization of mineral phases (e.g., plagioclase, pyroxene, hornblende, Fe-Ti oxides, etc.) gradually enriches non-crystallizing components in the melt. In the case of components like silica or sodium, their concentrations in the crystallizing phases are low relative to their concentration in the melt, resulting in their overall enrichment. Bulk lava compositions from these volcanoes range from basalt to dacite (lavas generally contain from 48 to 70 weight percent SiO_2), and the melt fraction between mineral grains is andesitic to rhyolitic (53–78 weight percent SiO_2). The glassy fragments in

volcanic ash are the non-crystalline part of the magma and, hence, have the lowest crystallization temperature. Conversely, the glass also has the lowest melting temperature. When volcanic ash is ingested into operating jet aircraft engines, it is the glass particles that will melt first. As aircraft engine operating temperatures are lowered in an effort to reduce the ash fusion within the engine (Campbell, this volume; Casadevall and others, 1991; Przedpelski and Casadevall, this volume), it is the melting temperature of glass particles that will determine the operating temperatures below which the ash will not melt in the engine. The purpose of this paper is to review the compositions of glasses found in volcanic ashes from typical circum-Pacific volcanoes and to estimate their melting temperatures by comparison to published phase diagrams available in the geological and engineering literature. We report here on the melting properties of the more common silica-rich glasses. Mafic (andesitic) glass, similar to that erupted in the 1992 eruption of Mt. Spurr (Alaska), is currently under study and will be the subject of a future report. Alaskan volcanoes in the eastern Aleutian arc were selected for study because of their recent activity and potential hazard to aircraft safety (Steenblik, 1990; Przedpelski and Casadevall, this volume; Kienle, this volume). Several Alaskan volcanoes in the eastern Aleutian arc (fig. 1) have produced widespread volcanic-ash deposits that have covered south-central Alaska. Ash may be produced in short-lived, large eruptions (Novarupta in 1912, Spurr in 1953 and 1992) or in a series of intermittent, small eruptions (Redoubt Volcano, 1989–90). Jet aircraft encounters with ash have been recorded from eruptions of Augustine in 1976 and Redoubt in 1989 (Steenblik, 1990; Casadevall, 1991; Kienle, this volume).

METHODS OF STUDY

All of the glass samples used in this study were obtained from volcanic ash deposits from south-central Alaska. The White River ash and the ash from Hayes Volcano are voluminous prehistoric ashes that covered south-central Alaska (Riehle, 1985; Westgate, 1990; Beget and others, 1991). Novarupta, which erupted in 1912, is the largest historic Alaskan eruption and spread ash throughout southern Alaska (Griggs, 1922; Hildreth, 1987). Ash from Augustine Volcano, the most active volcano in the eastern

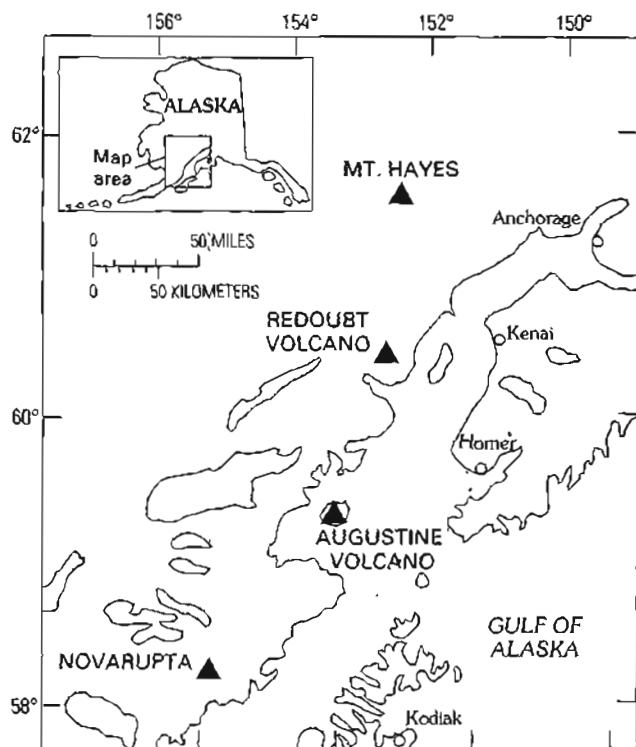


Figure 1. Volcanoes (solid triangles) in the eastern Aleutian volcanic arc, Alaska.

Aleutian arc, was collected from prehistoric deposits on Augustine Island that span approximately 2,700 years of eruptive history (Swanson and Kienle, 1986; Beget and Kienle, 1992). Ash from Redoubt Volcano is represented by samples from the 1989–90 eruption. Together, this suite of samples provides a representative collection of the ashes that is to be expected from eruptions of these Alaskan volcanoes.

ANALYTICAL TECHNIQUES

Glass from these ash samples was analyzed with a Cameca MBX electron microprobe at Washington State University using a 15-kV electron beam and a sample current of 13.5 nA. A beam spot diameter of 8 μ m was used, and the counting time was 10 seconds. The glass analyses are reported as oxides and are normalized to 100 percent. Actual totals ranged from 98 to 100 percent, depending on the degree of hydration (water in the glass.) Well-characterized natural glasses were used as standards (KCI was used for Cl measurements).

RESULTS

When compared with lavas, glass particles (shards of quenched melt) in the volcanic ash from Alaskan volcanoes are much richer in silica as a consequence of crystallization

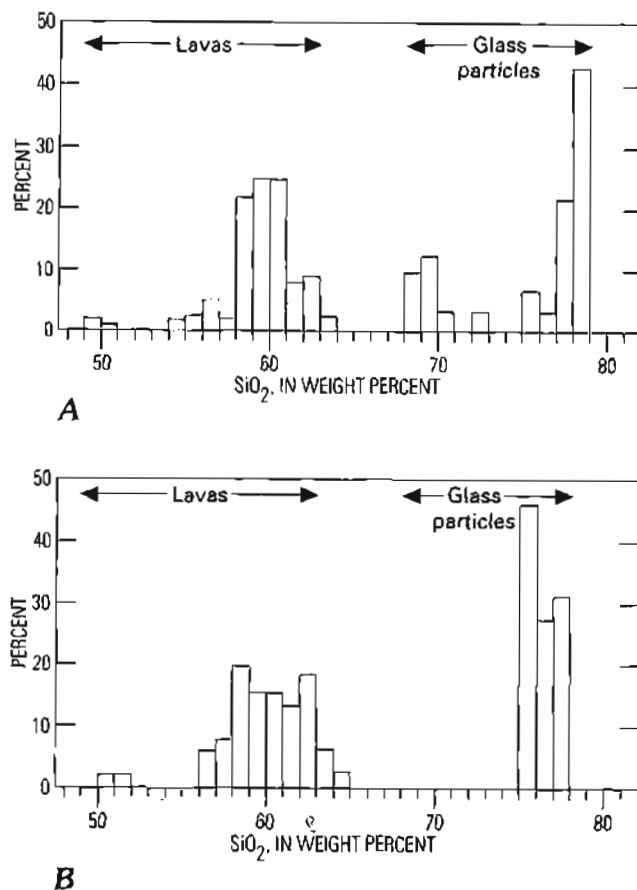


Figure 2. Silica contents of lavas (bulk samples) and glass particles (shards) in volcanic ashes from A, Redoubt and B, Augustine Volcanoes. The numbers of analyses of lavas and glasses from each volcano are in excess of 50 and have been normalized to 100 percent for comparison. Volcanic glass is consistently higher in silica than the whole-rock lavas. Glass analyses are from unpublished data in the authors' files (representative analyses given in table 1). Lava compositions for Augustine Volcano are from Kienle and others (1983) and Daley (1986); compositions for Redoubt Volcano are from Nye and others (in press) and Swanson and others (in press).

to form phenocryst minerals before eruption. For example, lavas from Redoubt Volcano have basaltic and andesitic bulk compositions (50–64 weight percent SiO_2 , fig. 2), whereas the glass in the volcanic ash from the 1989–90 eruption of Redoubt ranges from 69 to 78 weight percent SiO_2 (fig. 2). Similar relations are shown for Augustine Volcano (fig. 2), but the Augustine glasses show a more restricted range of compositions (75–78 weight percent SiO_2).

Representative glass compositions are shown in table 1 both as weight percent oxide and as normative minerals. The normative composition is the rock analysis recalculated to a set of standard anhydrous normative minerals. For silica-rich volcanic rocks or glasses, the abundant normative minerals are quartz (Q), albite (Ab), and orthoclase (Or), with lesser amounts of anorthite (An), corundum (C), hypersthene (Hy),

Table 1. Representative electron microprobe analyses of volcanic glass from ash from Alaskan volcanoes.

[Analyses are presented as weight percent of oxides and as normative minerals (see text for explanation of normative minerals). Numbers in parentheses represent units of standard deviation]

Quantity analyzed	Redoubt Volcano (12/15/89)				Augustine Volcano		Hayes Volcano	White River ash	Novarupta	
Analyses expressed as weight percent of oxides										
SiO ₂	69.35 (0.45)	71.91 (0.31)	75.94 (0.36)	77.81 (0.35)	75.38 (0.36)	76.36 (0.31)	73.65 (0.36)	73.77 (0.43)	78.20 (0.37)	76.94 (0.17)
TiO ₂	0.51 (0.11)	0.45 (0.03)	0.31 (0.07)	0.22 (0.01)	0.39 (0.04)	0.37 (0.06)	0.23 (0.03)	0.21 (0.02)	0.18 (0.06)	0.35 (0.07)
Al ₂ O ₃	15.59 (0.54)	14.75 (0.16)	13.32 (0.21)	12.40 (0.18)	12.98 (0.10)	12.58 (0.17)	14.50 (0.14)	14.54 (0.26)	12.00 (0.15)	12.29 (0.12)
Fe ₂ O ₃ total	3.26 (0.31)	2.58 (0.14)	1.46 (0.22)	1.22 (0.09)	2.30 (0.15)	2.06 (0.12)	1.94 (0.21)	1.71 (0.14)	1.34 (0.15)	1.87 (0.13)
MgO	0.87 (0.17)	0.67 (0.02)	0.30 (0.11)	0.23 (0.03)	0.49 (0.05)	0.43 (0.05)	0.54 (0.03)	0.36 (0.03)	0.14 (0.05)	0.26 (0.04)
CaO	3.25 (0.29)	2.48 (0.10)	1.57 (0.25)	1.16 (0.10)	2.28 (0.27)	2.04 (0.16)	2.23 (0.10)	1.85 (0.11)	0.85 (0.19)	1.27 (0.09)
Na ₂ O	4.37 (0.18)	4.21 (0.08)	3.92 (0.21)	3.71 (0.12)	3.95 (0.13)	3.89 (0.09)	3.93 (0.08)	4.16 (0.13)	4.07 (0.13)	3.98 (0.13)
K ₂ O	2.54 (0.12)	2.79 (0.11)	3.04 (0.14)	3.14 (0.17)	2.00 (0.27)	1.98 (0.08)	2.62 (0.11)	3.07 (0.10)	3.03 (0.10)	2.85 (0.08)
Cl	0.17 (0.08)	0.16 (0.02)	0.15 (0.04)	0.13 (0.06)	0.24 (0.11)	0.29 (0.07)	0.36 (0.03)	0.33 (0.03)	0.19 (0.03)	0.19 (0.03)
n ¹	11	7	5	7	18	16	15	15	18	10
Analyses recast as normative minerals										
Q	26.04	30.43	37.69	41.38	39.13	41.14	35.18	33.32	40.90	39.77
Or	15.01	16.49	17.97	18.56	11.82	11.70	15.48	18.14	17.91	16.84
Ab	36.98	35.62	33.17	31.39	33.42	32.92	33.25	35.20	34.44	33.68
An	15.70	12.30	7.7	5.75	11.31	10.12	11.06	9.18	4.22	6.30
C	0.00	0.30	0.73	0.79	0.17	0.33	1.14	1.01	0.48	0.35
Hy	2.17	1.67	0.75	0.57	1.22	1.07	1.34	0.90	0.35	0.65
Hm	3.26	2.58	1.46	1.22	2.30	2.06	1.94	1.71	1.34	1.87
Tn	0.30	0.00	0.00	0.00	0.00	0.00	0.00	0.00	0.00	0.00
Ru	0.39	0.45	0.31	0.22	0.39	0.37	0.23	0.21	0.18	0.35

¹ Number of points per analysis, n.

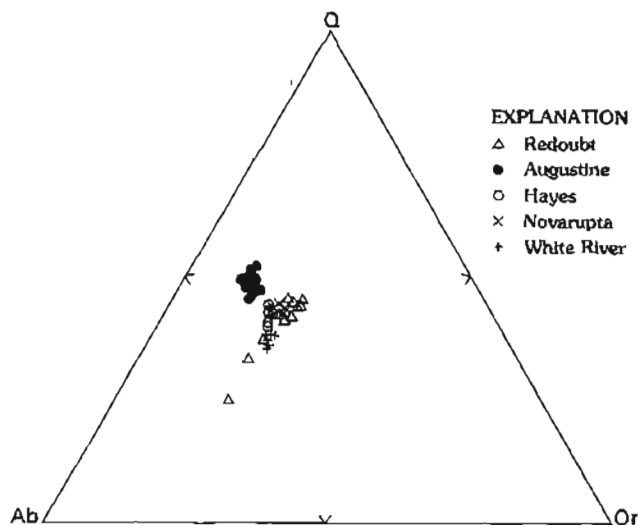


Figure 3. Normative compositions (in terms of albite, Ab; orthoclase, Or; and quartz, Q—see text for explanation) of glasses from the White River ash, the 1912 eruption of Novarupta, and eruptions of Mt. Hayes and Augustine and Redoubt Volcanoes. The Redoubt data are for glasses from the 1989–90 eruption. White River, Augustine, and Hayes data are from prehistoric ashes. Mt. Hayes data are from Beget and others (1991); other data are from the authors' unpublished files.

hematite (Hm), sphene (Tn), and rutile (Ru). The recalculation of the oxide components into normative minerals facilitates comparison of glass compositions to experimental laboratory results on melting temperatures of rocks.

Glass compositions displayed on triangular variation diagrams, with normative components as the variables, cluster into fields for each suite of glasses (fig. 3). Glasses from single, short-lived eruptions (e.g., White River ash and Novarupta) cluster in small fields, whereas glasses from multiple eruptions (Augustine and Hayes) define slightly larger fields. The 1989–90 Redoubt glasses form a range of compositions related to the mixing of two different magmas (with different compositions of melt quenched to glass) in the early (December 1989) stages of the eruption (Swanson and others, in press).

MELTING RELATIONS OF GLASSES

Liquidus phase relations (temperatures required to completely melt a solid) at a pressure of 1 bar in the system SiO_2 (quartz, Q)— KAlSi_3O_8 (orthoclase, Or)— $\text{NaAlSi}_3\text{O}_8$ (albite, Ab) are shown in figure 4. This system is well known to geologists as the "granite system" because of its use in describing the melting and crystallization behavior of granitic rocks. The triangular composition diagram is divided into primary phase fields by boundary curves. Isotherms (lighter solid lines that represent constant

temperature) describe the melting temperatures for any solid that contains the normative minerals quartz, orthoclase, and albite (fig. 4). The boundary curve between the primary phase fields of the SiO_2 polymorphs cristobalite (Cr) and tridymite (Tr), and alkali feldspar (Af) has a temperature minimum (m, fig. 4) at 960°C . For any combination of these three normative minerals (quartz-orthoclase-albite), melting at 1 bar will initially start at 960°C , and the composition of the first melt will correspond to m (fig. 4). The incongruent melting of K-feldspar (Or) at low pressure is represented by the boundary curve between alkali feldspar (Af) and leucite (Lc) phase fields (fig. 4). The small (10–20 bar) pressure increase within operating turbofan engines does little to change the 1 bar melting relations of figure 4.

In addition to the albite (Ab), orthoclase (Or), and quartz (Q) components, the volcanic glasses contain appreciable normative anorthite (An) (table 1). Addition of the anorthite component raises the melting temperatures relative to the anorthite-free albite-orthoclase-quartz compositions; however, the magnitude of this effect is difficult to predict, especially for this system without water. Experiments done on ingestion of dust containing appreciable anorthite component along with albite, orthoclase, and quartz into operating jet engines find that ash begins to melt at temperatures of about $1,000^\circ\text{C}$ (Kim and others, 1992). These results are in good agreement with the predictions from figure 4, where

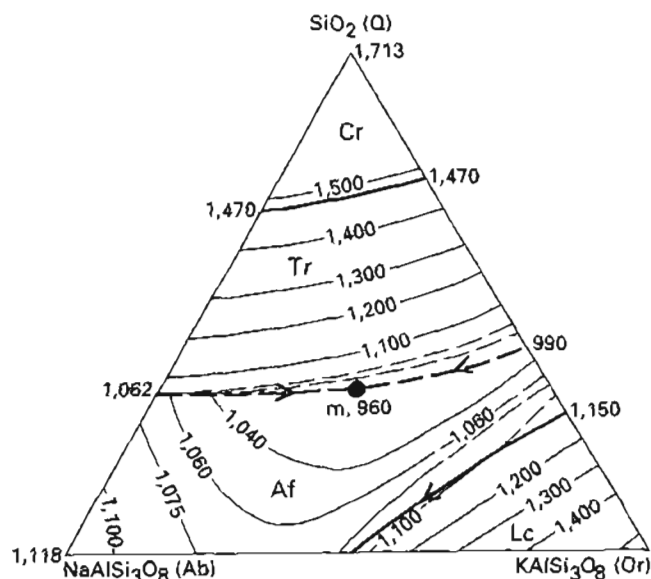


Figure 4. Liquidus phase diagram for the system Ab-Or-Q at one bar pressure, modified from Schairer (1950). Heavy lines are boundary curves with arrows indicating the direction to lower temperature. Primary phase fields are shown for cristobalite (Cr), tridymite (Tr), alkali feldspar (Af), and leucite (Lc). Symbol, m, indicates temperature minimum on boundary curve between cristobalite/tridymite and alkali feldspar. See text for further explanation.

the beginning of melting for anorthite-free compositions occurs at 960°C. Thus, the effect of anorthite on melting relations seems small and is probably on the order of less than 50°C. Melting of any volcanic glass that contains normative quartz, orthoclase, and albite can be modeled in the system albite-orthoclase-quartz, as illustrated for the glasses in this study on figure 5. Augustine glasses plot between the 1,200°C and 1,300°C isotherms; the glasses from the Hayes Volcano and Novarupta plot between the 1,100°C and 1,200°C isotherms; and White River glasses plot near the 1,100°C isotherm (fig. 5).

The large field of Redoubt glass compositions (fig. 5) is caused by variation in composition of glass shards erupted during December 1989 (table 1) and gives a melting range of 1,000°C–1,200°C. These glasses (with the higher silica contents—77 to 78 weight percent SiO₂) were erupted from December 1989 to April 1990; they melt at temperatures of 1,100°C to 1,200°C. Lower silica glasses (68 to 73 weight percent SiO₂) were only erupted during December 1989 and melt at lower temperatures: 1,000°C to 1,100°C.

Maximum-cruise operating temperatures of high performance turbofan engines currently used on long-range commercial aircraft (747-400, DC-10, etc.) are on the order of 1,400°C (E.E. Campbell, Boeing Co., oral commun., 1991; Kim and others, 1992). Most of the compositions in the system albite-orthoclase-quartz are above liquidus temperatures at 1,400°C (fig. 4)—this includes all the volcanic glasses modeled in this study (fig. 5). Indeed, some of the minerals found in the volcanic ash (e.g., sodic plagioclase) will also melt at 1,400°C. Ingestion of volcanic ash by turbofan engines effectively grinds the ash to fine particles ($\approx 7 \mu\text{m}$;

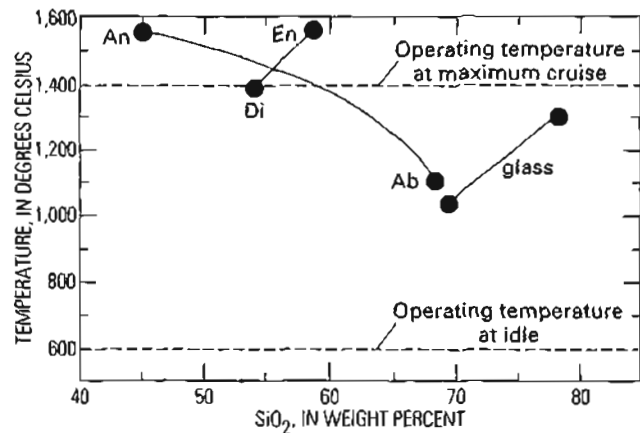


Figure 6. Melting relations of plagioclase (An-Ab), pyroxene (Di-En), and volcanic glasses (from fig. 5) at 1 bar pressure. Dashed lines represent the approximate operating temperatures of typical high-performance turbofan engines at idle and maximum-cruise conditions.

Casadevall and others, 1991) and, in the process, erodes the tips of the compressor airfoils (Przedpelski and Casadevall, this volume). This combination of small ash particle size and the high operating temperatures of the engine ensures that much of the volcanic ash will melt upon ingestion into an operating engine and be deposited on the turbine (specifically on the high-pressure nozzle guide vanes).

A reduction of engine thrust to idle has been recommended if a jet aircraft encounters volcanic ash in the air (Campbell, this volume; Przedpelski and Casadevall, this volume). Turbofan engines operating at idle run at about 600°C, considerably below the melting temperatures of all volcanic glass (fig. 6). Cooling of turbofan engines from normal operating temperatures (1,400°C) to idle temperatures is almost instantaneous. Volcanic ash will not melt when ingested into the engines at idle conditions (600°C). In addition, the rapid cooling from operating conditions to idle thrust setting induces a thermal shock related to the differential thermal expansion of the molten glass and the engine-metal substrate that can remove much of the previously melted glass that was deposited in the engine.

CONCLUSIONS

Ingestion of volcanic ash by high performance turbofan engines at operating conditions melts glass shards and some of the minerals that make up the ash (fig. 6). Volcanic glass compositions can show wide variations and still be melted upon ingestion into the engine because of high engine operating temperatures. Operating temperatures must be lowered below the lowest melting temperature ($\approx 1,000^\circ\text{C}$ for glass, fig. 6) to prevent melting of ingested volcanic ash. Reduction of engine operating conditions to idle settings ($\approx 600^\circ\text{C}$) will prevent melting of ingested volcanic ash.

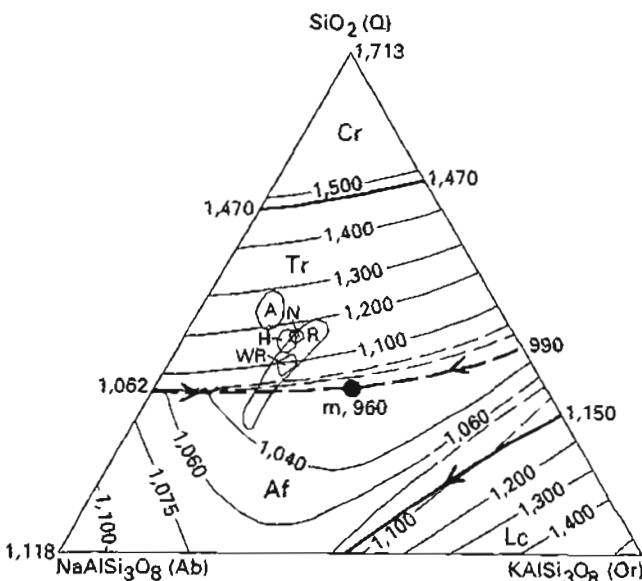


Figure 5. Composition fields of volcanic glasses (fig. 3) on liquidus Ab-Or-Q phase diagram at 1 bar pressure showing isotherms that define melting temperatures for various glasses. A, Augustine; N, Novarupta; H, Hayes; WR, White River; R, Redoubt.

RECOMMENDATIONS

Industry recommendations involving aircraft encounters with airborne volcanic ash (Lloyd, 1990; Campbell, this volume; Przedpelski and Casadevall, this volume; AIA, 1991) emphasize the need to exit the ash as quickly as possible and to reduce engine thrust to idle. Reduction of engine operating temperatures will prevent the melting of volcanic ash (including glass) ingested into the engines. Dynamic experiments done on ingestion of dust into operating engines (e.g., Kim and others, 1992; Dunn and Wade, this volume) should be done with volcanic ash (including an abundance of glass) at engine-idle temperatures. The question to be answered is whether glass particles can anneal and flow as a supercooled liquid above the glass transformation temperature (T_g), the temperature between lower temperature glass and higher temperature supercooled liquid (Carmichael and others, 1974). For most silicate glasses, T_g is about 0.66 of the melting temperature (Carmichael and others, 1974). Volcanic glasses in this study thus have glass transformation temperatures of about 700°–860°C. Will these volcanic glasses anneal at engine-idle conditions and adhere to the hotter parts of the engine? Probably not. The glass transformation temperatures are close to the idle operating temperatures ($\approx 600^\circ\text{C}$), and the transit time of the ash through the engine is short. M.G. Dunn does not believe that glass annealing will occur (CALSPAN, oral commun., 1991) and does not find an adhesion of ash below 1,000°C in his experiments (Kim and others, 1992; Dunn and Wade, this volume). However, such ash-ingestion experiments should be tried at engine-idle conditions with a volcanic ash rich in volcanic glass.

ACKNOWLEDGMENTS

Funding for this study was provided by the Alaska Volcano Observatory. Samples of Redoubt Volcano tephra were supplied by Robert G. McGimsey of the U.S. Geological Survey. Tephra glass analyses were done at Washington State University with the able assistance of Scott Cornelius and Diane Johnson. Discussions with Michael G. Dunn of CALSPAN and preprints of his papers on dynamic experiments with dust and jet engines provided a much needed "reality check" on some of the conclusions presented in this paper. Several industry people, including Ernie Campbell of Boeing Commercial Airplanes, Zygmunt Przedpelski of General Electric Aircraft Engines, and Peter Kingston of Rolls Royce Inc., provided useful copies of graphic materials.

REFERENCES CITED

AIA, 1991, AIA recommendations aimed at increased safety and reduced disruption of aircraft operations in regions with volcanic activity: Washington, D.C., Aerospace Industries Association of America, 7 p.

- Beget, J.E., and Kienle, J., 1992, Cyclic formation of debris avalanches at Mount St. Augustine Volcano: *Nature*, v. 356, p. 701–704.
- Beget, J.E., Reger, R.D., Pinney, D., Gillispie, T., and Campbell, K., 1991, Correlation of the Holocene Jarvis Creek, Tangle Lakes, Cantwell, and Hayes tephra in southcentral Alaska: *Quaternary Research*, v. 35, p. 74–189.
- Carmichael, I.S.E., Turner, F.J., and Verhoogen, J., 1974, *Igneous Petrology*: New York, McGraw-Hill, 739 p.
- Casadevall, T.J., ed., 1991, First International Symposium on Volcanic Ash and Aviation Safety: U. S. Geological Survey Circular 1065, 58 p.
- Casadevall, T.J., Meeker, G.P., and Przedpelski, Z.J., 1991, Volcanic ash ingested by jet engines [abs.], in Casadevall, T.J., ed., *First International Symposium on Volcanic Ash and Aviation Safety*: U.S. Geological Survey Circular 1065, p. 15.
- Daley, E.E., 1986, Petrology, geochemistry, and the evolution of magmas from Augustine Volcano, Alaska: Fairbanks, Alaska, University of Alaska Fairbanks, unpub. M.S. thesis, 106 p.
- Griggs, R.F., 1922, *The Valley of Ten Thousand Smokes*: Washington, D.C., National Geographic Society, 340 p.
- Hildreth, W., 1987, New perspectives on the eruption of 1912 in the Valley of Ten Thousand Smokes, Katmai National Park, Alaska: *Bulletin of Volcanology*, v. 47, p. 680–697.
- Kienle, J., Swanson, S.E., and Pulpan, H., 1983, Magmatism and subduction in the eastern Aleutian arc, in Shimozuru, D., and Yokoyama, I., eds., *Arc Volcanism: Physics and Tectonics*: Boston, D. Reidel, p. 191–224.
- Kim, J., Dunn, M.G., Baran, A.J., Wade, D.P., and Tremba, E. L., 1992, Deposition of volcanic materials in the hot sections of two gas turbine engines, in 1992 ASME International Gas Turbine Conference, Cologne, Germany, 1–4 June 1992, 31 p.
- Lloyd, A.T., 1990, Vulcan's blast: Boeing Airliner, April–June 1990, p. 15–21.
- Nye, C.J., Swanson, S.E., and Miller, T.P., in press, Geochemistry of the 1989–1990 eruption of Redoubt Volcano: Part I. Evidence from major and trace element chemistry: *Journal of Volcanology and Geothermal Research*.
- Riehle, J.R., 1985, A reconnaissance of the major tephra deposits in the upper Cook Inlet region, Alaska: *Journal of Volcanology and Geothermal Research*, v. 26, p. 37–74.
- Schairer, J.F., 1950, The alkali feldspar join in the system $\text{NaAlSi}_3\text{O}_8$ – KAlSi_3O_8 – SiO_2 : *Journal of Geology*, v. 58, p. 512–517.
- Steenblik, J.W., 1990, Volcanic ash, a rain of terra: *Air Line Pilot*, June/July p. 9–15, 56.
- Swanson, S.E., and Kienle, J., 1986, The 1986 eruption of Mt. St. Augustine, field test of a hazard model: *Journal of Geophysical Research*, v. 93, p. 4500–4520.
- Swanson, S.E., Nye, C.J., Miller, T.P., and Avery, V.F., in press, Geochemistry of the 1989–1990 eruption of Redoubt Volcano: Part II. Evidence from mineral and glass chemistry: *Journal of Volcanology and Geothermal Research*.
- Westgate, J.A., 1990, White River ash, in Wood C.A., and Kienle, J., eds., *Volcanoes of North America*: New York, Cambridge University Press, p. 92.

THE INJECTION OF VOLCANIC ASH INTO THE ATMOSPHERE

By Andrew W. Woods and Juergen Kienle

ABSTRACT

In this paper, we present some physical models that can describe the ascent of volcanic ash into the atmosphere during a volcanic eruption. We consider both sustained volcanic eruption columns and discrete volcanic thermal clouds. To test the modeling approach, we compare our predictions of the ascent rate of a model cloud with some observations of the ascent of the ash cloud during the April 15, 1990, eruption of Redoubt Volcano, Alaska. We also consider the radial spreading of ash as a gravity current following emplacement by the column and compare our theory with the observations from the April 21, 1990, eruption of Redoubt, Alaska. Both styles of eruption behavior are hazardous for aircraft.

INTRODUCTION

There is a range of styles of explosive volcanic eruption that can produce large convecting ash clouds and thereby inject ash high into the atmosphere. Ash can rise high into the atmosphere if the hot, erupted material can mix with and heat up a sufficient mass of air so that the bulk density of the mixture decreases below the ambient (Self and Walker, this volume). The typical ascent time of this ash to its maximum height is on the order of a few minutes; if this time is longer than the time over which the material is erupted and becomes buoyant, then the cloud will rise as a discrete volcanic thermal cloud (Wilson and others, 1978; Woods and Kienle, in press). Such volcanic thermal clouds formed, for example, during the April 15 and 21, 1990, eruptions of the Redoubt Volcano, Alaska. Figure 1 is a photograph of the April 21 eruption cloud, which ascended about 12 km into the atmosphere. The main eruption cloud has reached its maximum height and has begun to spread laterally into the atmosphere. A relatively small, vertical column may be seen below this main cloud. This column contains material rising from the ground after the ascent of the main cloud—this material is less energetic than that in the main thermal cloud. In the photograph, a small secondary lateral intrusion has begun to develop from this column.

In a more sustained eruption, lasting several hours, material is continually erupted from the vent. In this case, a maintained eruption column, injecting ash high into the atmosphere, will form if the hot ash can entrain and heat a sufficient quantity of air so that the bulk density of the mixture falls below that of the ambient. Two different mechanisms of buoyancy generation are possible, and, during the course of an eruption, the style of eruption may change from one to the other: (1) If the erupted material is ejected upward from the vent very rapidly, the dense jet may entrain sufficient air to become buoyant before its upward momentum is exhausted; in this case, the material continues rising upward, driven by its own buoyancy thereby forming a classical Plinian eruption column (Sparks, 1986; Woods, 1988) such as the A.D. 79 eruption of Mt. Vesuvius, Italy. (2) If the erupted material is ejected from the vent with smaller momentum, that material will collapse back and spread out along the ground as an ash flow in a similar manner to the motion of water in a fountain. However, the material in the spreading ash flow may become buoyant through entrainment and mixing with air and sedimentation of large particles as it propagates along the ground. It will then rise off the ground to form a maintained eruption column, in this case called a co-ignimbrite eruption column (Sparks and Walker, 1977; Woods and Wohletz, 1991). Historical examples of eruptions, which include phases in which co-ignimbrite eruption columns developed, include the massive 1815 eruption of Tambora, Indonesia, and the 1912 eruption of Katmai, Alaska. Co-ignimbrite eruption columns tend to form during massive eruptions (Woods and Wohletz, 1991).

Both discrete and maintained eruption clouds can inject vast quantities of ash into the atmosphere—they thereby pose a serious safety problem for aircraft. However, sustained eruption columns are perhaps more hazardous for aircraft because they may persist for hours and can therefore inject very large quantities of ash, which spreads over a very wide area in the atmosphere. In order to evaluate the dangers of an eruption for aircraft, it is important to know the extent of the region in which the mass loading of ash in the air is at hazardous concentrations. When ash has been carried upward to its maximum height by the eruption column, it

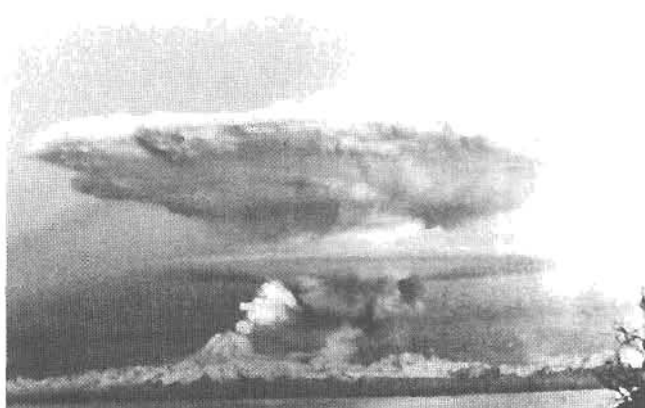


Figure 1. Photograph of the volcanic eruption cloud formed during the April 21, 1990, eruption of Redoubt Volcano, Alaska, seen from the Kenai Peninsula, east of the volcano. The main cloud ascended about 12 km, and the secondary intrusion ascended to an altitude of about 6 km. Photograph by Mark and Audrey Hodges.

spreads out laterally under gravity above its neutral buoyancy height and is carried by the wind to form a large, laterally spreading ash plume (fig. 2). The maximum ash concentration in this ash plume occurs at the top of the eruption column (before it is diluted through mixing with the ambient as it travels downwind).

In the following section, we describe the Plinian eruption-column model of Woods (1988) and the model of a volcanic thermal cloud of Woods and Kienle (in press). In order to test the modeling approach, we compare the predicted rate of ascent of a volcanic thermal, using the model of Woods and Kienle (in press), with the observed ascent of the thermal cloud during the April 15, 1990, eruption of the Redoubt Volcano, Alaska. We also investigate the radial spreading of the ash as a gravity current after it is emplaced into the atmosphere by the eruption; we compare a simple model with observations of the spreading umbrella cloud following the April 21, 1990, eruption of Redoubt Volcano. Details of the mass loading in eruption columns and the downwind dispersal of ash are given in other articles in this volume (Sparks and others, this volume; Bursik and others, this volume; Self and Walker, this volume).

MODELING THE DYNAMICS OF ERUPTION CLOUDS

Although the initial momentum of the material erupted from the vent accounts for the first few kilometers of the ascent, it is the generation of buoyancy that enables the material to ascend tens of kilometers (Woods, 1988). This buoyancy is generated through the entrainment of vast quantities of ambient air, which is heated and expands, ultimately lowering the density of the column below that of the surrounding

air. Once buoyant, the material rises through the atmosphere until reaching the height at which its density equals the ambient again, called the neutral buoyancy height. At this point, the inertia of the material causes the material to continue rising some distance until the material comes to rest. It then collapses downward toward the neutral buoyancy height and spreads out laterally. In this overshoot region, the density of the cloud exceeds that of the surroundings, and the cloud may actually become tens of degrees colder than the environment (Woods and Self, 1992). This undercooling of the eruption cloud causes difficulties in the interpretation of thermal satellite images of the top of eruption columns; in particular, it is very difficult to estimate the height of the cloud top using the observed cloud-top temperature and radiosonde measurements of the environmental temperature as a function of altitude (Woods and Self, 1992).

In the past 10–15 years, a number of models have been developed to describe the motion of maintained volcanic eruption columns. These are summarized and reviewed in the paper by Woods (1988), in which a dynamically consistent model is presented. This steady-state model is based upon the conservation of mass, momentum, and enthalpy, assuming that the column entrains ambient air at a rate proportional to the vertical velocity of the column at any height, following Morton and others (1956). The model incorporates a number of simplifications, which are good approximations in many explosive volcanic eruptions. These include the assumptions that (1) the material in the eruption column behaves as a single-phase, perfect gas, (2) there is little interphase mass or momentum transfer, (3) the system is in thermodynamic equilibrium, and (4) all of the solid material is fine-grained ash and therefore ascends to the top of the column.

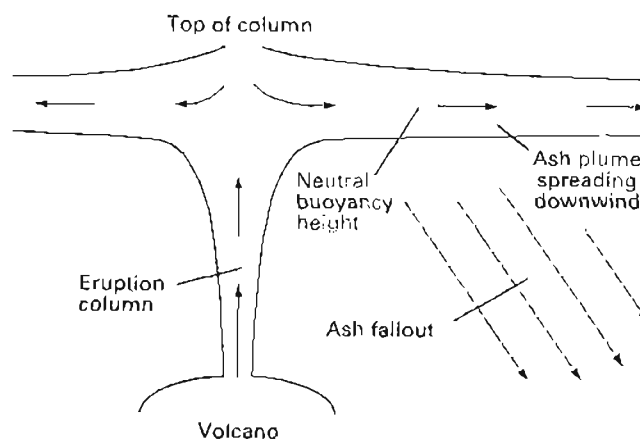


Figure 2. Schematic diagram of eruption column, spreading umbrella cloud, and downwind ash plume. Figure shows location of neutral buoyancy height.

In figure 3, we present a graph, calculated using this model, showing how the total height of rise of the column and the neutral buoyancy height of the column vary with the mass eruption rate for three different initial temperatures. In this graph, it may be seen that the rate of increase of column height decreases once it passes through the tropopause. This is because the temperature begins to increase with height in the stratosphere, causing the atmosphere to become much more stratified. It may also be seen that, because hotter columns generate more buoyancy, they tend to rise higher. Further details of the model are described in Woods (1988).

Woods and Bursik (1991) have extended this model to include the effects of fallout of the larger solid clasts below the top of the column. They showed that, if many of the clasts do fall out (as occurs in eruptions of larger mean grain size), then the eruption column becomes progressively smaller. This is because more of the thermal energy is removed by these solids, and, ultimately, the material in the column has insufficient thermal energy to become buoyant and a collapsed fountain forms. Woods and Wohletz (1991) have shown that the ascent of a co-ignimbrite eruption column rising off a hot ash flow (Sparks and Walker, 1977) may also be described using this model. In this case, the material being supplied to the column originates from a large area; initially it has little upward momentum and is only just buoyant relative to the surrounding ambient atmosphere. However, after entraining more air, the material rapidly expands and becomes buoyant and, as a consequence, accelerates upward. Woods and Wohletz (1991) calculated that the ascent height of these co-ignimbrite columns was much less than that of Plinian columns because, typically, only about one-third of the

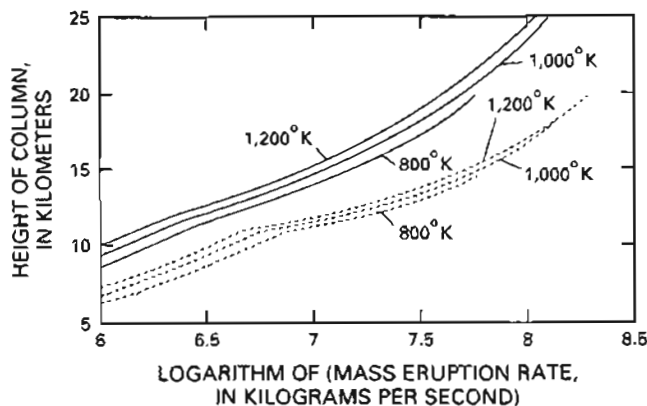


Figure 3. Calculations of neutral buoyancy height (dashed lines) and total column height (solid lines) as a function of erupted mass flux. Curves are given for three eruption temperatures (800°K, 1,000°K, 1,200°K). Calculations are based on the model of Woods (1988) using the standard atmosphere model described therein for which the tropopause is located at 11 km.

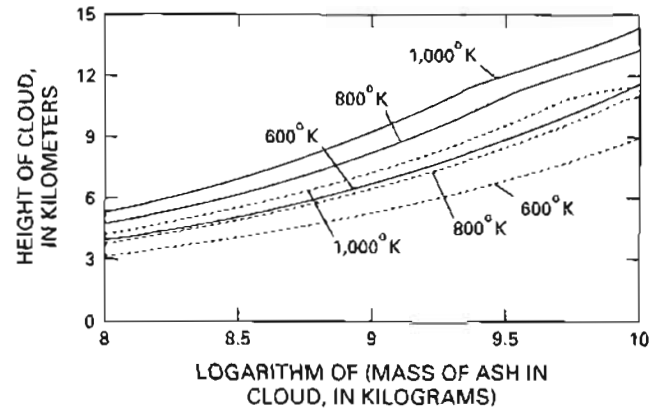


Figure 4. Calculations of neutral buoyancy height (dashed lines) and total cloud height (solid lines) as a function of erupted mass. Curves are given for three eruption temperatures (600°K, 800°K, 1,000°K). Calculations are based on the model of Woods and Kienle (in press) using the standard atmosphere as described in figure 3.

erupted ash and solid material is elutriated from the ash flow into the rising cloud. This reduces the source of thermal energy, which results in ascent of the cloud.

Using a similar approach, Woods and Kienle (in press) have presented a model of the ascent of discrete volcanic clouds. In this model, the discrete cloud is assumed to ascend as a sphere that entrains ambient air and therefore increases in radius as it ascends. The model calculates the altitude and radius of the cloud as well as the average density, temperature, and velocity in the cloud as functions of time. An important difference between the motion of a maintained, steady eruption column and a discrete volcanic thermal cloud is that, as a volcanic thermal rises, there is an additional drag exerted upon the cloud as a result of the air that must be displaced by the rising cloud. This is usually referred to as the virtual mass (Batchelor, 1967) and is incorporated in the model of Woods and Kienle (in press).

In figure 4, we present calculations using this model of the ascent height and neutral buoyancy height of a volcanic thermal cloud, such as that developed following the eruption Redoubt Volcano (fig. 1). We present calculations for three different initial temperatures as a function of the initial mass of the thermal cloud. The results are qualitatively similar to those in figure 3, which describe maintained eruption columns.

TESTING ERUPTION-CLOUD MODELS

Relatively few detailed observations of volcanic eruptions, recording the ascent height of the cloud as a function of time or the velocity in a maintained eruption column as a

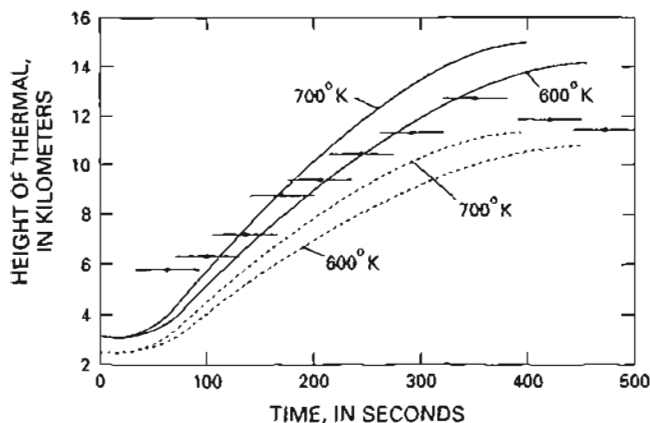


Figure 5. Comparison of observed ascent of the April 15, 1990, Redoubt eruption cloud with the model predictions of the total cloud height (solid lines) and the height of the center of the cloud (dashed lines). Calculations are shown for two initial, model cloud temperatures (600°K and 700°K), which represent bounds on the initial temperature of the cloud (Woods and Kienle, in press). The data were collected by analysis of video recordings of the cloud ascent. Horizontal lines through data points represent error bars.

function of height, have been published; such observations are necessary to test the accuracy of the modeling approach. Sparks and Wilson (1982) tracked several plume fronts rising from the crater of Soufriere St. Vincent and compared this with a model of a starting plume, and Sparks (1986) reported some satellite observations of the ascent of the lateral blast cloud of Mount St. Helens, May 18, 1980, and compared these with the theory of Morton and others (1956). More recently, Woods and Kienle (in press) have reported on some slow-scan video-camera recordings of the rise of the April 15, 1990, eruption cloud of Redoubt Volcano and compared this with a new model of a volcanic thermal.

During the April 15, 1990, eruption of Redoubt Volcano, a hot ash flow was produced from the explosion of a volcanic dome. This ash flow traveled along the ground for 3–4 km, following a natural ice canyon carved in a glacier. As the flow entrained and heated ambient air, the upper part of the flow became buoyant and rose into the atmosphere, forming a large, convecting volcanic thermal cloud. In figure 5, we present a graph showing the observed height of the cloud as a function of time as deduced from the slow-scan video recording. Post-eruption studies of the far-field air-fall (Scott and McGimsey, in press) and near-field flow deposits (C.A. Neal, oral commun., 1991) give estimates for the total mass of material erupted from the volcano during this eruption as approximately 2.5×10^9 kg. Using this data and the conservation of enthalpy in the flow (Sparks, 1986), we estimate that the temperature of the elutriated cloud was 600°K – 700°K , assuming that it was just buoyant on ascent. This data provides the initial conditions for our model of the ascent of the thermal cloud and, in figure 5, we also present

model ascent curves for clouds rising off the flow with temperatures of 600°K and 700°K . In these calculations, we have used meteorological radiosonde data from three stations near Redoubt Volcano taken at about the time of the eruption. It may be seen that the model is able to reproduce most of the features of the buoyant ascent very satisfactorily, especially the time scale of the ascent and the height of rise of the cloud. This gives us confidence in the accuracy, at least in terms of the order of magnitude, of the predictions of these models. Further details of this comparison and the field data are given in Woods and Kienle (in press).

In addition to field observations, some recent controlled laboratory experiments have been able to test aspects of these models (Woods and Caulfield, 1992). There are mixtures of methanol and ethylene glycol (MEG) with density less than that of water that, upon mixing with water, become more dense than water. Therefore, with sufficient initial momentum, a downward-propagating, but light, jet of MEG can entrain and mix with ambient water to become dense and thereby continue propagating downward (in an analogous fashion to a Plinian eruption column) (Woods and Caulfield, 1992). However, a relatively light jet of MEG, with sufficient initial downward momentum, comes to rest before it can mix with sufficient water to become dense; in this case, a collapsed fountain forms and the MEG mixture rises back up around the source. Woods and Caulfield (1992) developed a simple theoretical model of their laboratory experiments based on the same conservation laws as used in the eruption-column model of Woods (1988). The conditions under which experimental column collapse occurs were successfully compared with the model predictions; this further confirms the validity of the underlying physics in the models.

SPREADING UMBRELLA CLOUDS

We now describe the initial spreading of the umbrella cloud once it is emplaced into the atmosphere by the eruption column—the subsequent dispersal and fallout of ash has been described by Bursik and others (1992; this volume). Following injection into the atmosphere by the eruption column, the first stage of ash dispersal consists of the radial gravitational spreading of the cloud toward its neutral buoyancy height. This is the dominant mechanism causing lateral spreading of the ash cloud during the first few minutes after the ash is injected into the atmosphere. However, when the rate of spreading decreases below typical velocities associated with the ambient wind field and ambient turbulence, this gravitational spreading may become of secondary importance in comparison to the wind as an ash-dispersal mechanism. During the May 18, 1980, eruption of Mount St. Helens, the ash plume spread out under gravity from a radius of about 20 km to nearly 50 km in about 10 minutes (Sparks, 1986, fig. 5), whereas the April 21, 1990,

eruption cloud at Redoubt Volcano spread out from a radius of about 6 km to over 15 km in about 10 minutes under gravity before being carried downwind. Woods and Kienle (in press) have described a simple model of the gravitational spreading of an ash cloud following Simpson (1987). In the model, the radial inertia of the cloud balances the gravitational force, which results from the vertical displacement of the air by the cloud. Woods and Kienle (in press) predict that an instantaneously emplaced cloud spreads radially at a rate proportional to $(\text{time})^{1/3}$, and an umbrella cloud continually supplied from below spreads at a rate proportional to $(\text{time})^{2/3}$ until the dispersal becomes dominated by wind. As can be seen in figure 6, this model compares favorably with direct observations from the spreading of the April 21, 1990, eruption cloud of Redoubt Volcano, which was emplaced nearly instantaneously.

CONCLUSIONS

We have described models of both instantaneous and maintained eruption columns. These models are based upon the conservation of mass, momentum, and enthalpy. We have compared our model of a thermal cloud with the observations of the Redoubt Volcano eruption of April 1990. We have also discussed simple models of the radial spreading of the umbrella cloud and have shown that the simple model compares favorably with observations from the April 21, 1990, eruption of Redoubt Volcano. The models have shown that even relatively small eruption clouds can ascend up to tens of kilometers into the atmosphere, causing a serious hazard for aircraft, which typically fly in the troposphere below about 11 km. Once the ash cloud has reached its neutral buoyancy height, the ash may then spread several hundred or even thousands of kilometers before settling from the atmosphere. A particularly important result of the modeling is that the upper surface of an eruption column may actually become tens of degrees colder than the surrounding environment, owing to the inertial overshoot of the erupted mixture above the neutral buoyancy height. This can lead to difficulties in interpreting the height of eruption clouds from thermal satellite images (Woods and Self, 1992). In a companion paper in this volume (Sparks and others, this volume), the models described herein have been used to calculate the ash loading at the top of eruption columns.

REFERENCES CITED

Armienti, P., Macedonio, G., and Pareschi, M.T., 1988, A numerical model for simulation of tephra transport and deposition: Applications to May 18, 1980 Mount St. Helens eruption: *Journal of Geophysical Research*, v. 93, p. 6463–6476.

Batchelor, G.K., 1967, *An Introduction to Fluid Dynamics*: Cambridge, Cambridge University Press, 615 p.

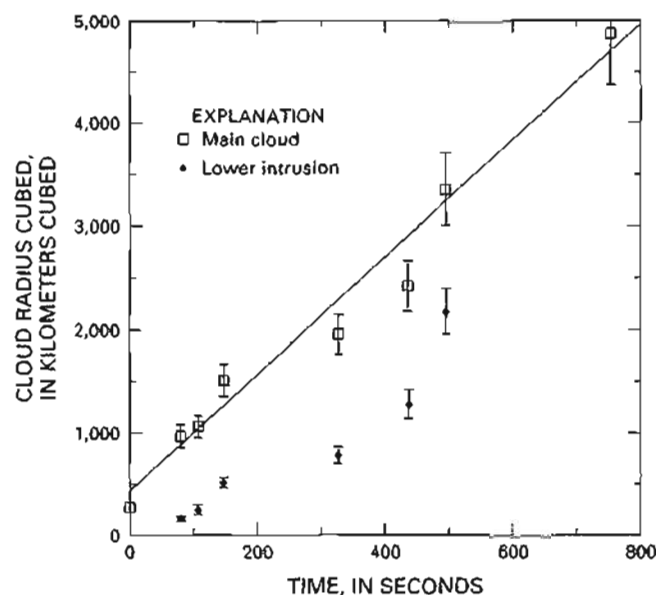


Figure 6. Comparison of observed spread of umbrella cloud that formed following the April 21, 1990, eruption of Redoubt Volcano and a simple model of a radially spreading gravity current, after Woods and Kienle (in press). The graph shows the rate of spread of the main cloud as well as the lower secondary intrusion, which can be seen in figure 1. The data were obtained from analysis of photographs by Mark and Audrey Hodges. Vertical lines through data points indicate error bars.

Bursik, M.I., Sparks, R.S.J., Gilbert, J., and Carey, S., 1992, Dispersal of tephra by volcanic plumes: A study of the Fogo A eruption, Sao Miguel (Azores): *Bulletin of Volcanology*, v. 54, p. 329–344.

Morton, B., Taylor, G. I., and Turner, J. S., 1956, Turbulent gravitational convection from maintained and instantaneous source: *Proceedings of the Royal Society, Series A*, v. 234, p. 1–23.

Scott, W.E., and McGimsey, R.G., in press, Character, mass, distribution, and origin of tephra-fall deposits of the 1989–1990 eruption of Redoubt Volcano, Alaska: *Journal of Volcanology and Geothermal Research*.

Simpson, J., 1987, *Gravity Currents in the Environment and the Laboratory*: Chichester, Ellis Horwood, 244 p.

Sparks, R.S.J., 1986, The dimensions and dynamics of volcanic eruption columns: *Bulletin of Volcanology*, v. 48, p. 1–16.

Sparks, R.S.J., and Walker, G.P.L., 1977, The significance of vitric-rich airfall deposits: *Journal of Volcanology and Geothermal Research*, v. 2, p. 329–341.

Sparks, R.S.J., and Wilson, L., 1982, Explosive volcanic eruptions, V—Observations of plume dynamics during the 1979 Soufriere eruption, St. Vincent: *Geophysical Journal of the Royal Astronomical Society*, v. 69, p. 551–570.

Wilson, L., Sparks, R.S.J., Huang, T.C., and Watkins, N.D., 1978, The control of eruption column heights by eruption energetics and dynamics: *Journal of Geophysical Research*, v. 83, p. 1829–1836.

- Woods, A.W., 1988, The fluid dynamics and thermodynamics of eruption columns: *Bulletin of Volcanology*, v. 50, p. 169–191.
- Woods, A.W., and Bursik, M.I., 1991, Particle fallout, thermal disequilibrium and volcanic plumes: *Bulletin of Volcanology*, v. 53, p. 559–570.
- Woods, A.W., and Caulfield, C.P., 1992, An experimental investigation of explosive volcanic eruptions: *Journal of Geophysical Research*, v. 97, p. 6699–6712.
- Woods, A.W., and Kienle, J., in press, The dynamics and thermodynamics of volcanic clouds: Theory and observations from the April 15 and April 21, 1990 eruptions of Redoubt Volcano, Alaska: *Journal of Volcanology and Geothermal Research*.
- Woods, A.W., and Self, S., 1992, Thermal disequilibrium at the top of volcanic clouds and its effect on estimates of the column height: *Nature*, v. 355, p. 628–630.
- Woods, A.W., and Wohletz, K., 1991, The dimensions and dynamics of coignimbrite eruption columns: *Nature*, v. 350, p. 225–227.

VOLCANIC ASH-AIRCRAFT INCIDENTS IN ALASKA PRIOR TO THE REDOUBT ERUPTION ON 15 DECEMBER 1989

By Juergen Kienle

ABSTRACT

Commercial and military propeller-driven and jet aircraft have encountered airborne volcanic ash in the Cook Inlet region three times prior to the near crash of a Boeing 747-400 jet downwind from Redoubt Volcano on 15 December 1989. Aircraft flew into ash plumes in 1953 when Mt. Spurr erupted and in 1976 and 1986 when Augustine Volcano erupted. Damage to aircraft in all incidents was restricted to severe sandblasting, and no engine failures occurred.

INTRODUCTION

The volcanoes of the Cook Inlet region, Alaska, make up the eastern end of the Aleutian volcanic arc. Air routes connecting Europe and North America with the Far East follow great-circle routes, which parallel much of the volcanic chain. Three volcanoes in Cook Inlet, Mt. Spurr, Redoubt Volcano, and Augustine Volcano (fig. 1), have erupted several times this century for a total of 10 eruptions between 1900 and 1992, or about once every 10 years on average. In recent decades, the eruption rate has almost doubled. Since 1950, Augustine erupted three times, Redoubt twice, and Spurr twice, totaling seven eruptions in the past 43 years or once every 6 years on average. Each eruptive cycle of the three volcanoes produced multiple explosions and associated ash plumes. Iliamna Volcano, located between Redoubt and Augustine Volcanoes (fig. 1), has not had an ash eruption in historic times, although large steam plumes have been reported frequently to the Alaska Volcano Observatory (AVO).

The Alaska Volcano Observatory gives special attention to the four Cook Inlet volcanoes, which are west and southwest of Anchorage (fig. 1). AVO operates remote, continuously recording, radio-telemetered seismic stations on all four Cook Inlet volcanoes and slow-scan television cameras, which are focused on Spurr and Redoubt. For the recent eruptions of Spurr (1992), Redoubt (1989-90), and Augustine (1986), this has allowed scientists to forecast eruptive activity and to give adequate warnings to the

commercial aircraft industry and to the U.S. military, either before or at the onset of explosive, ash-producing eruptions. Because ash is mainly advected by tropospheric winds, plume-path predictions issued in recent years by AVO have been used by carriers to avoid aircraft-ash encounters (Casadevall, in press).

This paper gives a brief description of aircraft-ash incidents over Cook Inlet between 1953 and 1986, before the near-fatal encounter of a Boeing 747-400 jet with a Redoubt ash plume on 15 December 1989.

AIRCRAFT-ASH ENCOUNTERS OVER COOK INLET, 1953-86

MT. SPURR, 1953

On 9 July 1953, at about 17:00 local time, the Crater Peak vent on the southern flank of Mt. Spurr erupted suddenly, without much warning, sending a dark, ash-rich column to a height of 21 km (70,000 ft). Juhle and Coulter (1955) report that the ash cloud, carried by gentle westerly winds, drifted over Anchorage by noon. Heavy ash fall lasted for about 3 hours and darkened the skies so much that the city lights had to be turned on from noon until 15:00. Eventually 3 to 6 mm (1/4 inch) of fine dust settled over the city, including Anchorage Airport and Elmendorf Air Force Base, disrupting air traffic for 2 days.

By chance, the eruption was witnessed at close range by pilots of two U.S. Air Force planes on a reconnaissance mission near the volcano (Juhle and Coulter, 1955; Wilcox, 1959). The following pilots' account is quoted from an Air Force press release of 10 July 1953 (taken from Wilcox, 1959):

At 05h 05m Lieutenant Metzner noticed a column of smoke 60 miles ahead that was about 15,000 ft high and one-eighth mile wide. As he approached the smoke it was apparent that the eruption causing it was becoming increasingly severe with the smoke growing rapidly in height. At about 25 miles distance, the volcano was recognized as the 11,070-foot high Mt. Spurr. Both planes approached the mountain at about 15,000 ft and circled the volcano at about 05h 25m. They noticed the continuing increase in the intensity and size of the column of smoke with lightning flashes through its core every 30 seconds. Smoke issued from the volcano in violent billows at

the 7,000-foot level of the mountain caused by huge subterranean explosions. Tremors on the mountainsides were visible from the aircraft and were followed by snow slides on the mountain. The smoke had by now reached the 30,000-foot level, rolling upward and assuming the shape of the atomic bomb mushroom. Clouds of smoke were every shade of gray from black at the crater to pure white at the top. By this time the width had increased to about a mile at the base and 30 miles at its widest part.

About 05h 40m Lieutenant Metzner climbed in order to estimate the height of the mushroom. The top of the stalk, or the bottom of the mushroom, was 30,000 ft and the top of the mushroom had climbed to 70,000 ft. Lightning was now flashing from top to bottom of the mushroom at three-second intervals.

At about 6h 00m volcanic ash began falling from the mushroom on all sides and finally made the entire area hazy. A clear definition of the volcano and the mushroom rapidly faded and the patrol returned to its base.

Another pilot report confirmed that ash was still being erupted vigorously 4 hours later, at 09:00. The activity declined toward noon but resumed at 15:30; other eruptions took place later that day (Wilcox, 1959). Wilcox further states that, on the next day, 10 July, the vent was only steaming, except for a strong ash-laden surge at 15:30, which rose to 6 km (20,000 ft). Juhle and Coulter were in the field at the volcano from 11 to 14 July and again on 16 July, during which time they observed steam clouds to heights of 6 km, with occasional puffs of black dust (Wilcox, 1959).

One of the two F-94 jet aircraft that were flying near Mt. Spurr on the morning of 9 July flew through the cloud and had its Plexiglas cockpit canopy frosted by the "sand-blasting" action of the ash (Juhle and Coulter, 1955). The following information is summarized from a U.S. Air Force report on the Mt. Spurr eruption (U.S. Air Force, 1955):

During the peak of eruptive activity, three jet aircraft of the 66th Fighter-Interceptor Squadron were dispatched through the ash plume to bring back first-hand, eyewitness accounts of the eruption. [There is a conflict with the report of Juhle and Coulter (1955), which says that only one jet flew through the eruption cloud.] Upon return to Elmendorf AFB, all three jets had sandblasted wing leading edges, windshields, side panels, and front portions of the canopies, greatly reducing pilot visibility. Some panels later had to be replaced.

As a precaution, all aircraft of the U.S. Air Force's 5039th Air Transport Squadron in flyable condition (26 planes) were evacuated to Laird and Eielson Air Force Bases near Fairbanks. However, only four F-94 interceptors were able to engage in the evacuation; loss of power in the dusty air on take-off grounded the other interceptors. These were hangared in time, except for several large C-124 transport aircraft (Globe Trotters). Float-equipped L-28's of the 5th Liaison Squadron were moved from Anchorage to Lake Louise. Wheel-equipped Beavers were placed inside hangars. Two radar stations in the Anchorage area, one on Fire Island, were taken off the air to prevent damage to the antenna drive and generators.

Most seriously affected by the ash fall were the propeller-driven C-124 transport aircraft stored outside, which required 10 days of cleanup to remove the fine volcanic ash from the aircraft. From 9 to 13 July, tactical aircraft were unable to take to the air over Elmendorf because of dusty conditions and remobilized ash on runways and taxiways. The 10th Air Division of the Alaska Air Command lost its ability to meet its air defense mission and it passed the responsibility for fighter interception and radar control to the 11th Air Division at Laird AFB. It was only on 17 July, eight days after the eruption, that the three Elmendorf fighter-interceptor squadrons returned to normal operations. For all practical purposes, Elmendorf AFB was closed to air traffic from 9 to 17 July. The east-west runway was

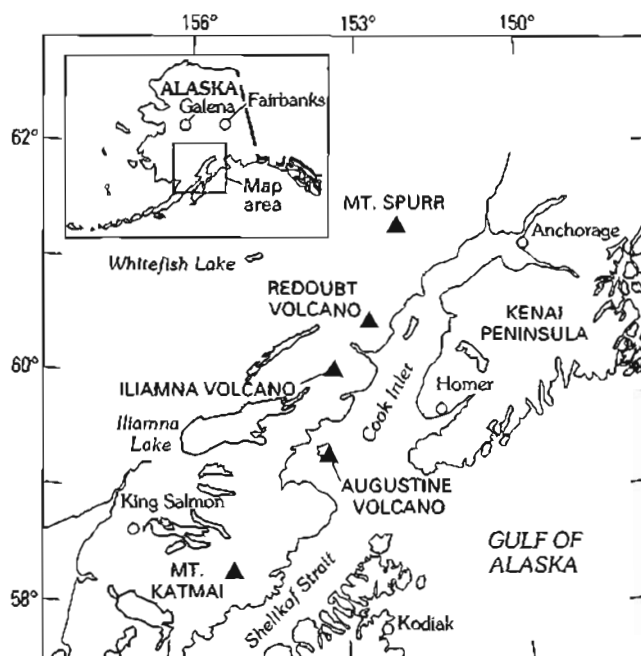


Figure 1. Location of volcanoes in the area of Cook Inlet (solid triangles) and places mentioned in the text. Elmendorf Air Force Base is located near Anchorage.

cleared for emergency flying only. Aircraft landed, but had to immediately cut off engines while on the runway before being towed to the hangar. The reverse procedure was used for emergency takeoffs to reduce exposure of the airplanes to the pervasive dust.

The cleanup operation produced many engineering headaches. The soft, clinging ash first had to be cleared from all aircraft surfaces, taxiways, runways and parking ramps. All moving parts, air intakes, accessory cases, filters and screens required thorough cleaning to prevent corrosion and contamination.

A truck-mounted jet engine, originally designed to remove ice from railroad tracks, proved to be the most useful tool in clearing ash from large swaths of ground; for example, within 40 hours this jet-blower cleared some 440,000 m² of pavement at the Anchorage International Airport.

There are no known records of commercial aircraft being affected by the 9 July eruption of Mt. Spurr. As became clear after encounters between volcanic ash and aircraft at Galunggung, Indonesia, in 1982, and more recently at Redoubt, propeller-driven airplanes that operate at low engine temperatures fare much better than jets in severe, dusty conditions.

AUGUSTINE VOLCANO, 1976

Augustine Volcano, located in lower Cook Inlet (fig. 1), erupted in January 1976 after 12 years of dormancy (fig. 2). Sub-Plinian eruptions occurred from 22 to 26 January and spread ash generally northward and eastward over the Kenai Peninsula, with fine ash falling as far away as Sitka, 1,100 km (684 mi) downwind (Kienle and Shaw, 1979).

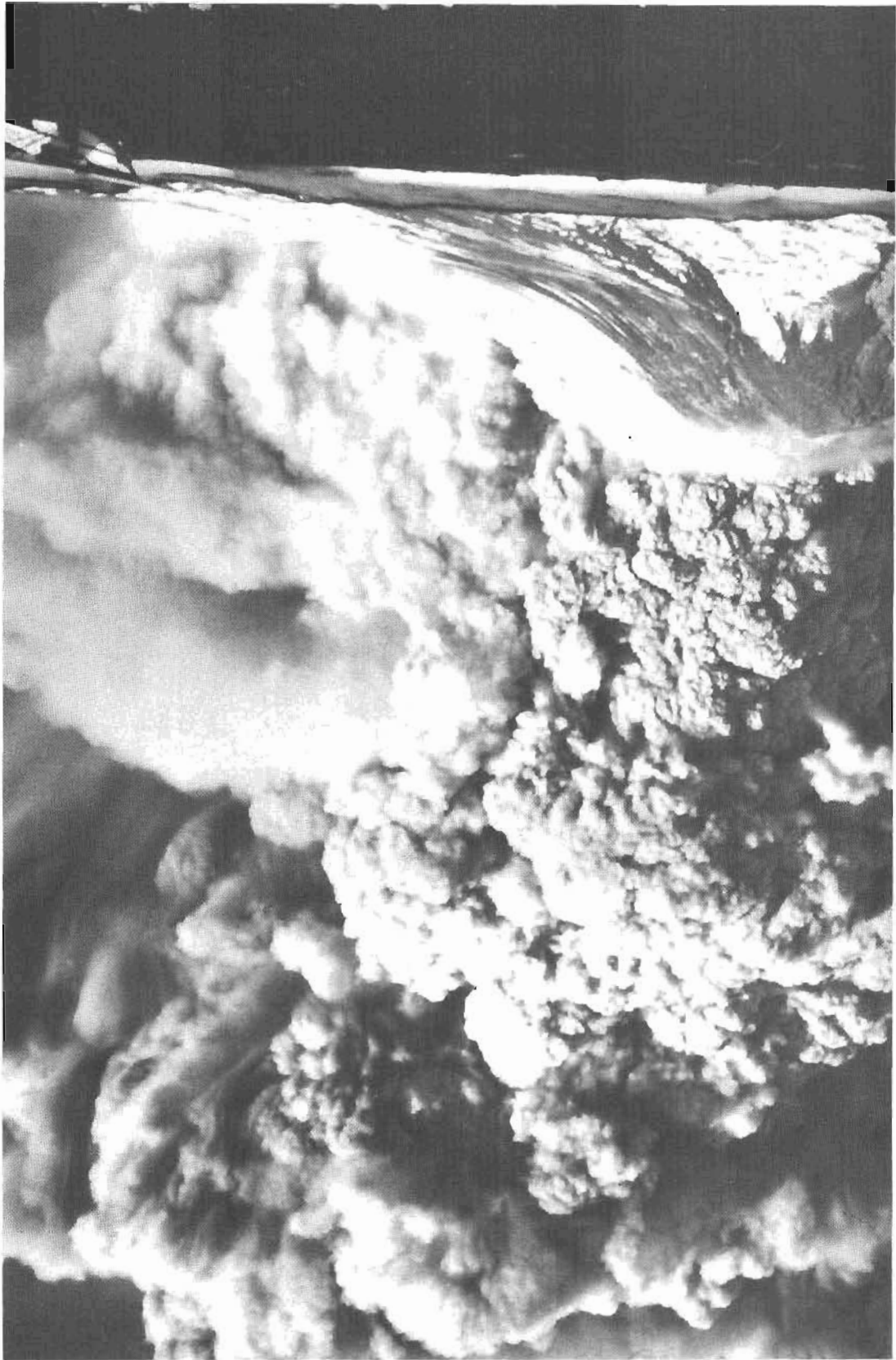


Figure 2. Augustine Volcano in eruption on 6 February 1976. Photograph from the west coast of Augustine Island, courtesy of Gary Gunkel.

One of the 22 January Augustine eruptions occurred in the midst of a U.S. Air Force defense exercise. Reports of greatly reduced visibility were received from pilots in two F-4E Phantom jets flying in formation through an eruption cloud. These observations were used by Kienle and Shaw (1979) to estimate the minimum mass concentration of particulate material contained in that eruption cloud. No mechanical problems or serious power loss were reported by the pilots. The following is an excerpt of a report by the two F-4E Phantom jet pilots who had taken off from Galena, Alaska, on 22 January 1976, heading south for King Salmon (from Kienle and Shaw, 1979; U. S. Air Force, 1976):

The two jets were flying in clouds, cruising at 9 km (31,000 ft). We were still in the weather when suddenly at 14:30 AST the ordinary gray clouds slightly darkened for a moment or two, then there was instant complete darkness. There was no turbulence associated with this darkness. The two jets were flying in close formation about 10 meters apart. Had the lead plane not immediately turned on its lights, the following pilot would have lost contact; he could barely see the lead plane 10 meters away with its lights on. Upon landing in King Salmon, the canopy of the aircraft was seen to be scoured, and the paint at the wing tips was sandblasted off. Very fine, jewelers-rouge-colored material was ingested into the cockpit through the engine air intakes. The material was sticky and was found in every nook and cranny of the planes.

A second incident concerns three Japan Airline jet airplanes en route to Tokyo on the afternoon of 25 January 1976. As recounted by Mr. K. Noguchi of Japan Airlines (Kienle and Shaw, 1979):

After cargo flight JL 672 took off from Anchorage at 16:00 AST, the DC-8 was about to reach its cruising altitude of 10 km (33,000 ft), 25 minutes after takeoff, traveling along air route J-501 when it suddenly encountered an ash cloud near Whitefish Lake (25 km southeast of Sparrevohn). Upon landing in Tokyo the scoured center windshield had to be replaced. Much ash had adhered to the plane and slight abrasion damage was found on external radio parts, landing gears and the air-conditioning system, but none of these parts needed to be replaced.

Two other passenger planes, a Boeing 747 and a DC-8, also bound for Tokyo and departing within 1 hour after flight JL 672, reported ash suddenly adhering to the planes at cruising altitude (about 10 km) near Sparrevohn, which also caused minor damage but not as extensive as that to the DC-8 flight JL 672.

Kienle and Swanson (1985), in a report on volcanic hazards for Augustine Volcano, discussed the hazard of volcanic ash to aircraft and delineated very high risk, high-risk, moderate, and low-risk hazard zones in the vicinity of Augustine Island.

AUGUSTINE VOLCANO, 1986

Augustine erupted again in 1986, with strong eruptive activity concentrated in the period between 27 and 31 March. The sequence of events was similar to the 1976 eruption, with an initial, highly explosive vent-opening phase lasting 4 days, followed later in the year by less explosive activity associated with the extrusion of a new lava dome (Swanson

and Kienle, 1988). The eruptive cycle ended in September 1986, but from April on, the eruption did not present a substantial hazard to aircraft.

During the March 1986 eruption of Augustine Volcano, airborne ash again presented a hazard to aircraft operations throughout the Cook Inlet basin and to airports in Anchorage because of predominantly southerly winds (Yount and others, 1987). The eruption was anticipated by Alaskan volcanologists (Kienle and others, 1986; Kienle, 1986), and T. Miller and M. E. Yount of the U.S. Geological Survey office in Anchorage held briefings with the Federal Aviation Administration (FAA) and the U.S. Air Force on 18 March 1986, 9 days prior to the eruption, to warn about the possibility of an eruption and the consequences to aircraft operations.

Early on the morning of 27 March 1986, just after the eruption had begun, the U.S. Air Force evacuated planes from Anchorage and kept them away until 30 March. Even though the Anchorage International Airport was never officially closed during the most explosive phase of the eruption, most commercial carriers either canceled or diverted their Anchorage flights between 27 and 29 March.

The following is a summary taken from Aviation Week and Space Technology (1986):

From March 27 to 29, air carrier service to Anchorage was nearly at a standstill. Subsequently, the wind shifted to a northerly direction carrying the ash away from the Cook Inlet bowl, now affecting the airline traffic between Anchorage and airports at Kodiak and King Salmon. Volcanic ash generally stayed below 15,000 ft (4.5 km) but a stronger eruption on March 31 sent an ash plume up to 30,000 ft (9 km).

Alaska Airlines had its worst day on 28 March, when it canceled 40 out of 68 Anchorage arrivals and departures. Twenty-seven to 29 March, the Anchorage stop of the airline's Seattle-Anchorage-Fairbanks flights, coming and going, were deleted. Western Airlines canceled all of its flights to and from Alaska 27-28 March and flew some flights on 29 March. United Airlines, Northwest Airlines and other international carriers that fly from Europe and Far East Asia over the North Pole canceled service during the worst ash conditions. United canceled 35 flights between 27 and 29 March. Local commuter airplane traffic between Anchorage and the Kenai Peninsula also was largely shut down and the Federal Aviation Agency [sic] (FAA) temporarily shut down its air-route surveillance radar at Kenai for two days. With shifting winds on 31 March 1986, ash was cleared from the air over most of the Cook Inlet basin, and normal air operations resumed.

CONCLUSIONS

A comparison of the eruptions of these volcanoes demonstrates that, as we learn to live with the high activity level of Cook Inlet volcanoes, we improve our ability to cope with the problem of volcanic ash and aviation safety. Air traffic has increased dramatically in Alaska since the eruption of Mt. Spurr in 1953. High-bypass, turbine-powered jet aircraft have replaced larger, propeller-driven passenger planes; both factors increase the risk of danger from encountering airborne volcanic ash. On the other hand, the volcanological community in Alaska has come together since 1953. The 1953 Mt. Spurr eruption caught everyone off-guard, but we

were better prepared in 1976 and 1986 for the Augustine eruptions, having instrumented that volcano with radio-telemetered seismographs starting in 1970. In 1986, briefings with the aviation community were held by U.S. Geological Survey volcanologists 9 days prior to the onset of the eruption that paralyzed air traffic in Cook Inlet for 4 days. Significantly, there were no encounters of aircraft, either private or military, with volcanic ash during the most vigorous phase of the 1986 Augustine eruption.

The close cooperation among volcanologists of the U.S. Geological Survey, the Alaska Geological Survey, and the University of Alaska, Fairbanks, that had developed during the 1986 Augustine eruption was formalized in March 1986 with the founding of the Alaska Volcano Observatory. Since then, AVO has instrumented all four Cook Inlet volcanoes with at least four seismometers at each volcano. In addition, remotely controlled slow-scan television cameras have been installed to continuously observe Mt. Spurr and Redoubt Volcano, and we have plans to do the same for Augustine Volcano. Satellite surveillance of the volcanoes and eruptive plumes has become routine at the AVO laboratory in Fairbanks (Dean and others, this volume), and an array of lightning detectors can track electrified plumes in Cook Inlet. Radars and television cameras have been used to track rising eruption columns and their dispersal by wind.

During the two recent eruptions in Cook Inlet at Redoubt Volcano (1989–90) and at Mt. Spurr (1992), AVO went on 24-hour watches for several months. Communication with the carriers and Federal agencies involved with air traffic (Federal Aviation Administration, National Weather Service) were increased and resulted in the production of daily updates on the status of the active volcano and the forecasting of potential plume trajectories every 6 hours (or more often during active phases of ongoing eruptions) (Murray and others, this volume).

In spite of the better level of preparedness in recent years, there was a near fatal encounter of a Boeing 747-400 with an ash plume of Redoubt Volcano on 15 December 1989 (Casadevall, in press). The aviation and volcanology communities in Alaska must jointly strive to avoid any other encounters of this type.

ACKNOWLEDGMENTS

I thank Tina Neal and one anonymous reviewer for their constructive editing of the original draft. This work was supported by the Alaskan Volcano Observatory through U.S. Geological Survey Grant 14-08-0001-0574.

REFERENCES CITED

- Aviation Week and Space Technology, 1986, Alaska air traffic disrupted by ash from volcano: v. 124, no. 14, p. 36.
- Casadevall, T.J., in press, The 1989–1990 Eruption of Redoubt Volcano, Alaska: Impacts on aircraft operations: *Journal of Volcanology and Geothermal Research*.
- Juhle, W., and Coulter, H.W., 1955, The Mt. Spurr eruption, July 9, 1953: *Transactions of the American Geophysical Union*, v. 36, p. 188–202.
- Kienle, J., 1986, Augustine Volcano: Awake again?: *Eos, Transactions of the American Geophysical Union*, v. 67, p. 172–173.
- Kienle, J., Davies, J.N., Miller, T.P., and Yount, M.E., 1986, The 1986 eruption of Augustine Volcano: Public safety response by Alaskan volcanologists: *Eos, Transactions of the American Geophysical Union*, v. 67, p. 580–582.
- Kienle, J., and Shaw, G.E., 1979, Plume dynamics, thermal energy, and long distance transport of Vulcanian eruption clouds from Augustine Volcano, Alaska: *Journal of Volcanology and Geothermal Resources*, v. 6, p. 139–164.
- Kienle, J., and Swanson, S.E., 1985, Volcanic hazards from future eruptions of Augustine Volcano, Alaska: University of Alaska Geophysical Institute, Report UAG R-275, 122 p.
- Swanson, S.E., and Kienle, J., 1988, The 1986 eruption of Mt. St. Augustine: Field test of a hazard evaluation: *Journal of Geophysical Research*, v. 93, p. 4500–4520.
- U.S. Air Force, 1955, History of the Alaskan Air Command, Part 2, natural phenomenon, Mt. Spurr eruption: Anchorage, Alaska Air Command, Elmendorf Air Force Base, p. 73–80.
- , 1976, History of the 21st composite wing: Anchorage, Alaska Air Command, Elmendorf Air Force Base, v. 1, 121 p.
- Wilcox, R.E., 1959, Some effects of recent volcanic ash falls with especial reference to Alaska: *U.S. Geological Survey Bulletin* 1028-N, p. 409–476.
- Yount, M.E., Miller, T.M., and Gamble, B.M., 1987, The 1986 eruption of Augustine Volcano, Alaska: Hazards and effects: *U.S. Geological Survey Circular* 998, p. 4–13.

IMPACT OF VOLCANIC ASH FROM 15 DECEMBER 1989 REDOUBT VOLCANO ERUPTION ON GE CF6-80C2 TURBOFAN ENGINES

By Zygmunt J. Przedpelski and Thomas J. Casadevall

ABSTRACT

The 1989–90 eruptions of Redoubt Volcano, Alaska, and the near tragedy on 15 December 1989 of KLM flight 867, a Boeing 747-400 aircraft powered by General Electric (GE) CF6-80C2 engines, underscore the threat to aircraft safety from volcanic ash clouds.

An eruption of Redoubt at 10:15 a.m. Alaska Standard Time (AST) produced an ash-rich eruption column that climbed to approximately 40,000 ft altitude. Wind speeds at high altitudes at the time were 100 knots from south-southwest. At 11:46 a.m., KLM flight 867 entered the volcanic ash cloud at approximately 25,000 ft altitude, 150 nautical miles northeast of Redoubt. Immediately the aircrew increased power and attempted to climb out of the ash cloud. Within 1 minute, the four engines decelerated below idle. The aircraft descended approximately 13,000 ft before the crew restarted the four engines and resumed flight to Anchorage. Even though there were no injuries to passengers, the damage to engines, avionics, and aircraft structure from this encounter was significant. Similar engine thrust loss and engine and aircraft damage was experienced by two Boeing 747 aircraft during 1982 volcanic eruptions of Galunggung Volcano in Indonesia.

The primary cause of engine thrust loss in these events was the accumulation of melted and resolidified ash on the stage-1-turbine nozzle guide vanes. These deposits reduced the effective flow of air through the engine causing compressor stall. Reduction of thrust level while in an ash cloud significantly reduces the rate of engine-performance degradation.

STATEMENT OF PROBLEM

The loss of thrust on all engines during an approximately 1-minute exposure to the Redoubt volcanic ash cloud could have resulted in a major tragedy. Fortunately the alert flight crew was able to restart all engines and make a safe landing at Anchorage. The events preceding and subsequent to the cloud encounter and the engines' response and physical conditions were analyzed to identify

procedures that would reduce the probability of future occurrences of similar events, which threaten flight safety. Additional discussion of the Redoubt activity and its effects on aircraft operations and airplane damage may be found in reports by Brantley (1990), Campbell (1991), Casadevall (in press), and Steenblik (1990).

METHODS OF STUDY

The following data sources were used to reconstruct the event, to establish the specific cause(s) of thrust loss and to recommend appropriate preventive/corrective actions:

- Interviews with and statements from the flight crew of KLM flight 867.
- Tape recordings and transcripts of radio communications between air traffic controllers and KLM flight 867 and other flights in the Anchorage area prior to and during the event.
- Forecasted and recorded wind aloft data.
- Digital flight-data recorder (DFDR), aircraft condition monitoring systems (ACMS), and the non-volatile memory (NVM) of the engine full-authority digital electronic controls (FADEC).
- Event descriptions and findings from other aircraft-volcanic cloud encounters.
- CF6-80C2 engine steady-state and transient operating characteristics with normal and degraded component efficiencies.
- On-site (Anchorage) external inspection of the aircraft and all engines and borescope inspection of engines 1 and 2.
- Complete analytical disassembly and inspection of engine 1 at the KLM maintenance facility at Schiphol Airport, Amsterdam.
- General Electric experience with engines exposed to sand/dust environment in the field and during controlled factory tests.
- Analysis of samples of volcanic ash recovered from the four engines.

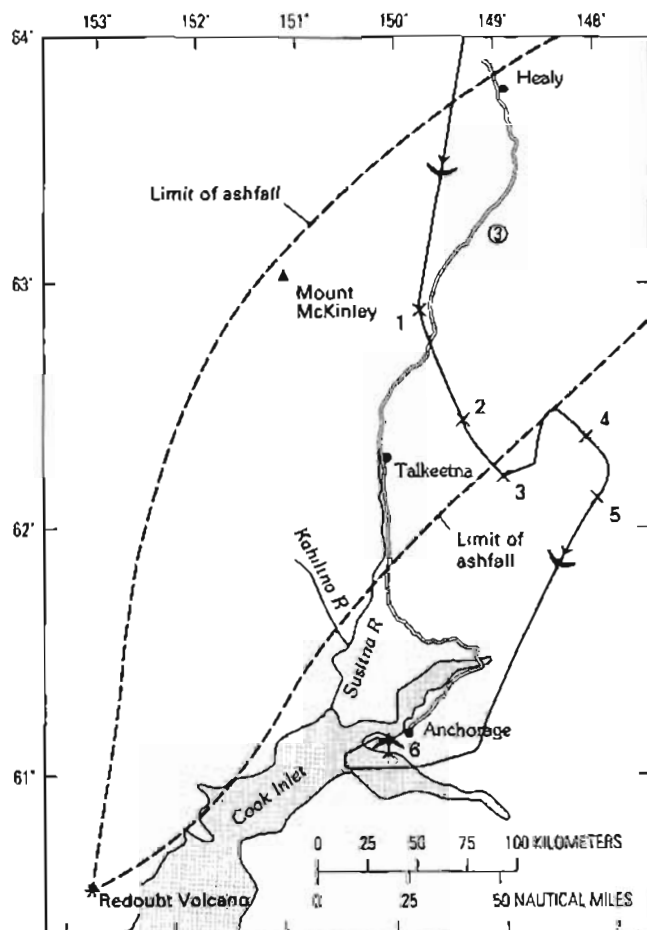


Figure 1. Map showing flight path of KLM 867 (heavy solid line) and limits of detectable ash fall (heavy dashed lines) from 15 December 1989 eruption of Redoubt Volcano. Numbers on map, explained below, are keyed to principal events for KLM flight 867. AST, Alaska Standard Time. 1, 11:40 AST, airplane begins descent from 35,000 ft; alters course to avoid ash cloud. 2, 11:46 AST, airplane encounters ash cloud at 25,000 ft. 3, 11:47 AST, airplane loses power on all four engines after climbing to 27,900 ft. 4, 11:52 AST, airplane engines 1 and 2 restart at 17,200 ft. 5, 11:55 AST, airplane engines 3 and 4 restart at 13,300 ft; flight is resumed to Anchorage. 6, 12:25 AST, airplane lands at Anchorage International Airport. Map modified from Casadevall (in press). Flight-route data provided by National Transportation Safety Board (1991) and FAA Flight Standard Division, Anchorage. Ash-fall data modified from Scott and McGimsey (in press).

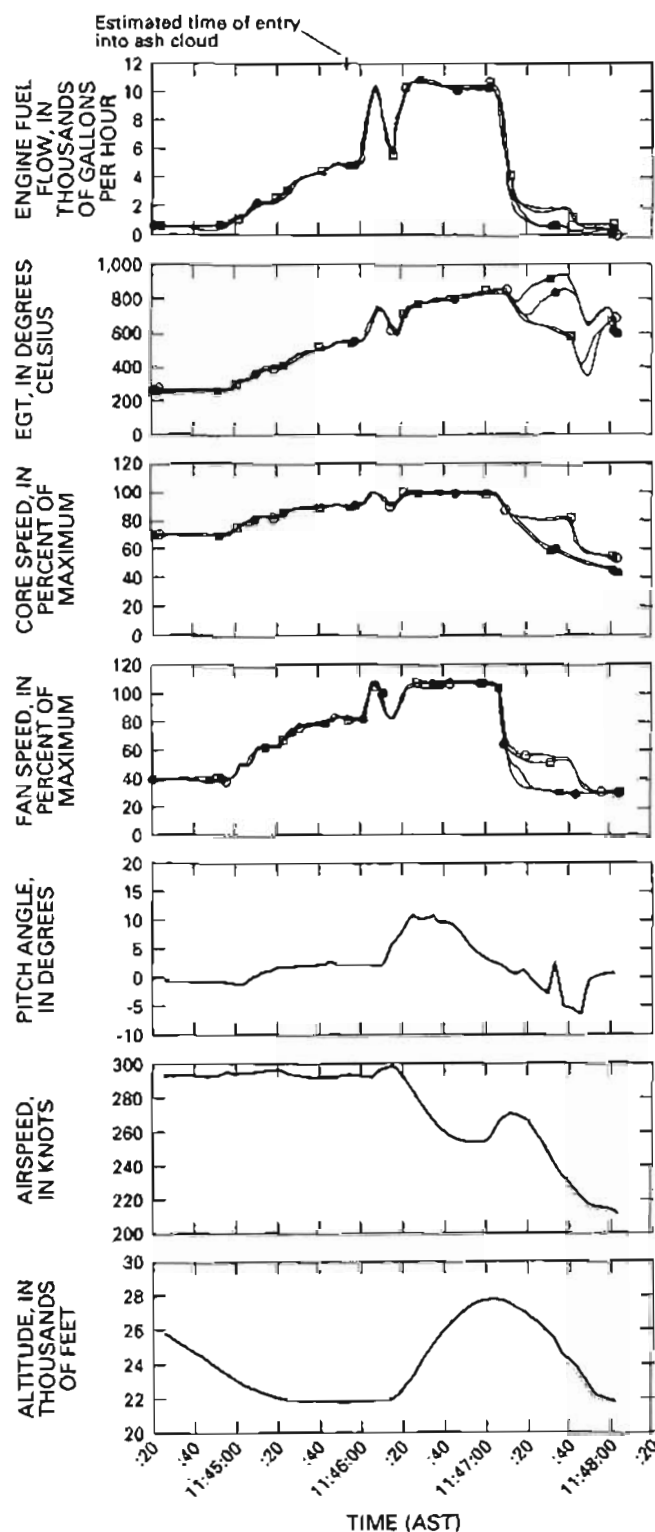


Figure 2 (facing column). Encounter of KLM flight 867 with ash from Redoubt Volcano, 15 December 1989: engine and aircraft parameters (engine fuel flow, exhaust-gas temperature (EGT), core speed (N2), fan speed (N1), pitch angle, airspeed, and altitude) from cloud entry to shutdown. AST, Alaska Standard Time.

EXPLANATION

- Engine 1 ● Engine 3
- Engine 2 ○ Engine 4

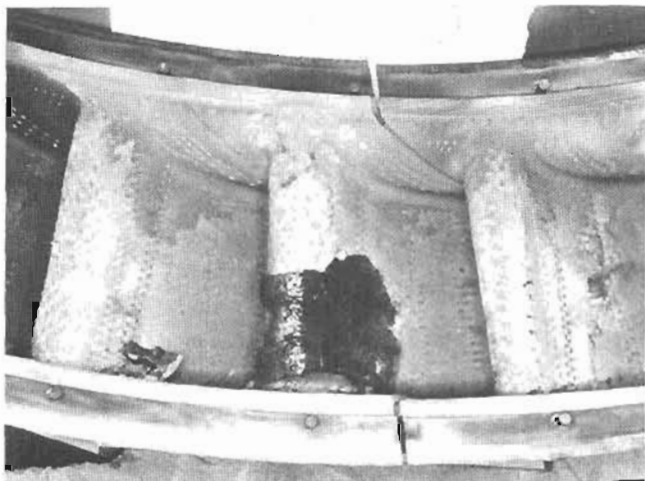


Figure 3. Dark, glassy deposits of remelted volcanic ash on leading edge of stage-1 high-pressure-turbine (HPT) nozzle guide vane (NGV).

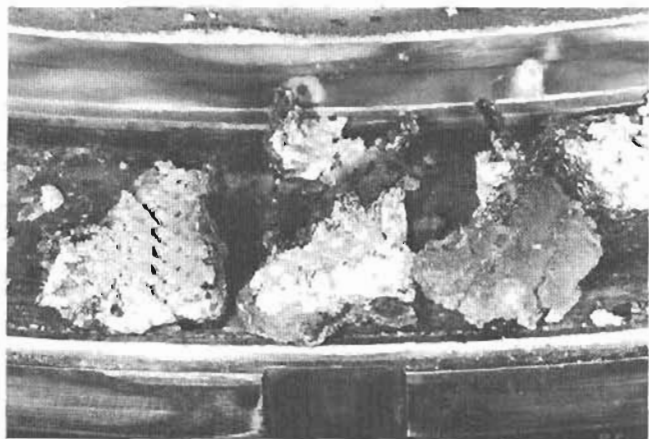


Figure 4. Leading-edge deposits dislodged during disassembly of stage-1 high-pressure-turbine (HPT) nozzle guide vanes (NGV's).

RESULTS AND OBSERVATIONS

A major eruption of Redoubt Volcano occurred at 10:15 a.m. AST on 15 December 1989 and lasted for about 1 hour. This was the third large eruption from the volcano on this day (Brantley, 1990). At 11:46 a.m. AST, while leveling off at an altitude of 25,000 ft, KLM 867 entered a heavy volcanic cloud. Maximum power climb was selected and approximately 1 minute later, after climbing to approximately 27,900 ft, all engines decelerated. Engines 1 and 3 decelerated to sub-idle core rotor speed (N2), while engines 2 and 4 settled down at 80 percent N2 for approximately 20 seconds before decelerating to sub-idle N2. The time sequence of events is shown on the annotated aircraft flight path in figure 1. Aircraft and engine response during this critical period is shown in figure 2.

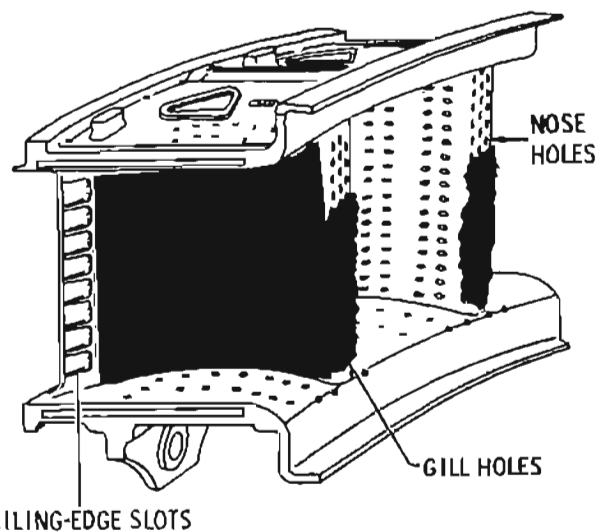


Figure 5. Sketch of deposits on stage-1 HPT nozzle guide vanes, based on borescope inspection of engine 1.

The location of the ash cloud (154 nautical miles from Redoubt on 217° true heading) was consistent with the forecasted and pilot-reported winds aloft and with the ash release at the beginning of the eruption cycle. Prior to the encounter, the exact location of this cloud was not known by the crew of KLM 867. Pilot reports (Pireps) and radar data available to Anchorage air traffic controllers indicated either the presence of more than one ash cloud and (or) a large dispersion of the main cloud resulting from the high velocity gradient of winds aloft as a function of altitude.

The fire warning bell and the displayed message "CARGO FIRE FWD" occurred shortly after engine deceleration and was interpreted by the Captain to be a false message. This was confirmed by inspection, which showed no evidence of compartment fire.

The engines' operation during the high-power climb was consistent with rapid reduction of the stage-1 nozzle guide vane (NGV) flow area and associated reduction in high-pressure-turbine (HPT) efficiency. Approximately one-half of the maximum deterioration was still present following the successful restarts. Visual inspection of the number 1 engine revealed thick deposits of melted and resolidified ash material on some of the stage-1 NGV's (fig. 3). These deposits were brittle at room temperature, and many pieces fell off during engine transportation and disassembly (fig. 4). The remaining deposits could be easily removed by hand. It was inferred that these deposits built up to maximum just prior to engine deceleration and gradually became dislodged during the start attempts and during subsequent engine operation. Based on borescope inspections conducted at Anchorage, approximately 40 percent of the NGV's were still covered by thick deposits after landing (fig. 5).

Engine fuel levers were moved to the "OFF" position and engine restarts were initiated immediately after the loss



Figure 6. Accumulation of unmelted volcanic ash in the high-pressure-turbine rotor.

of power. Engines 1 and 2 were successfully started at an altitude of 17,200 ft (after five or six attempts). Engines 3 and 4 were successfully started at an altitude of 13,300 ft (after eight or nine attempts). "Autostart" mode was used and at least one start appeared to have been correctly terminated by the FADEC start/stall logic just before being terminated by the crew. The windmilling N2 was in excess of 30 percent, and the entire start sequence varied from approximately 30 seconds to 60 seconds during each attempt.

The engines did not overheat during deceleration or during subsequent aborted starts. The highest exhaust-gas temperature (EGT) of 930°C was recorded on engine 1 during the initial deceleration. There was no unusual thermal distress observed during disassembly of this engine.

The general condition of all hardware in engine 1 was consistent with the performance level recorded prior to landing. In addition to the remains of the heavy, stage-1 nozzle deposits, the following performance-related observations were made:

- No measurable erosion or other damage to the low-pressure system (fan, booster, and low-pressure turbine (LPT)).
- Minor compressor erosion, most pronounced in the mid and aft rotating stages.
- Stage-1 high-pressure-turbine (HPT) blade tips were "ground off" (approximately 0.060 inches of tip material was missing).
- Buildup of hard material on stage-1 HPT shrouds.
- Thin but hard deposits on stage-1 HPT blade pressure surfaces.
- Engine 1 inspection indicated that there was no significant plugging of any of the HPT cooling circuits; however, there was a heavy, fine, powdery ash buildup within the HPT rotor cavities (fig. 6).

The general physical conditions (distress and presence of ash deposit) of all four engines were very similar. The compressor-discharge-pressure (P_{S3}) sensing line on engine 1 was unobstructed. The P_{S3} readings obtained from the ACMS system during and after the deceleration indicated that P_{S3} signals to the engine electronic controls were unrestricted. The DFDR was not recording for 2 minutes 5 seconds after the initial engine deceleration when all four electrical generators dropped off line. The engine FADEC remained powered and was controlling the engines during that time and provided valuable information stored in the NVM.

CONCLUSIONS

SPECIFIC

Engine deceleration from high power to below idle was initiated by high-pressure-compressor (HPC) stall. The stall margin loss was caused by stage-1 HPT nozzle effective-flow-area restriction and associated HPT efficiency loss. The stage-1 HPT bucket-clearance increase was caused by local buildup of hard, resolidified ash material on the shroud surface (fig. 7), which ground off the bucket-tip material.

The stage-1 nozzle effective-flow-area restriction was caused by resolidification and buildup of melted ash particles on the leading edges and pressure surfaces of the individual NGV's. This effective-flow-area restriction was estimated to be 8 percent. This buildup also resulted in an increase in pressure loss across the nozzle and a reduction in HPT efficiency. Total HPT efficiency loss, including the stage-1 HPT blade-clearance increase was estimated to be 7 percent. High-pressure-compressor (HPC) erosion (fig. 8), caused by ingestion of ash particles, resulted in minor stall-margin decrease and compressor-efficiency loss estimated to be 1 percent.

The lowering of the temperature following manual fuel supply cut-off increased the viscosity and brittleness of the built-up material. The thermal and pressure/velocity transients associated with the fuel off/on/off cycle dislodged some of the nozzle deposits. The density of these deposits was low, and, consequently, there was no downstream airfoil

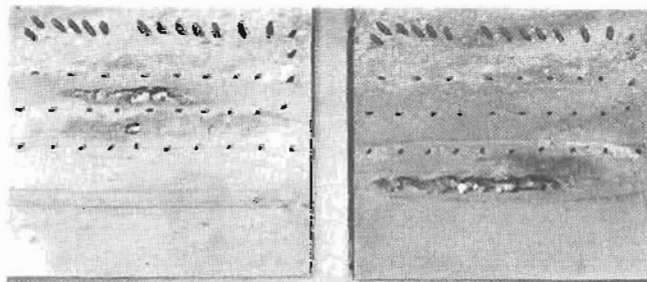


Figure 7. Deposits of solidified, remelted ash on stage-1 high-pressure-turbine shrouds.

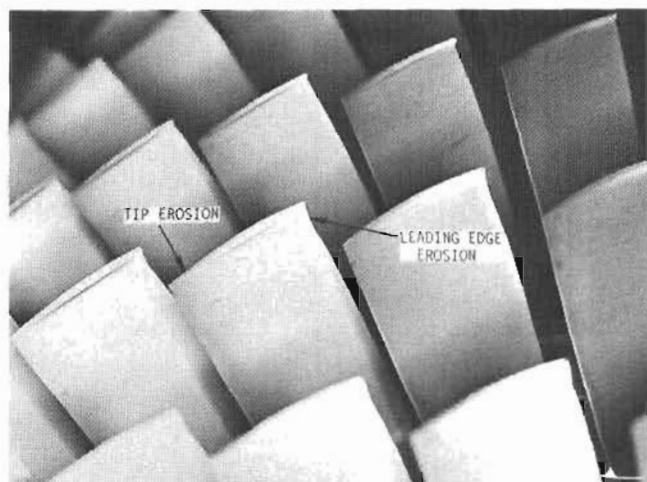


Figure 8. High-pressure-compressor (HPC) blades, showing erosion of leading edges and blade tips.

damage. Successful starts were achieved after a portion of these deposits were dislodged.

During the starts, "autostart" mode was used and at least one start appeared to have been correctly terminated by the FADEC start/stall logic. Most of the starts, however, were terminated by the crew overriding the autostart sequence and thus negating the adaptive automatic restart features of the control system while, in some of these cases, the engine or engines appeared to be on the way to a successful start (fig. 9). Continued engine operation, following successful restarts, dislodged additional stage-1 deposits. Permanent engine performance degradation was the result of compressor erosion and the stage-1 HPT blade-clearance increase.

The absence of any thermal damage to the engines was the result of the combination of decisive and skillful actions of the crew and the responsiveness and built-in protection in the FADEC system.

The presence of ash particles set off the fire warning bell in the cargo compartment and displayed the "CARGO FIRE FWD" message (the cargo-compartment fire detector is a smoke/particle detector—unlike the engine-compartment detector, which is activated by temperature).

The ash concentration at 25,000 ft altitude was estimated at 2 g/m^3 , based on the rate of nozzle-deposit buildup compared to the rates measured during engine tests conducted by Calspan (Dunn and Wade, this volume).

Ash particles exiting the fan air stream ranged in size from 10 to 100 microns and most closely represent the size of particles encountered by KLM 867 in flight. The particles found within HPT passages, which were believed to be representative of the size distribution entering the combustor, were typically 6–10 microns in size. The ash contained some volcanic-glass material with a melting point of $1,200^\circ\text{C}$. This material is considered to be responsible for rapid buildup of deposits on the stage-1 NGV's; however, components of the

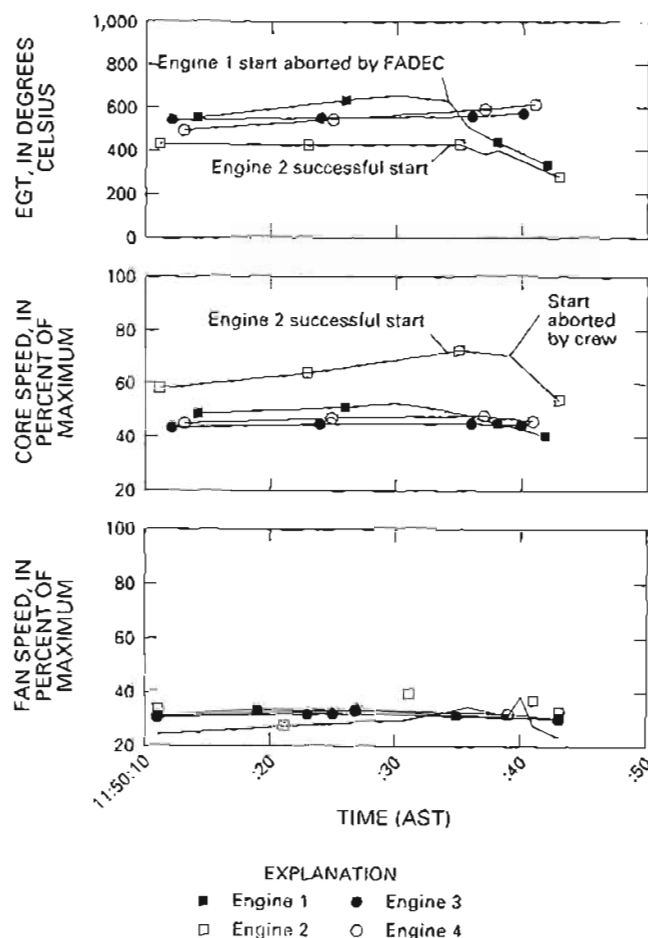


Figure 9. Encounter of KLM flight 867 with ash from Redoubt Volcano, 15 December 1989: engine parameters (exhaust-gas temperature (EGT), core speed (N2), and fan speed (N1)) during first recorded restart attempt. AST, Alaska Standard Time; FADEC, full-authority digital electronic controls.

ash with higher and lower melting points were also present in the NGV deposits. The unmelted particles adhered to the semi-molten layer of glassy material on stage-1 NGV's (Casadevall and others, 1991).

GENERAL

Relatively "new" (within hours of eruption) volcanic clouds contain concentrations of ash that can cause complete loss of engine power in approximately 1 minute when the engine is operating at combustor-discharge temperatures in excess of the melting temperature of the ash. The primary mechanism of engine power loss during these high-engine-power and high-ash-concentration exposures is the buildup of melted and resolidified ash material on the stage-1 NGV's, resulting in flow-area reduction, turbine-efficiency loss, and compressor stall. Permanent damage to the engine under these conditions is limited if the engine is

not exposed to overtemperature during the stall or subsequent restart attempt(s).

Time, altitude, and airspeed permitting, the engine can be restarted by the fuel off/on/off cycles, breaking up the deposit material, which is brittle at low temperatures. FADEC with built-in start/stall/overtemperature logic in the autostart mode simplifies and speeds up the restart sequence and prevents further engine damage.

Reduction of engine power to flight idle upon inadvertent entry into a volcanic cloud will eliminate the stage-1 NGV buildup because the combustor-discharge temperature at idle is below the melting point of volcanic-ash constituents.

Operation in an ash cloud will result in compressor airfoil and flowpath erosion and eventual compressor stall. Compressor stall is an airflow discontinuity resulting in loss of thrust and internal temperature increase. The time required to reach this condition is at least an order of magnitude longer than the time to produce significant ash accumulation on the NGV's at the high-power level (assuming the same ash concentration). Compressor erosion is permanent, and engine operability and available thrust will be adversely affected. The compressor-erosion rate can be significantly reduced by decreasing the core engine rotational speed (N2).

Damage mechanisms in the longer term include the restriction of HPT cooling circuits, which may result in hot-section distress, and the contamination of the lubrication system, which may result in premature bearing distress. Another possible damage mechanism is the restriction of air-flow passages around the fuel nozzles—this leads to poor fuel atomization and the inability to start the engine.

SAFETY RECOMMENDATIONS

CREW ACTIONS

Entering into a volcanic ash cloud can be recognized by St. Elmo's Fire/corona discharge (night or day), dust and smell in the cockpit/cabin, and outside darkness (day time only) (Campbell, this volume). If a volcanic ash cloud is inadvertently entered, disconnect the autothrottle, reduce power to flight idle, increase compressor air bleed to maximum possible, and exit the cloud as quickly as possible. Bleed air is air extracted from the compressor for use in various aircraft systems. Increased extraction increases stall margin. There is no universal "best" procedure for exiting the cloud; however, generally a 180° turn will result in the fastest cloud exit. Avoid rapid throttle movements (up or down) to prevent a possible compressor stall (Campbell, this volume; Müller, this volume).

If power reduction to flight idle is not possible, reduce power to the lowest level consistent with other requirements and exit the cloud as quickly as possible. Monitor exhaust-gas temperature as the primary engine instrument indicating ash accumulation at the stage-1 high-pressure-turbine nozzle

guide vanes. If EGT exceeds the red line or increases rapidly, the throttle should be closed and fuel levers moved to "OFF" to minimize engine thermal damage and increase the probability of successful restart.

Restarts should be initiated immediately. More than one attempt may be required to obtain a successful start. Autostart should be used (if available) because it simplifies the starting procedure and provides engine overtemperature protection. Compressor bleed should be turned on during restarts and during subsequent engine operation to maximize stall margin. Following restart, the engine performance/stall margin/EGT may improve with time, but it will not reach the pre-ash-encounter level. Rapid throttle movement and maximum-power operation should be avoided, if possible, because stall margin is decreased and some cooling-circuit plugging may be present.

REGULATORY AGENCIES

The greatest threat to aircraft and engines is presented by "new" clouds (within hours of eruption) that contain large concentrations of ash particles. The communication network between volcanic-activity-monitoring agencies and air-traffic-control agencies should be improved so that volcanic activity of the type that can result in substantial release of ash into the atmosphere can be communicated immediately to the affected air crews. In early phases following the eruption, the cloud position should be continuously tracked at all altitudes utilizing winds aloft, pilot reports, and other available means. Appropriate air-traffic-control measures should be taken to provide aircraft-cloud separation.

The ash-particle size distribution and concentration in volcanic eruption clouds should be documented. In addition, engine and (or) combustor tests should be sponsored by the Federal Aviation Administration (FAA) to establish threshold values for "safe" levels of ash concentration and the "safe" range of combustor temperature. This information, combined with updated dispersion and theoretical fallout models (and with improved cloud tracking) can establish when an ash cloud ceases to be a flight hazard. These efforts will enhance aviation safety and reduce air traffic delays resulting from volcanic activity.

ACKNOWLEDGMENTS

During this investigation, many GE engineers contributed to the hardware reviews and engineering analysis. The following individuals, outside the GE organization, provided background data and constructive suggestions that made this report possible: Captain K.F. van der Elst, Commander of KLM flight 867; Mr. Roy C. Daw, NTSB (National Transportation Safety Board), Anchorage Regional Office, Alaska; and Dr. Michael G. Dunn, Arvin/Calspan, Buffalo, New York. In addition, special thanks go

to the KLM maintenance personnel at Schiphol Airport who performed the disassembly and inspections of the engines involved in this event.

REFERENCES CITED

- Brantley, S.R., 1990, The eruption of Redoubt Volcano, Alaska, December 14, 1989–August 31, 1990: U.S. Geological Survey Circular 1061, 33 p.
- Casadevall, T.J., in press, The 1989–1990 eruption of Redoubt Volcano, Alaska: Impacts on aircraft operations: *Journal of Volcanology and Geothermal Resources*.
- Casadevall, T.J., Meeker, G.P., and Przedpelski, Z.J., 1991, Volcanic ash ingested by jet engines [abs.], in Casadevall, T.J., ed., First International Symposium on Volcanic Ash and Aviation Safety, Program and Abstracts: U.S. Geological Survey Circular 1065, p. 15.
- Campbell, E.E., 1991, 747-400 airplane damage survey following a volcanic ash encounter [abs.], in Casadevall, T.J., ed., First International Symposium on Volcanic Ash and Aviation Safety, Program and Abstracts: U.S. Geological Survey Circular 1065, p. 14.
- National Transportation Safety Board [NTSB], 1991, Aircraft Accident Report ZAN ARTCC #100, KLM 867, H/B74F December 15, 1989 2048 UTC: unpub. report, 726 p.
- Scott, W.E., and McGimsey, R.G., in press, Character, mass, distribution, and origin of tephra-fall deposits of the 1989–1990 eruption of Redoubt Volcano, south-central Alaska: *Journal of Volcanology and Geothermal Research*.
- Steenblik, J.W., 1990, Volcanic ash: A rain of terra: *Air Line Pilot*, June/July 1990, p. 9–15, 56.

ECONOMIC DISRUPTIONS BY REDOUBT VOLCANO: ASSESSMENT METHODOLOGY AND ANECDOTAL EMPIRICAL EVIDENCE

By Bradford H. Tuck and Lee Huskey

ABSTRACT

The eruptions of Redoubt Volcano in 1989–90 imposed significant economic costs on Alaska residents, airlines and other businesses serving Alaska, government agencies, and travelers going to or coming from Alaska. This paper presents a set of principles, or guidelines, for the classification and aggregation of costs and benefits associated with the eruptions. These costs include both market-measured costs and non-market-measured costs, such as waiting time.

INTRODUCTION

This paper describes a social accounting framework designed to classify real economic costs and benefits, as well as related redistributions of economic activity associated with the eruptions of Redoubt Volcano between December 1989 and April 1990. Conceptually, we are trying to compare economic activity that would have occurred if the eruptions had not taken place with activity that actually took place. The difference between these two situations represents the net economic cost of the eruptions.

There are two major reasons for measuring these costs. The first is to provide an aggregate measure of the net economic costs associated with the Redoubt Volcano eruptions and the distribution of those costs among geographic areas. Estimates such as these are often instrumental in obtaining Federal or State government assistance (if available in a timely fashion). The second use is to provide an indication of those costs that could be avoided or lessened with the implementation of various mitigation measures. This is essential information for the evaluation of investment in mitigation measures.

DESIGNING THE ACCOUNTS

There are several issues that have been considered in the design of the accounting framework. A review of these will help in understanding both what is and what is not being measured. Readers interested in substantially more detailed

discussions of social income accounting may consult Yanovsky (1965) or Eisner (1989).

The present accounting framework is intended to reflect three measures of economic activity: real economic costs, real economic benefits, and redistributions of costs or benefits.

Costs are incurred as a result of using up factors of production, or inputs, and may be of two types: direct damage costs and mitigation costs. Direct damage costs are defined as costs resulting directly from the volcanic eruption, such as a jet engine repair, ash cleanup and removal, and "waiting time" costs of individuals. These are costs that would not have occurred except for the eruptions. Mitigation costs includes those costs associated with mitigation of the effects of present or future volcanic eruptions. These are costs intended to reduce future damages. Included in this category would be airborne radar to track ash clouds, costs of monitoring volcanic activity, and installation of special dikes to protect the Drift River oil-loading facility.

Some real economic benefits may also have resulted from the eruptions (e.g., volcanic ash used in pottery, the inevitable T-shirt, or tourist flights around the volcano). More difficult to value, but of greater potential long-run significance, might be increased knowledge related to predicting eruptions, appropriate flight procedures when encountering volcanic ash clouds, etc. However, we expect that most perceived benefits are really redistribution effects.

The third category of measurement addresses redistributions of economic activity. Distributional effects related to volcanoes are discussed in detail in Blong (1984). These redistributions occur when economic activity shifts from one geographic locale to another as a result of the eruptions. For example, a flight scheduled to land in Anchorage is diverted to Fairbanks. Fairbanks gains income that is lost in Anchorage. Redistribution also occurs when components of income are shifted from one owner to another. For example, when a damaged jet engine is replaced, there is a redistribution of economic profit from the aircraft owner (or insurer) to the firm doing the repair.

The inclusion of costs, benefits, and redistributions arising from transportation delays (and cancellations) is

another major aspect of accounting for economic costs related to the Redoubt eruptions. Consequences of travel delays, trip cancellations, and, to a lesser extent, freight and postal service delays are not directly measured by the market but are likely to be substantial.

Benefits, costs, and distributional effects depend on both the geographic area encompassed and timing. The geographic frame of reference in the present study is global, in the sense that costs, benefits, and redistributions associated with the eruptions are included regardless of where they occurred. Geographic sub-units are established to identify localized effects. The timing of costs may also provide useful information, and, where possible, we will measure costs relative to specific eruptions.

THE BASIC RULES

Before looking at some illustrations of the application of our accounting principles, it is helpful to summarize the specific rules that we are using to measure volcano-related economic impacts.

1. Any economic action (i.e., the use of factor inputs, such as labor, capital, or purchased intermediate inputs) that occurs because of an eruption, which otherwise would not have occurred, is treated as a change from the "without eruption" state. If the action can be expected to increase the consumer's utility, or "economic well-being" compared to the non-eruption case, the change is treated as a benefit. If the action is to maintain (or attempt to maintain) a consumer's pre-eruption utility level or restore their utility level, then the change is treated as a cost. As indicated above, these costs are further divided into two categories: direct damage costs and mitigation costs.
2. Benefits or costs may be measured either by the monetary value of factor inputs used in the production process (the value added measure) or by the market price of the good or service produced but, however measured, cannot be counted twice (i.e., double counted).
3. The estimate of the net economic cost of the eruptions is the difference between measured total costs and total benefits.

SOME EXAMPLES

We can now illustrate the use of the accounting framework with several examples. First considered is the privately owned Drift River Oil Terminal, located on the west shore of Cook Inlet at the mouth of the principal river draining the north flank of Redoubt Volcano. Oil produced from Cook Inlet platforms is transported by pipeline to the Drift River facility for storage and loading on to tankers. Debris flows from the eruptions caused flooding, threatened the physical integrity of Drift River Terminal, forced the closing of the

facility, and lead to cessation of production from the Cook Inlet fields. Subsequently, the facility was repaired, levees were installed to protect the facility, and operation of the facility and production from Cook Inlet fields resumed. From a conceptual point, what costs should be charged against the eruptions?

Firstly, the cost of levees should clearly be included because the levees were a State-imposed precondition for reopening the facility. Secondly, other modifications to the facility to prevent the recurrence of adverse flooding effects would also be included. These are examples of mitigation costs. Costs of shutting down and restarting Cook Inlet production facilities should also be included and should reflect direct damage costs. State royalty income at the time of the eruptions was about \$39,000 per day (Brantley, 1990). The economic cost of replacing the revenue flow (e.g., as measured by the cost of borrowing to replace the revenue flow) would also be a direct cost. The same principle would apply to the delay in producer earnings.

A second example considers the repair of damage to aircraft. A highly reported incident occurred when a Boeing 747-400 flew through an ash cloud on December 15, 1989, and lost power in all four engines. Although the engines were restarted and the plane landed safely, the aircraft required extensive repair work (Przedpelski and Casadevall, this volume). All four engines were replaced, as were portions of the electrical and avionics systems. In addition, the aircraft required a thorough cleaning to remove ash. The reported repair costs were estimated at approximately \$80 million (Steenblik, 1990).

How do the account principles treat these expenditures? First, the repair and cleaning costs are a direct result of the eruption and reflect the use of resources to repair damage caused by the eruptions. Secondly, only a portion of the costs of engine and electronics replacement should be included. The portion that should be included would be equal to the cost of replacing the remaining economic life of the damaged equipment. For example, if an engine had 20 percent of its economic life remaining at the time of the incident, then replacement of that 20 percent should be charged against the eruption (i.e., a cost of the eruption), whereas the balance would be treated as new investment and not counted as a cost of the eruption.

A third illustration of our account principles relates to the treatment of a canceled or rescheduled event. The annual Anchorage "Christmas Carol" production scheduled for several performances prior to Christmas had to be postponed. The actors, actresses, and stage crew were in Anchorage, but the shipment of stage sets (to be transported by air freight) was delayed several times. Although the production did finally take place after several reschedulings, there was a significant loss in revenue.

What are the losses associated with this event? Following the principle of "resources used," the loss should be equal to the resources used in the "non-production." This

would include the opportunity cost of the actors, actresses, and stage crew (as measured by their compensation), their housing and transportation costs, the earnings that the Performing Arts Center could have obtained if used for an alternative event, the cost of promotional activity, etc. There is also an economic cost reflected in the time invested by volunteer participants.

A final example addresses the issue of waiting time. Disruption of flight schedules and outright cancellation of flights resulted in extensive, and often lengthy, delays for air travelers. In many cases, the end result was complete trip cancellation on the part of the individual traveler. There are two dimensions to these waiting-time costs with which we try to deal. The first is the temporary non-utilization of factor inputs where the foregone use cannot be recaptured in the future. For example, a business traveler stranded in Seattle on a trip from San Francisco to Anchorage (and unable to conduct business from the airport) spends a certain number of hours waiting to complete the trip. This waiting time is a cost of production and a use of the factor input, labor. As such, it can be valued at its regular rate of compensation.

The second type of waiting-time cost is associated with final consumption of air travel (i.e., consumer travel). In this case, the cost of waiting is the value of leisure time that the consumer has given up. For example, a student returning home to Anchorage for the Christmas holidays has to spend two days in the Seattle airport. These two days are days that the student does not get to spend with family

(or friends already back from other schools). Typically, the value of leisure time is measured by its opportunity cost, or what the individual could have earned if they had chosen to work rather than to have taken leisure time. We follow that convention in these accounts. Thus, the cost of the student's waiting time would be equal to what the student could have been earning had that student chosen to work (instead of being a student). Discussion of the measurement and use of leisure time is more fully treated in Kendrick (1987) and Eisner (1989).

SUMMARY

In summary, we have attempted to state a set of "rules" to guide the classification and aggregation of economic costs and benefits associated with the eruptions of Redoubt Volcano during 1989–90. Compilation of these costs and benefits provides both an indication of the overall costs to society of the eruptions and a reference against which future mitigation efforts can be evaluated.

ADDENDUM

Since this report was prepared, we have completed the study of economic consequences of the 1989–90 Redoubt Volcano eruptions (Tuck and others, 1992). Table 1 contains a summary of the findings regarding the economic impact of the Redoubt Volcano eruptions on the aviation industry.

Table 1. Estimated economic impacts of the 1989–90 eruption of Redoubt Volcano on the aviation industry.¹

("Big Four," United, Delta, Northwest, and Alaska Airlines; ?, no estimate available for economic impact for this category; Na., estimated economic impact not allocated to this category; AIA, Anchorage International Airport. All figures in U.S. dollars)

Category	December 1989	January 1990	Total
Domestic passenger traffic			
"Big Four" (B4)	837,884	349,138	1,187,022
Domestic total – B4	433,511	35,673	469,184
International passenger traffic	?	?	?
Domestic freight	Minimal	Minimal	Minimal
International freight	Na.	Na.	15,000,000
AIA revenues			
Landing fees	177,464	77,696	255,160
Concessions	508,216	487,339	995,555
Fuel flowage fees	135,060	205,460	340,520
Airport support industries			
Fuel distribution	Na.	Na.	50,000
Ground crews and service	Na.	Na.	600,000
Catering	Na.	Na.	43,500
Concessions	Na.	Na.	285,000
Passenger waiting time	1,144,800	689,000	1,833,800
Estimated production losses	Na.	Na.	21,059,741
Equipment damage costs	Na.	Na.	80,070,000
Total aviation costs			101,129,741

¹ Source of information: Tuck and others (1992).

REFERENCES CITED

- Blong, R.J., 1984, *Volcanic Hazards: A Sourcebook on the Effects of Eruptions*: Sydney, Academic Press, 424 p.
- Brantley, S.R., ed., 1990, The eruption of Redoubt Volcano, Alaska, December 14, 1989–August 31, 1990: U.S. Geological Survey Circular 1061, 33 p.
- Eisner, Robert, 1989, *The Total Incomes System of Accounts*: Chicago, University of Chicago Press, 416 p.
- Kendrick, J.W., 1987, Happiness is personal productivity growth: *Challenge*, v. 30, p. 37–44.
- Steenblik, J.W., 1990, Volcanic ash—A rain of terra: *Airline Pilot*, June/July, p. 9–15.
- Tuck, B.H., Huskey, L., and Talbot, L., 1992, The economic consequences of the 1989–90 Mt. Redoubt eruptions: University of Alaska, Anchorage, Institute of Social and Economic Research, [unpub. report prepared for the U.S. Geological Survey Alaska Volcano Observatory], 39 p.
- Yanovsky, M., 1965, *Social Accounting Systems*: Chicago, Aldine Publishing Company, 237 p.

ALASKA VOLCANO-DEBRIS-MONITORING SYSTEM: NEW TECHNOLOGIES TO SUPPORT FORECASTING VOLCANIC-PLUME MOVEMENT

By Gary L. Hufford

ABSTRACT

The eruptions of Redoubt Volcano during 1989–90 revealed a number of deficiencies in National Weather Service (NWS) operations that greatly hampered the forecaster's ability to accurately forecast and issue timely advisories on the movement of airborne volcanic debris. The forecaster lacked knowledge of (1) the physical properties of airborne volcanic debris, (2) the initial location of debris in the atmosphere, both vertically and horizontally, (3) real-time winds near and downstream of the volcano, and (4) rapid access to volcanic-debris-tracking models.

To help resolve these deficiencies, an Alaska volcano debris monitoring system has been designed, acquired, and installed at the NWS offices in Anchorage, Alaska. The system consists of a wind-profiling Doppler radar that provides hourly vertical profiles of winds near the volcano, a satellite downlink and processing system for tracking volcanic plumes using a variety of polar-orbiting satellites, a C-band radar to provide vertical and horizontal extent of the plume at and near the volcano, a new volcanic-debris-tracking model, and an upgrade to the regional computer and communications network for processing, applications, and display of the volcano debris monitoring system database.

INTRODUCTION

Volcanic ash injected into the atmosphere from the 1989–90 Redoubt eruptions became the most common and widespread hazard (Brantley, 1990) from this series of eruptions. The ash caused significant damage to property, especially aircraft, and severely disrupted normal activities in south-central Alaska, where about 60 percent of the State's population lives.

Redoubt Volcano is one of four active volcanoes that lie along the west side of Cook Inlet (fig. 1). These four volcanoes have erupted for a combined total of seven times in the

last 80 years. Some of those eruptive episodes have lasted over a 2-year period. The four volcanoes are part of an active chain that extends from upper Cook Inlet, southwest along the Alaska Peninsula, to the western Aleutians. This chain includes a total of 35 volcanoes active during the last century (Simkin and others, 1981).

During the last eruptive episode of Redoubt Volcano, the NWS found that there were a number of deficiencies in information that greatly hampered the forecaster in accurately forecasting and issuing timely advisories on the movement and concentration of volcanic debris injected into the atmosphere. The forecaster had no information on (1) ash particle size and concentration, (2) initial height or horizontal extent of the plume into the atmosphere, (3) real-time vertical profiles of the winds near and downstream of the volcano, and (4) rapid access to volcanic-ash-trajectory models.

The potential for future hazardous eruptions near Cook Inlet led Congress to support a volcano monitoring program for south-central Alaska to minimize the affects on the population and commerce. A major participant in the monitoring program is the NWS. The purpose of this paper is to describe the technologies that have been chosen by NWS for the task of ash detection, monitoring, and tracking in Alaska. The system, called the Alaska volcano debris monitoring system, consists of new remote-sensing instrumentation, development of new predictive models, and an upgrade of the NWS regional computer and communications network for processing, applications, and display of the integrated database from the monitoring system.

REMOTE-SENSING TECHNOLOGIES

The remote sensing instrumentation in the Alaska volcano debris monitoring system consists of a Doppler wind profiler, a non-Doppler weather radar (C-band), and a polar satellite downlink, processing, and display system.

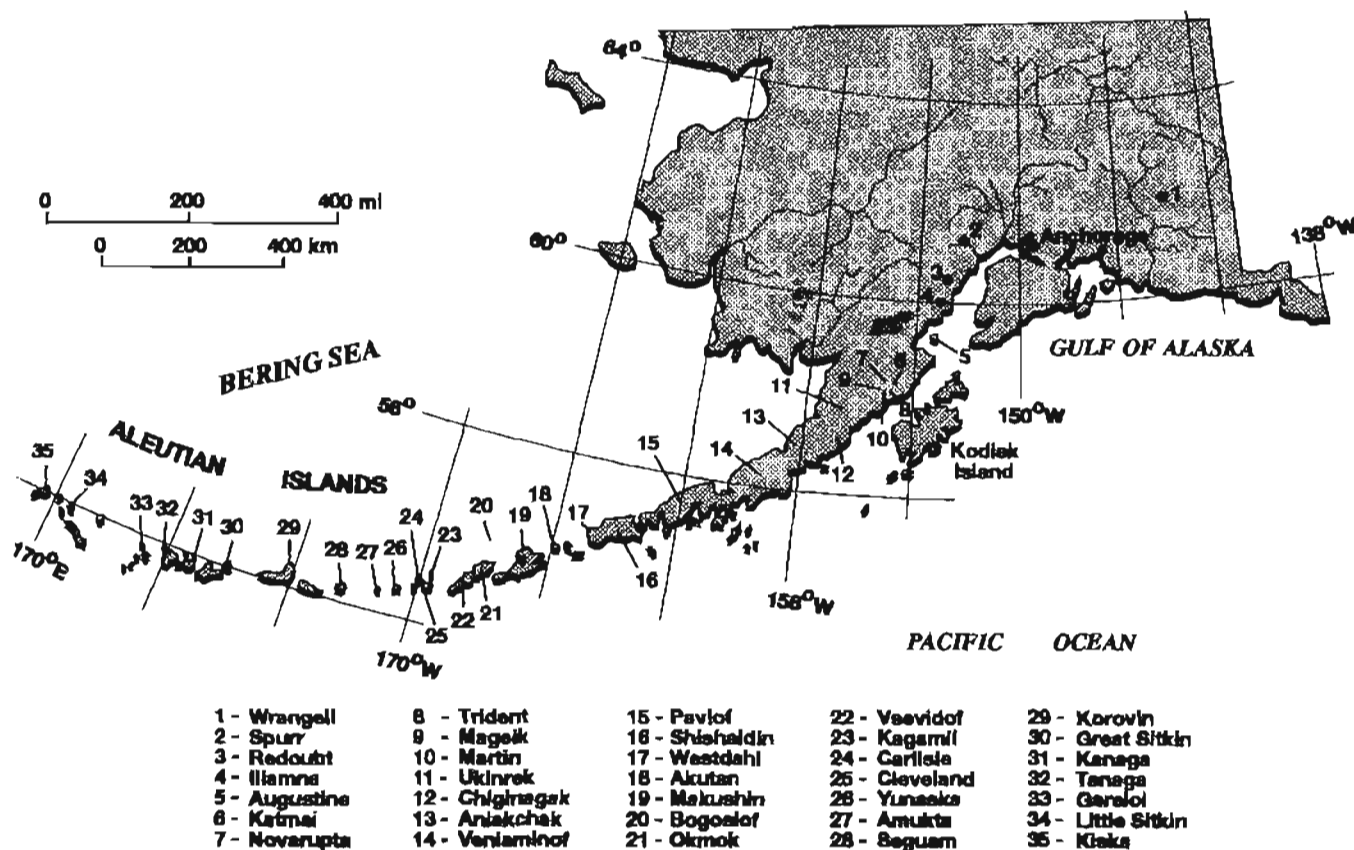


Figure 1. Volcanoes along Cook Inlet, Alaska, that have shown activity in the last century, including Mt. Spurr (2), Redoubt Volcano (3), Iliamna Volcano (4), and Augustine Volcano (5). Source: Alaska Volcano Observatory.

WIND PROFILER

A wind-profiling Doppler radar observes the weak back-scatter from turbulent inhomogeneities in the atmospheric radio refractive index. The ultra high frequency (UHF) system (405 MHz) is suited for high-resolution, clear-air wind observations from 1 km to 16 km producing data every 6 minutes that is arranged into hourly, vertically averaged wind profiles (Balsley and Gage, 1982). Many studies have been made of the precision of profiler wind measurements. Thomas and Williams (1990) report that, in a comparison of profiler and rawinsonde (balloon) winds, the standard deviation was close to 3 m/s, with an inherent accuracy for the profiler of less than 1 m/s.

To support the Alaska volcano debris monitoring system, the wind profiler was installed in Homer, Alaska, about 100 km from Redoubt Volcano (fig. 2) in December 1990. The Homer site provides hourly vertical profiles of winds near the Cook Inlet volcanoes. Figure 3 shows an example of the wind measurements from the Homer profiler. Other profiler sites are proposed for Talkeetna and Middleton Island, Alaska (fig. 2). These two sites will give hourly vertical wind profiles at locations downwind from the Cook Inlet volcanoes. These sites will also provide winds along two major

air-traffic corridors over south-central Alaska that have relatively poor upper-air network coverage (fig. 4).

C-BAND RADAR (5 CENTIMETER)

Ground-based radar observations and calculations can provide significant information on estimating (1) the height of the eruptive column above the volcano, (2) the maximum vertical and horizontal dimensions of the ash cloud downwind, and (3) the location and horizontal velocity of the ash cloud. NWS radar observations of ash clouds from Mount St. Helens demonstrated that weather radar (5 cm) can yield timely information during and following volcanic eruptions (Harris and Rose, 1983). However, there are some constraints.

One- to 10-cm radars sometimes cannot discriminate between ash clouds and meteorological clouds and rain targets (Stone, this volume). Thus, on cloudy, rainy days, ash plumes may go undetected by weather radar if the radar is the only source of detection. In addition, once an ash cloud is in the dispersed stage, particle sizes may be too small to be detectable by radar. Radar must be used in conjunction with

other observational measurements to be an effective data source.

In October 1990, a 5-cm C-band radar was located in Kenai, Alaska, approximately 90 km from Redoubt (fig. 2). The radar is mounted on a modified recreational motor home and is portable. The unit can be moved rapidly to optimize observations of the other volcanoes in the Cook Inlet area. Data from the radar site is sent, in real time, by telephone to the forecaster in Anchorage for display on remote monitors.

HIGH RESOLUTION PICTURE TRANSMISSION PROCESSING SYSTEM

NOAA/TIROS (National Oceanic and Atmospheric Administration—television and infrared observing satellite)

polar-orbiting satellites have been used in some cases to detect and track ash clouds utilizing a number of instruments on the platform. Advanced very high resolution radiometer (AVHRR) visible and infrared imagery have been used to track volcanic clouds in Alaska (Holasek and Rose, 1991; Schneider and Rose, this volume) and southeast Asia (Prata and others, 1985) using standard methods to track meteorological clouds. Infrared imagery has been used to discriminate volcanic clouds from ordinary water/ice clouds utilizing two signatures in the brightness temperatures (Prata, 1989). The first signature is based on the emission characteristics of silicates in the ash cloud. Silicates have a lower emissivity at $11\ \mu\text{m}$ than at $12\ \mu\text{m}$ where water/ice show peak emissivity. This effect is seen as a negative temperature difference between channels 4 and 5 of the AVHRR instrument. The second signature is a lower emissivity for sulfuric acid

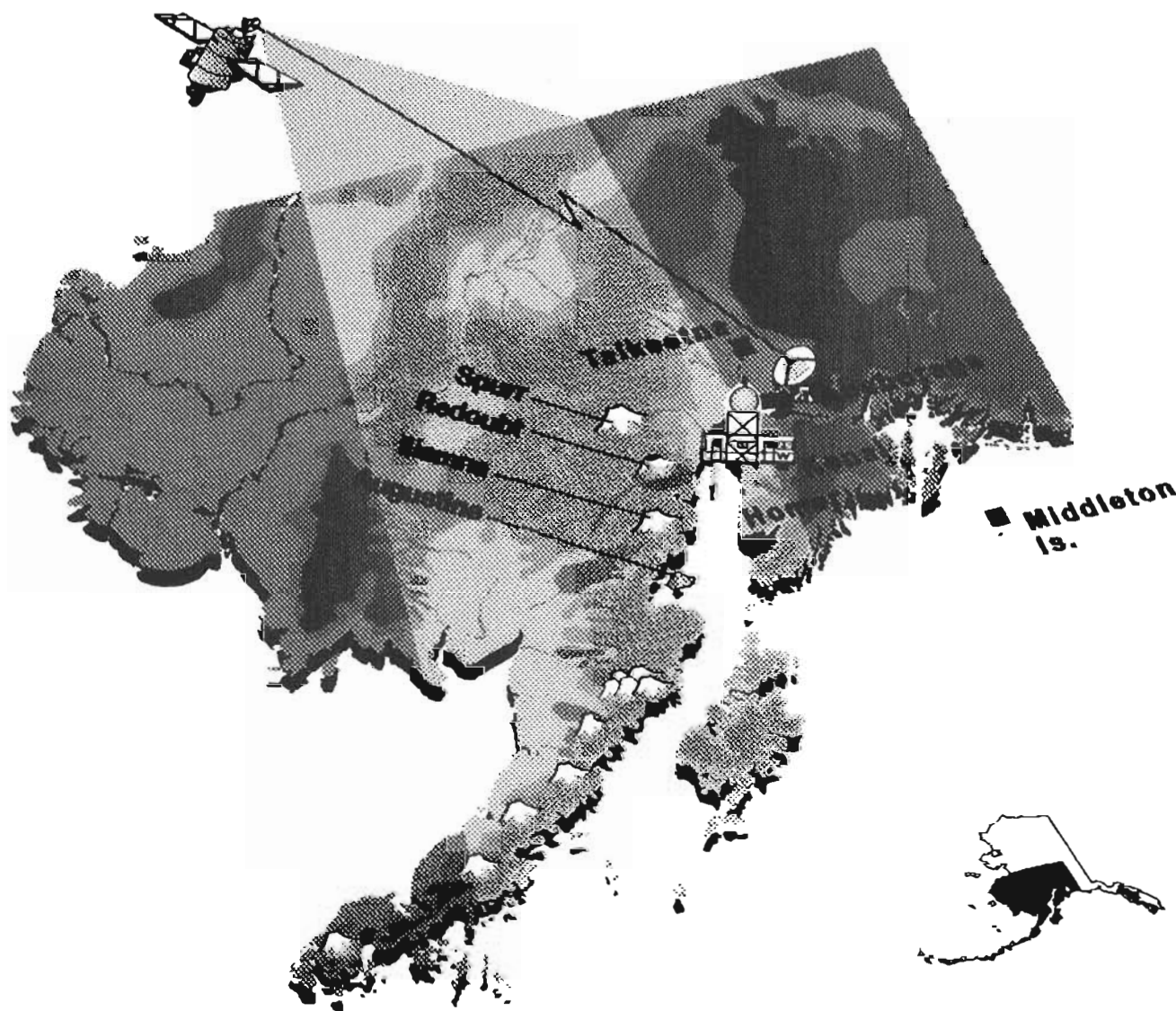


Figure 2. Location of remote-sensing instrumentation of the Alaska volcano debris monitoring system in relation to the four volcanoes along Cook Inlet.

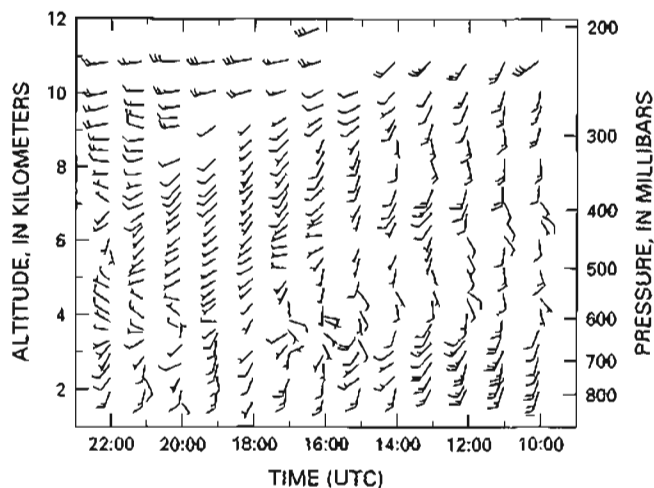


Figure 3. Hourly vertical profiles of wind from the Homer, Alaska, profiler for April 2, 1991. Orientation of "arrow" shaft indicates wind direction and has a precision of $\pm 10^\circ$. "Flag" length indicates wind speed: a "half-flag" has a value of 5 knots; a "full-flag" has a value of 10 knots. UTC, Coordinated Universal Time.

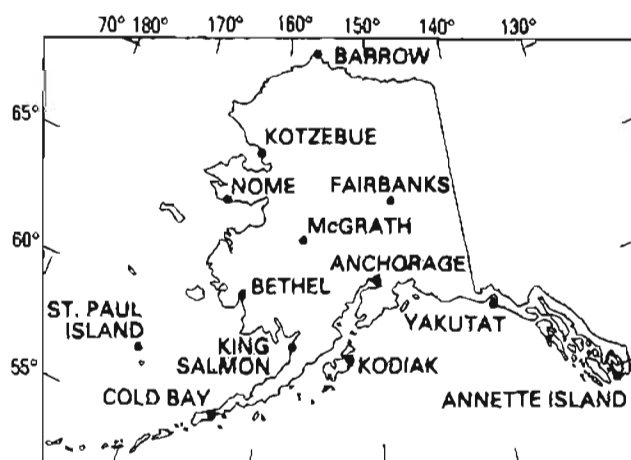


Figure 4. Location of the upper-air (rawinsonde balloon release) network in Alaska.

droplets or acid-coated particles ($11 \mu\text{m}$) when compared to water/ice particles ($12 \mu\text{m}$).

The high spatial resolution of the NOAA/TIROS polar-orbiting satellites (1 km), their great spectral range, and frequent coverage make these satellites a significant monitoring and tracking tool over Alaska. At low latitudes, the polar orbit limits the view of the same point to only four times per day for two satellites. Because the orbits of the satellites are near polar and sun synchronous, their orbital paths tend to converge at the poles, and, in the higher latitudes, coverage can be up to 18 passes per day from the same two polar satellites.

There are other operational instruments on-board the NOAA/TIROS polar-orbiting satellites that have potential to support the monitoring and tracking of volcanic plumes. The TIROS observational vertical sounder (TOVS) on the polar-orbiting satellites should be able to provide considerable information on volcanic clouds and conditions around them. TOVS consists of a high-resolution infrared radiation sounder (HIRS) that contains 20 infrared channels and a passive microwave sounding unit (MSU). TOVS also provides vertical profiles of temperature, moisture, and geostrophic wind down to the surface in areas of no clouds. This data can be used to estimate the maximum height and trajectory of ash clouds.

A high-resolution image-processing system (HIPS) was installed in Anchorage, Alaska, in June 1991 (fig. 2). The system includes a tracking antenna located at the international airport, an ingest/synchronization computer, a main processor, and four workstations at the three Alaska forecast offices (Anchorage, Juneau, and Fairbanks) and the Center Weather Service Unit in Anchorage. Eighteen polar-orbiting passes over Alaska can be processed to produce at least 12 satellite-image products per pass; these are distributed via the Alaska region operational communications network (ARO-NET). The HIPS system was also designed to ingest data from other polar-orbiting satellites, including those of the defense meteorological satellite program (DMSP), to increase coverage so that an image is available over any given point in Alaska every 1.5–2 hours. The aerial coverage for HIPS is within a 1,500-km radius from Anchorage.

Satellite data are displayed on workstations, and interactive software allows for complete digital manipulation of the imagery and sounding data, including animation, graphic overlay, cartographic projections, multispectral classification, windowing, and full color enhancement.

COMPUTER, COMMUNICATIONS, DATA INTEGRATION, AND MODELS

COMPUTER AND COMMUNICATIONS NETWORK

To insure the optimization of the NWS Alaska computers and communications to handle the large volume of data from the volcano monitoring system and the gridded data sets from various prediction models, the next-generation Alaska region operational computer and communications network (ARO-NET) was developed and made operational in October 1991 (fig. 5). Computer standards such as UNIX (OSF/1 compliance), X-Windows (Motif), and IEEE 802.3 Ethernet with TCP/IP network protocol have been selected to minimize the difficulties inherent in a heterogeneous computer environment. This allows a number of different kinds of computers to be used as workstations and coupled with an advanced wide- and local-area network

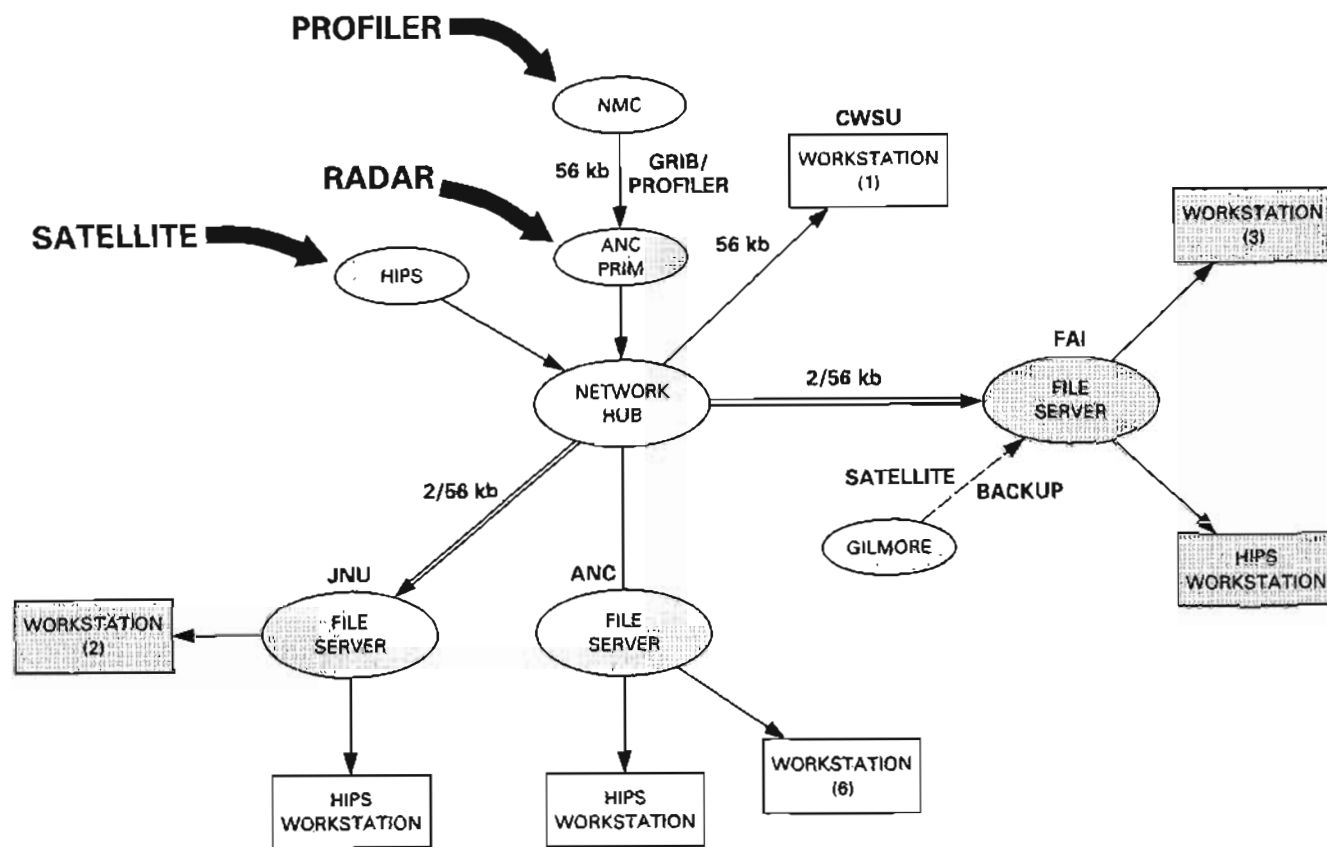


Figure 5. Schematic of Alaska region operational computer and communications network (ARO-NET). JNU, Juneau; FAI, Fairbanks; ANC, Anchorage; NMC, National Meteorological Center; CWSU, Central Weather Service Unit; HIPS, high-resolution image-processing system; GRIB, gridded binary format.

to integrate data from a combination of sources. New RISC (reduced instruction set chip) computers are used as application and file servers on the network, and high-speed digital communications lines (56 kb) have been incorporated to handle the increased volume of data.

INTEGRATED DATABASE

The data from the Alaska volcano debris monitoring system, integrated with other conventional data sources in Alaska, provides the forecaster with a powerful tool to assist in producing effective and timely forecasts. Comparing the integrated database to digital predictive-model output fields and adjusting the model when necessary will provide the forecaster with capabilities never available in field offices in the past. As an example, during eruptive events, forecasters will have available forecaster-selected, multilevel winds valid at 3-hour intervals from the time of initial eruption out to 12 hours, and thereafter every 6 hours out to 72 hours. These constant-height winds will come from gridded, digital-model output and can be displayed as streamlines (wind

paths). The forecaster will place observed winds from the profilers, satellites, rawinsonde balloon releases, and other observations over the streamlines. This overlay capability will assist the forecaster to initialize, verify, or adjust the predicted model winds.

ASH DISPERSION MODEL

The air resources laboratory of NOAA is developing a four-dimensional dispersion model for airborne volcanic debris (Heffter and others, 1990; Stunder and Heffter, this volume). This model will utilize wind data from the technologies described above as well as inputs from NOAA's forecast systems laboratory mesoscale analysis and prediction system (MAPS) and National Meteorological Center (NMC) boundary-layer forecast meteorological fields. Designed to serve aviation and local forecasting, MAPS over Alaska will define the tropospheric and lower stratospheric wind fields every few hours after eruption. Over the longer term, NMC forecast winds will be utilized. In addition, satellite imagery

will provide information on the location and horizontal extent of the ash cloud. The C-band radar will supply initial vertical height and direction of the ash plume at the volcano. The dispersion model will forecast concentrations and deposition of volcanic debris for forecast periods from eruption to up to 48 hours. The model should be ready for operational use in late 1992.

SUMMARY

The 1989–90 eruptions of Redoubt Volcano have resulted in the establishment of a volcano debris monitoring system to improve the accuracy and timeliness of NWS forecast warnings and advisories to the public during eruptions of Alaskan volcanoes. The long history of frequent eruptions from volcanoes along Cook Inlet clearly indicates that future eruptions are inevitable.

It is anticipated that improved forecast products will have their greatest impact on aviation safety in the Cook Inlet region. Because ash is not possible to detect during flight with present onboard sensors, effective and timely warnings will allow aircraft to avoid ash clouds.

These more accurate forecast products will be in both alphanumeric and graphic form. New products will include a graphical advisory, four-dimensional trajectories, and descriptive statements to the public and emergency-management agencies.

REFERENCES CITED

- Balsley, B.B., and Gage, K. S., 1982, On the use of radars for operational wind profiling: *Bulletin of the American Meteorological Society*, v. 63, p. 1009–1018.
- Brantley, S.R., ed., 1990, The eruption of Redoubt Volcano, Alaska, December 14, 1989–August 31, 1990: U.S. Geological Survey Circular, 1061, 31 p.
- Harris, D.M., and Rose, W.I., Jr., 1983, Estimating particle sizes, concentrations, and total mass of ash in volcanic clouds using weather radar: *Journal of Geophysical Research*, v. 88, p. 969–983.
- Heffter, J.L., Stunder, B.B., and Rolph, G.D., 1990, Long-range forecast trajectories of volcanic ash from Redoubt Volcano eruptions: *Bulletin American Meteorology Society*, v. 71, p. 1731–1738.
- Holasek, R.E., and Rose, W. I., Jr., 1991, Anatomy of 1986 Augustine Volcano eruptions as recorded by multispectral image processing of digital AVHRR weather satellite data: *Bulletin Volcanology*, v. 53, p. 420–435.
- Prata, A.J., 1989, Observations of volcanic ash clouds in the 10–12 μm window using AVHRR/2 data: *International Journal of Remote Sensing*, v. 10, p. 751–761.
- Prata, A.J., Wells, J.B., and Ivanac, M.W., 1985, A satellites view of volcanoes on the Lesser Sunda Islands: *Weather*, v. 40, p. 245–250.
- Simkin, T., Siebert, L., McClelland, L., Bridge, D., Newhall, C.G., and Latter, J.H., 1981, *Volcanoes of the World*: Stroudsburg, Pa., Hutchinson Ross, 242 p.
- Thomas, D.R., and Williams, S.R., 1990, Analysis of comparative wind profiler and radiosonde measurements, in *Proceedings of the 10th Annual Geoscience and Remote Sensing Symposium*: New York, v. 1, p. 537–540.

USING A PERSONAL COMPUTER TO OBTAIN PREDICTED PLUME TRAJECTORIES DURING THE 1989-90 ERUPTION OF REDOUBT VOLCANO, ALASKA

By Thomas L. Murray, Craig I. Bauer, and John F. Paskievitch

ABSTRACT

The Alaska Volcano Observatory (AVO) and the Anchorage Weather Service Forecast Office (WSFO) obtain predicted plume trajectories daily for Redoubt Volcano, Alaska. A model developed by the National Oceanic and Atmospheric Administration (NOAA) Air Resource Laboratory calculates predicted plume trajectories. The model, running on NOAA's NAS/9000 mainframe computer in Suitland, Md., uses forecast wind fields obtained from the NOAA National Meteorological Center. The model uses measured and forecast winds to predict the path of a weightless particle released at various pressure-altitudes above a specified location. The paths indicate the general direction and speed that ash from an eruption at that location will travel.

In response to the 1989-90 Redoubt eruption, we programmed an IBM-XT-style personal computer to automatically dial the NAS/9000 mainframe computer and obtain the predicted trajectories. Twice daily, after the predicted wind fields are updated, AVO and WSFO can easily collect and plot the trajectories predicted for the next 72 hours. Thus, the trajectories are immediately available in the event an eruption should occur. The predicted trajectories are plotted on a map of Alaska, showing the predicted location of the ash plume at 3-hour intervals for different altitudes between 5,000 and 53,000 ft. The plots are easily telefaxed to interested parties. The program has been modified to enable the user to obtain predicted plume trajectories for other U.S. volcanoes.

INTRODUCTION

Volcanic ash ejected into the atmosphere can cause severe problems to airplanes and to municipal and industrial facilities, as well as to people on the ground downwind from the volcano. Knowing where ash will travel is vital to

mitigating its effects. If notified in time, people in the path of the ashfall can take precautionary measures as complex as shutting down portions of a power facility or as simple as canceling a dinner date. Conversely, in areas unlikely to be affected by ashfall, industry can avoid wasting resources in preparation for ash that is not traveling in their direction. In this report, we describe a method to routinely acquire predicted wind speeds and directions (trajectories) at various pressure-altitudes and to plot and display the data in a simple, easy-to-distribute format. The predicted plume trajectories currently provide the only method that predicts, before an eruption, where ash will be blown (as opposed to tracking already-erupted ash). AVO and WSFO took advantage of this capability and informed other agencies daily as to where ash from Redoubt would go if the volcano were to erupt. In the event of an eruption, the predicted plume trajectory, having been plotted earlier, is ready for immediate use, thereby saving valuable time.

During the Redoubt eruption, plots were especially useful to the aviation industry. They were sent daily to Anchorage International Airport authorities, who then distributed them to the airlines, many of which required their flight crews to use them in flight planning (Casadevall, in press).

DESCRIPTION OF PREDICTED PLUME TRAJECTORIES

A computer model, developed by NOAA's Air Resource Laboratory (ARL), provides predicted plume trajectories based on forecast wind fields. The wind fields are calculated twice daily by the National Weather Service (NWS) from observations taken at 00:00 and 12:00 Greenwich Mean Time (GMT) (Heffter and others, 1990). Using the latitude and longitude of the volcano and the time of the hypothetical eruption, the model predicts the locations of dimensionless, weightless particles at 3-hour increments

after they are released into the atmosphere at various pressure-altitudes above the volcano. The model ignores effects from gravity and dispersion. Unlike volcanic ash, the model's ideal particles never fall to Earth, but remain at the pressure-altitude at which they were released forever.

The model accepts times for hypothetical eruptions up to 48 hours into the future in 3-hour increments. AVO can always have the latest predicted trajectories by obtaining the predicted trajectories from the NOAA computer twice daily after the latest weather observations are processed. Owing to the time required to process weather observations and calculate the predicted wind fields, the latest predictions are typically available about 3 hours after the actual measurements, at 03:00 and 15:00 GMT (or 18:00 and 06:00 AST).

OBTAINING PREDICTED PLUME TRAJECTORIES

Predicted plume trajectory plots were first used to predict trajectories of volcanic ash during the 1980 eruptions of Mount St. Helens, Washington (Miller and others, 1981; Smith, 1980). At that time, the technique to acquire trajectories was time consuming, requiring the full attention of a person for an hour or more (E. Brown, oral commun., 1991). As the level of activity at Mount St. Helens declined, the U.S. Geological Survey discontinued obtaining plume trajectory data.

In 1988, NOAA signed a memorandum of understanding with the Federal Aviation Administration (FAA) to provide the FAA with predicted plume trajectories (Heffter and others, 1990). During the 1989-90 eruptions of Redoubt Volcano, NOAA provided trajectory information to the FAA within 1 hour of NOAA's notification of the eruption and typically within 3 hours of the actual eruption (Heffter and others, 1990). Because an ash plume can move hundreds of kilometers during a 3-hour delay, AVO and the Anchorage WSFO felt that they needed trajectory information more quickly in order to issue timely warnings. Ideally, the trajectory information would be available before an eruption. This would allow AVO and WSFO to concentrate on the myriad other tasks involved in monitoring an eruption (data analysis, notifying interested agencies, answering media inquiries, etc.) and would avoid using personnel or phone and computer resources during an eruption to obtain the information. It would also allow AVO to include the information in daily updates sent to various public agencies and other users, including the aviation community, that could be affected by ashfall. Finally, it enabled AVO and WSFO to have the information ready for immediate distribution should an eruption occur.

In order to acquire the plume trajectories daily, even when there was little chance of an eruption, the process had to be simplified, or, as was the case with Mount St. Helens, it would fall into disuse. We were able to do this by using

computer hardware and software unavailable in 1980. The necessary equipment consists of an IBM XT (or compatible) personal computer, a 1,200-baud Hayes-compatible modem, a printer, the software package PROCOMM Plus (for communication with the NOAA computer), and Geograf Utilities (for the screen and printer graphics drivers). Users initiate the program with a few keystrokes and are prompted to answer a few questions. Then the program dials the NOAA NAS/9000 computer in Suitland, Md., runs the plume trajectory program for various hypothetical eruption times and pressure-altitudes, logs the data on the XT, and finally produces plots of the paths of the predicted plume trajectories on the user's printer. The entire process takes less than 20 minutes.

PLOTS OF PROJECTED PLUME TRAJECTORIES

Following the format of Smith (1980), trajectories at different pressure-altitudes for a single hypothetical eruption time are plotted as a map on a single 8½-by-11-inch sheet. The map shows the paths traveled by ideal particles released above the volcano at different pressure-altitudes at the hypothetical eruption time indicated on the plot (figs. 1 and 2). Symbols along the paths indicate positions of the particles at 3-hour time intervals. Stronger winds will blow the particles faster along their paths, and the symbols will be spaced correspondingly farther apart than for light winds. By plotting

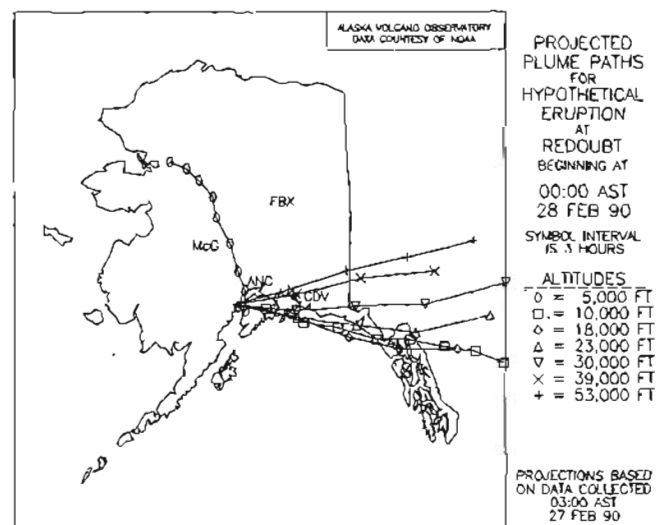


Figure 1. Example of predicted plume trajectories plotted over the State of Alaska for a hypothetical eruption beginning at 00:00 Alaska Standard Time (AST), February 28, 1990. Cordova (CDV), McGrath (McG), Fairbanks (FBX), and Anchorage (ANC) are approximately located. Trajectories for ideal particles released at various pressure-altitudes above Redoubt Volcano are plotted. The location of the symbols on the trajectory paths indicate the positions of the ideal particles at 3-hour intervals after eruption time.

all trajectories on a single map, the user can quickly visualize where the ash is likely to go without paging back and forth between seven plots of trajectories at individual altitudes. The data are plotted on maps of two different scales. One covers Alaska (fig. 1), and the second covers Cook Inlet and surrounding areas (fig. 2).

USE OF PREDICTED PLUME TRAJECTORIES

Users of the projected plume trajectories must understand that the trajectories give only a general indication of where ash will travel. The accuracy of the trajectories is limited by the accuracy of the predicted winds and the model's assumption of a weightless, dimensionless particle. For instance, the plots always show a travel path extending for 24 or more hours for an ideal particle. Users need to be informed that, although they may lie in the path of the ideal particle as indicated by the plot, gravity will likely cause the actual, non-ideal ash to settle before it reaches them.

The model also does not consider the effect of dispersion of the ash as it travels along the trajectory. Users should not be fooled into thinking that they will not be affected by ash simply because they are not located directly on the line predicted by the model. Until current research (Sparks and others, this volume; Stunder and Heffter, this volume; Tanaka, this volume) is incorporated into the model, we suggest qualitatively defining the area that may be affected by ash as an arc of $\pm 30^\circ$ along the trajectory as it travels away

from the volcano. This would also allow for inaccuracies in the predicted trajectory.

For small to moderate size eruptions, such as those at Redoubt, the major factor in the path's accuracy is the accuracy of the predicted winds. Rather than focusing attention on one plot at a given altitude, users should look through the suite of plots for each day to develop an idea of the stability of the weather system. Stable systems will generally have all trajectories for all altitudes, except perhaps 5,000 ft, traveling in about the same direction. The effects of the 5,000-ft trajectory are usually ignored both because the erupting vents at most volcanoes are usually above 5,000 ft in altitude and because they usually eject ash into higher altitudes where the winds are generally stronger. For stable systems, where the winds above 10,000 ft blow in the same general direction throughout the day, we feel the accuracy of the predicted winds to be quite good. Such was the case for the February 24, 1990, eruption of Redoubt (fig. 3). On days when the winds change or even reverse direction, it may be difficult to predict with any certainty where ash will travel (fig. 4). It is best to err on the side of caution during such times. Heffter and others (1990) provide a more detailed analysis of the accuracies of the trajectories.

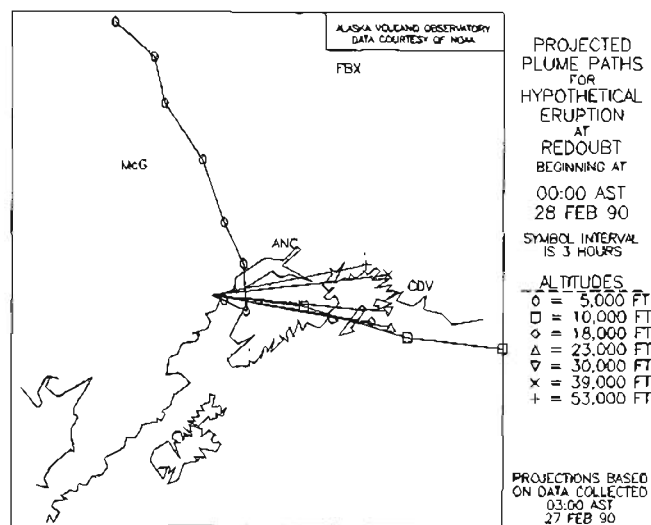


Figure 2. Example of predicted plume trajectories in figure 1 plotted over a map of Cook Inlet and surrounding areas for a hypothetical eruption beginning at 00:00 Alaska Standard Time (AST), February 28, 1990. Cordova (CDV), McGrath (McG), Fairbanks (FBX) and Anchorage (ANC) are approximately located.

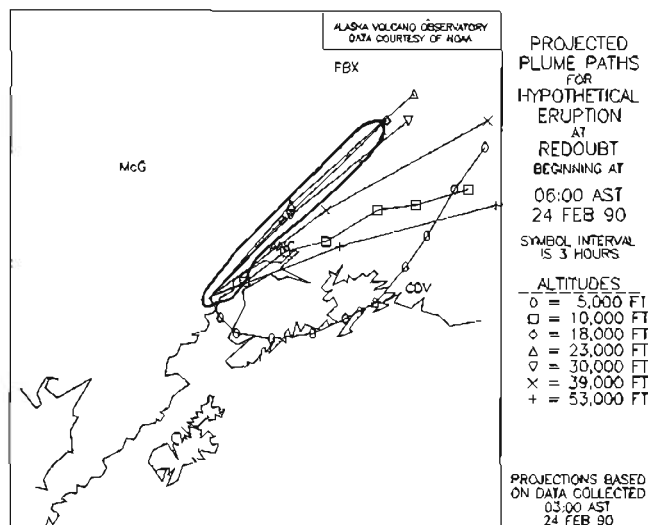


Figure 3. Predicted plume trajectories for the February 24, 1990, eruption of Redoubt Volcano with the actual ground deposition (heavy line) outlined (from Scott and McGimsey, in press). Because the eruption plume reached an altitude of only 28,000 ft (Brantley, 1990), the winds at 39,000 and 53,000 ft did not affect ash deposition. Note that the spacing between symbols for the winds at 18,000, 23,000, and 30,000 ft are more than twice that for winds at 5,000 and 10,000 ft—this indicates that the wind speed at higher altitudes is more than twice that at lower altitudes. For this reason, the pattern of ground deposition was influenced predominantly by the winds at 18,000, 23,000, and 30,000 ft. Cordova (CDV), McGrath (McG), Fairbanks (FBX) and Anchorage (ANC) are approximately located.

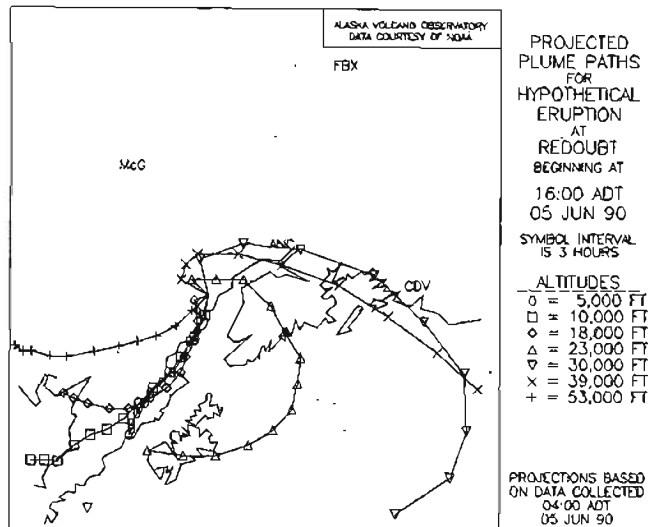


Figure 4. Plot showing the difficulty in determining where ash will travel when wind directions are expected to change. The 23,000- and 30,000-ft altitudes show the ash first going north and then curling to the southeast. The winds at 10,000- and 18,000-ft altitudes move the ash south as it falls through those altitudes. Note also that the spacing between symbols is significantly less than that in figure 3, indicating that the winds are much milder than on February 24, 1990. With this pattern of plume trajectories, it is not possible to say much more than the ash is likely stay in the Cook Inlet area (because of the low wind speed) and could affect any or all of the area. Cordova (CDV), McGrath (McG), Fairbanks (FBX) and Anchorage (ANC) are approximately located.

Major eruptions (such as the June 15, 1991, eruption of Mt. Pinatubo, Philippines, or those with strong horizontal wind components, such as the May 18, 1980, blast of Mount St. Helens) are special cases. They can disperse large quantities of ash in any or all directions for many kilometers before prevailing winds control the path traveled by the ash (Self and Walker, this volume).

CONCLUSIONS

Projected plume trajectories are an important tool for mitigating hazards associated with ashfall resulting from volcanic eruptions. This is the only currently used method

that predicts plume paths before an eruption. By simplifying the procedure to obtain plume-trajectory data, we enabled AVO and WSFO to obtain trajectory plots on a routine basis. AVO included the trajectory information in its daily updates that were sent to various governmental agencies and businesses (including Anchorage International Airport, where authorities distributed them to all 26 carriers located there) (Casadevall, in press). In the event of an eruption, projected plume paths were ready for immediate distribution. Thus, AVO and WSFO were able to make full use of predicted plume trajectories, both before and after eruptions.

We recommend that the ARL model be improved to include the effects of dispersion and gravity on volcanic ash. Such improvements would greatly enhance the effectiveness of plume trajectories without adding to the operational cost of acquiring them.

REFERENCES CITED

- Brantley, S.R., ed., 1990, The eruption of Redoubt Volcano, Alaska, December 14, 1989–August 31, 1990: U.S. Geological Survey Circular 1061, 33 p.
- Casadevall, T.J., in press, The 1989–1990 eruption of Redoubt Volcano, Alaska: Impacts on aircraft operations: *Journal of Volcanology and Geothermal Research*.
- Heffter, J.L., Stunder, B.J.B., and Rolph, G.D., 1990, Long-range forecast trajectories of volcanic ash from Redoubt Volcano eruptions: *Bulletin American Meteorological Society*, v. 71, no. 12, p. 1731–1738.
- Miller, C.D., Mullineaux, D.R., and Crandell, D.R., 1981, Hazard assessments at Mount St. Helens, in Lipman, P.W. and Mullineaux, D.R., eds., *The 1980 Eruptions of Mount St. Helens*, Washington: U.S. Geological Survey Professional Paper 1250, p. 789–802.
- Scott, W.B., and McGimsey, R.G., in press, Character, mass, distribution, and origin of tephra-fall deposits of the 1989–1990 eruption of Redoubt Volcano, south-central Alaska: *Journal of Volcanology and Geothermal Research*.
- Smith, W.K., 1980, A plotting program for producing ashfall prediction maps from output of the NOAA forecast trajectory program: Application to examples from the 1980 Mount St. Helens eruptions: U.S. Geological Survey Open-File Report 80-2005, 36 p.

A MESOSCALE DATA ASSIMILATION SYSTEM ADAPTED FOR TRAJECTORY CALCULATIONS OVER ALASKA

By Thomas W. Schlatter and Stanley G. Benjamin

ABSTRACT

Soon after a volcanic eruption, it is possible to locate the ash plume from satellite imagery, at least if the sky is clear. However, as the plume disperses and thins, remote detection becomes more difficult. A series of numerical analyses of atmospheric observations, which can supply wind data to a trajectory model at frequent intervals, is one way to accurately track the ash plume.

National Oceanic and Atmospheric Administration's (NOAA) Forecast Systems Laboratory has developed a mesoscale analysis and prediction system (MAPS) for assimilating surface and tropospheric weather observations over the contiguous United States every 3 hours. Designed to serve aviation and local nowcasting, MAPS was implemented at the National Meteorological Center in 1992. It relies heavily on automated aircraft reports supplied by Aeronautical Radio, Inc. (ARINC) through the aircraft communications addressing and reporting system (ACARS). These reports use isentropic coordinates (surfaces of constant potential temperature) in the free atmosphere and terrain-following coordinates near the ground.

MAPS is being adapted for use over Alaska where a special high-resolution topography field has been created to account for the rough terrain. However, more ACARS reports over all of Alaska must be collected in real time so that the tropospheric and lower stratospheric wind field can be adequately defined every few hours.

INTRODUCTION

When a volcano spews ash high into the atmosphere, it is not difficult to identify the location of the eruption unless dense clouds hide the ash plume from satellites. If the eruption is sufficiently powerful, ash may enter the stratosphere, above the clouds. Aircraft in the immediate vicinity of the eruption are subject to the life-threatening hazard of engine shutdown. Other substantial hazards remain long after the eruption, sometimes far from its origin, and aircraft must avoid the drifting ash plume. It is important, therefore, to know where the plume is and where it is likely to drift.

Satellites can track the ash plume as long as it can be detected. However, after the plume spreads and disperses, tracking becomes more difficult, and the levels where ash is concentrated are hard to discern. Trajectories calculated from a series of wind analyses or from a numerical forecast are solutions to the problems of tracking and predicting the plume location.

Trajectories are only as accurate as the analyses and forecasts on which they depend. At NOAA's Forecast Systems Laboratory, in Boulder, Colo., a team of meteorologists, a mathematician, and a systems programmer have been working for several years to develop a mesoscale analysis and prediction system (MAPS), which exploits several sources of atmospheric observations that are available almost continuously. Even now, analyses of upper-air conditions from the National Meteorological Center (NMC), in Washington, D.C., are available only twice a day, at 00:00 and 12:00 UTC. Over the contiguous 48 United States, sufficient observations are available to support upper-air analyses every 3 hours. MAPS assimilates these surface and tropospheric observations every 3 hours to better describe atmospheric conditions and make accurate short-term forecasts out to 12 hours.

A version of MAPS for the lower 48 States is already running experimentally at the National Meteorological Center, and another version is being developed for Alaska. The analyses and predictions from MAPS can be used as input for trajectory calculations whenever Alaskan volcanoes erupt. Simkin and others (1981) list 39 volcanoes on the Aleutian Islands, 27 on the Alaskan Peninsula, and 18 elsewhere in the State as being active at least once during the past 10,000 years. Beget and others (1991) estimate that Alaskan eruptions large enough to disrupt air traffic have an average recurrence interval of 5–10 years. The eruption of Redoubt Volcano on the west side of Cook Inlet during 1989 and 1990 is a recent example (Brantley, 1990).

In this paper, we describe how MAPS works, why it is useful for trajectory calculations, how it compares to the nested grid model (NGM) (the limited-area model currently in use at NMC), how MAPS is being adapted for use over Alaska, and some changes that must be made before the

Alaska version performs as well as the version for the lower 48 States.

HOW MAPS WORKS

MAPS provides high-frequency analyses and short-range forecasts that incorporate "off-time" observations as well as synoptic observations (at 00:00 and 12:00 UTC). The current resolution of the MAPS grid is 60 km. The main users of MAPS are commercial aviation and operational forecasters who need short-term guidance for 6–12 hours into the future. The main components of MAPS are shown in figure 1.

EXTERNAL DATA SOURCES

The upper-air assimilation system relies on two external sources of data: (1) a variety of meteorological observations from the surface, troposphere, and lower stratosphere (see following section), and (2) time-dependent boundary conditions supplied by NMC's nested grid model (NGM).

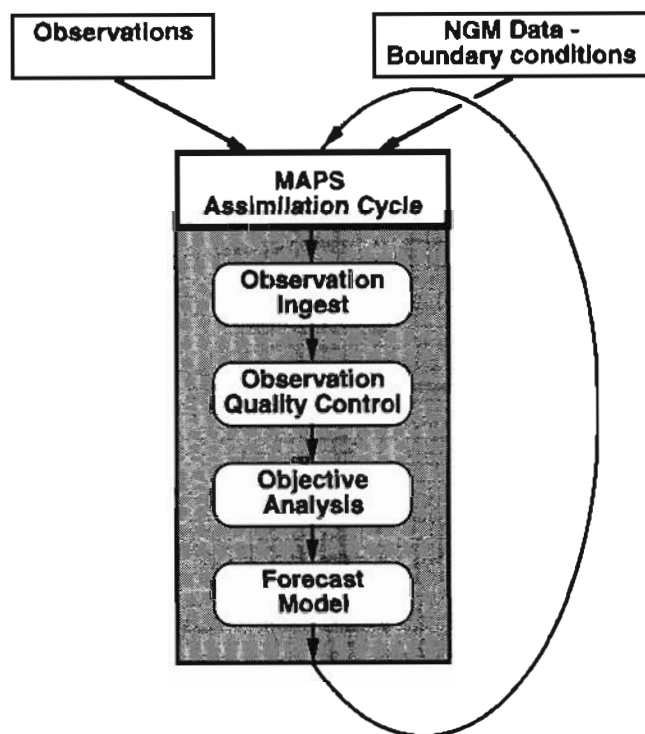


Figure 1. The major components of the mesoscale analysis and prediction system (MAPS). The upper-air assimilation cycle is self-contained except for the external inputs noted at the top. Observations of wind, temperature, pressure, and humidity by balloons, aircraft, radars, or observers are included. NGM, nested grid model at the National Meteorological Center, which supplies time-dependent lateral boundary conditions for the MAPS forecast model.

These boundary conditions are needed for the MAPS hybrid prediction model. They specify the evolution of the variables along the four edges of the forecast area, which pass through southern Canada, northern Mexico, and the coastal waters of the Atlantic and Pacific Oceans.

OBSERVATIONS

The upper-air assimilation cycle begins with the incorporation of observations from four major sources in the contiguous United States and adjacent portions of Canada and Mexico:

- **Rawinsondes**—About 80 every 12 hours, providing observations of winds, altitudes, temperatures, and moisture.
- **Wind profiler demonstration network** in the Central United States—Twenty of the 30 expected profilers were operating by mid-December 1991. Wind profiling radars provide accurate hourly profiles of the horizontal wind in the troposphere and lower stratosphere.
- **Surface observations**—Six hundred to 900 surface observations per hour depending on the time of day plus about 25 moored buoys. These observations are used to analyze low-level altitudes, winds, temperatures, and moisture.
- **ACARS aircraft reports**—These are fully automated reports of wind and temperature collected from the airlines by ARINC (Aeronautical Radio, Inc.) and made available through ACARS, the ARINC aircraft communications addressing and reporting system. An average of 380 to 1,550 reports were available every 3 hours during December 1991 (fig. 2). For peak travel time, the density of reports can be quite remarkable (fig. 3).

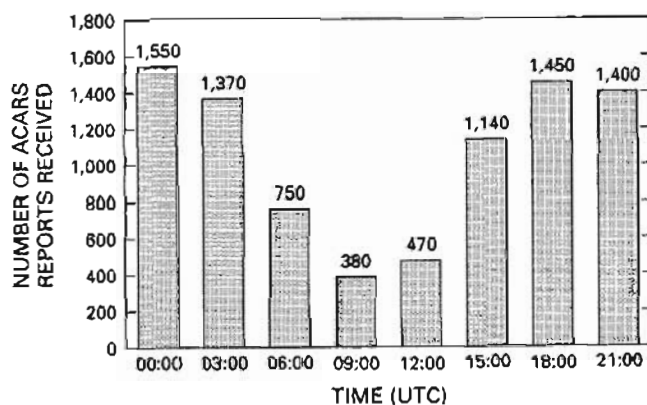


Figure 2. Average number of fully automated ACARS aircraft reports received in 3-hour windows during December 1991. There are peaks in air traffic at midday and during the late afternoon.

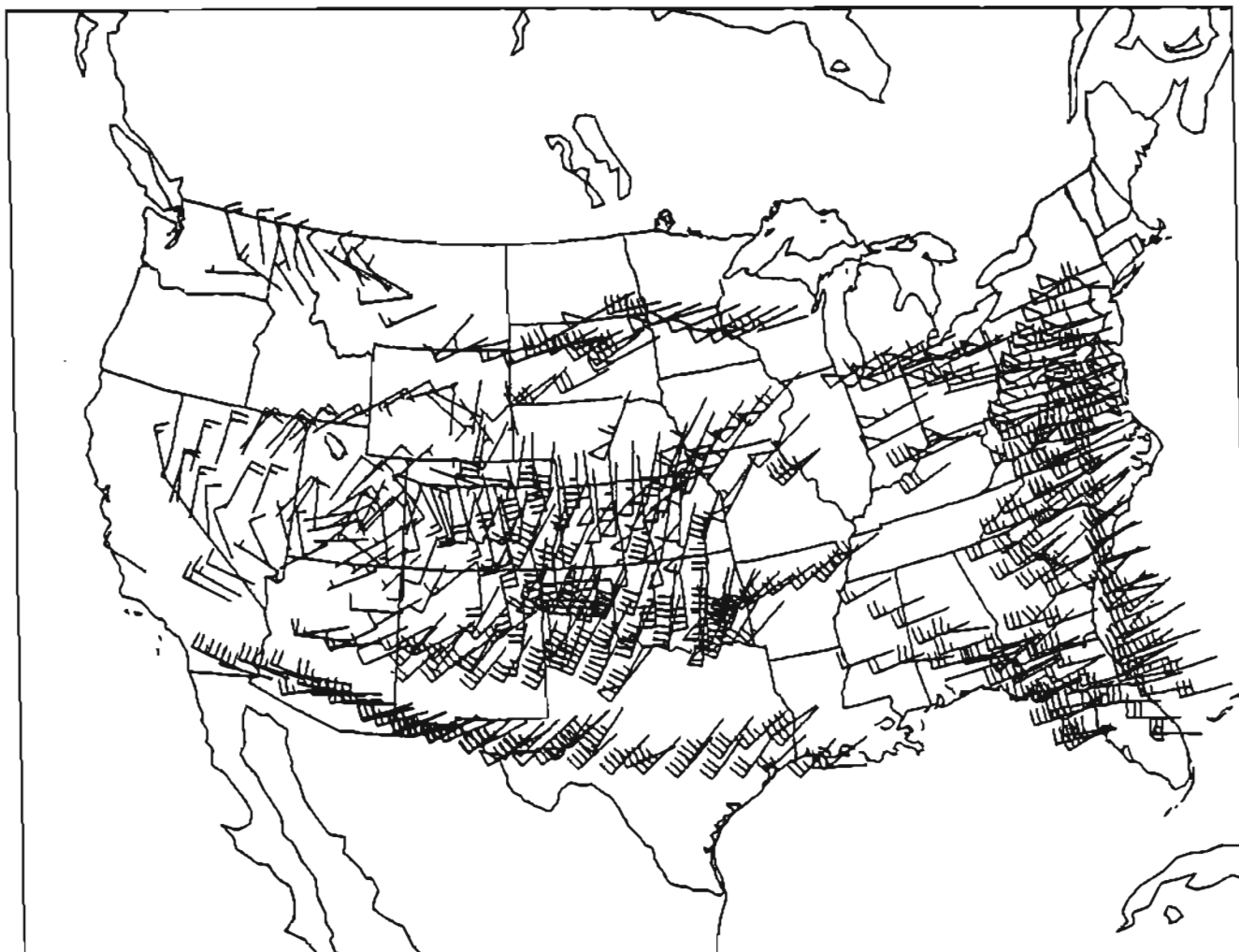


Figure 3. ACARS aircraft reports from between 175 and 225 mb (from 36,000 to 41,000 ft altitude) received between 16:30 and 19:30 UTC 19 January 1990. This represents 40 percent of the number received at all levels. The data plot is interpreted as follows: The staff extends into the wind; thus, winds along the East Coast are approximately from the west. Barbs on the staff give wind speed: small barbs represent 5 m/s; full barbs represent 10 m/s; and flags represent 50 m/s. The observations depict a jet stream from Kansas to the mid-Atlantic States.

ACARS observations are the single most important synoptic data source for the MAPS 3-hour assimilation cycle (Benjamin, 1991). They are numerous, distributed fairly evenly over the lower 48 States, and are mostly from between 400 and 150 millibars (mb) (altitudes between 24,000 and 45,000 ft). Some ascent and descent data are also available. These will soon become much more common and will be triggered as aircraft pass through specified altitudes. Profilers provide excellent wind data in the lower troposphere, an area where ACARS reports are still sparse.

Satellite radiances (values of upwelling radiation measured in different wavelength intervals) offer the hope of estimating layer temperatures and vertically integrated moisture content. So far, we have been unable to demonstrate that

this data source improves analyses or forecasts when the other sources of data are present. However, over Alaska, where observations are sparse in comparison to the lower 48 States, radiances from the polar-orbiting television and infrared observation satellites (TIROS) may prove more valuable. Satellite data are not assimilated in the present version of MAPS.

All incoming observations are subjected to several stages of quality control. The most rigorous of these is a "buddy" check. At each observation location, a value from neighboring observations is interpolated. If the interpolated value differs significantly from the observed value at that point, we run further tests to determine whether the central observation or one of its neighbors is at fault.

OBJECTIVE ANALYSIS

For a meteorologist, the words "objective analysis" refer to a programmable method for estimating meteorological parameters on a regular set of points, usually a three-dimensional grid. The estimates depend upon the available observations, which are usually distributed irregularly in space and time. Numerical prediction models are often made part of the objective analysis for the reasons mentioned in the next section. In the case of MAPS, a 3-hour numerical forecast, valid at the analysis time, provides a first guess for the analysis.

The method of objective analysis employed in MAPS is known as optimum interpolation and is statistical in nature. The method, popularized by Gandin (1963) and still widely used, accounts for the errors in different observing systems. It also accounts for the geographical distribution of stations relative to each other and to the point being analyzed and allows observations of one variable to influence the analysis of another. For example, observations of the altitude of constant pressure surfaces influence the analysis of wind. Finally, the method mixes information from the forecast model and observations in a logical way.

NUMERICAL PREDICTION MODEL

A numerical prediction model is an essential component of any system that assimilates meteorological data. First, the equations in these models summarize our understanding of atmospheric behavior. Second, our best a priori estimate of the current state of the atmosphere comes from a numerical prediction model, which provides the background for subsequent analysis. Moreover, the statistics of model performance tell us how to weight the model prediction (i.e., the background) relative to the observations. Third, the model imposes dynamic consistency on the system and retains the effects of all past observations.

The prediction model in MAPS is an outgrowth of the model introduced by Bleck (1984) and is based on the so-called primitive equations. These consist of three prognostic equations (for thermodynamic energy and the two components of horizontal momentum) and three diagnostic equations (the ideal gas law, the mass continuity equation, and the hydrostatic approximation). Calculations for both the analysis and the prediction are performed on a 60-km grid at each of 25 vertical levels. The model allows for stratiform and convective precipitation; turbulent transfer of heat, momentum and moisture in the vertical; and a diurnal heating cycle (Benjamin, Brewster, and others, 1991; Benjamin, Smith, and others, 1991).

Figure 4 summarizes the assimilation cycle. New observations are introduced every 3 hours, followed by a 3-hour forecast, which extrapolates atmospheric conditions forward to the next analysis time. Twice daily, at 00:00 and 12:00

UTC, the forecast runs out to 12 hours, mainly for comparison with NMC's nested grid model. As soon as NGM results are available, the time-dependent lateral boundary conditions for the MAPS domain are updated.

USING MAPS FOR TRAJECTORY CALCULATIONS

MAPS itself does not compute trajectories; rather, it supplies a series of analyzed or predicted wind fields to NOAA's Air Resources Laboratory, in Washington, D.C., which has long experience in generating trajectories. See Stunder and Heffter (this volume) for details on trajectory calculations.

Why should wind fields from MAPS be particularly good for the generation of trajectories? The immediate answer is that frequent assimilation of "off-time" observations permits sharper definition of mesoscale flow features that are tens to hundreds of kilometers in size, thus leading to a more accurate wind field.

A less obvious answer is related to the choice of vertical coordinate. Analyses and predictions in MAPS are computed in hybrid vertical coordinates (Benjamin, Smith, and others, 1991), which are a combination of two kinds of coordinates. In the free atmosphere, we use isentropic coordinates (19 surfaces of constant potential temperature). In adiabatic flow when there are no heat sources or sinks, air on a particular isentropic surface will remain on that surface. Under this assumption, trajectory calculations become two-dimensional. The vertical spacing of isentropic coordinates is tied to the stability of the atmosphere; the surfaces are close together when the atmosphere is stably stratified and widely

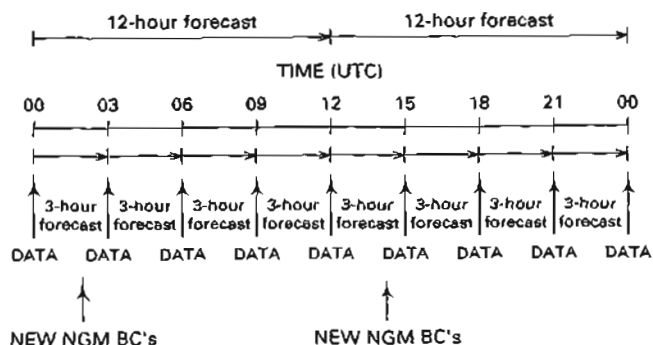


Figure 4. A 3-hour assimilation cycle. Every 3 hours, newly observed data are used to analyze atmospheric conditions. These analyses supply the initial conditions for a numerical prediction, which advances the atmospheric state forward to the next analysis time, when another batch of observations is assimilated. Twice a day, at 00:00 and 12:00 UTC, the forecast goes out to 12 hours. Each time the nested grid model (NGM) runs at NMC, a new set of time-dependent lateral boundary conditions (BC) replaces the old set.

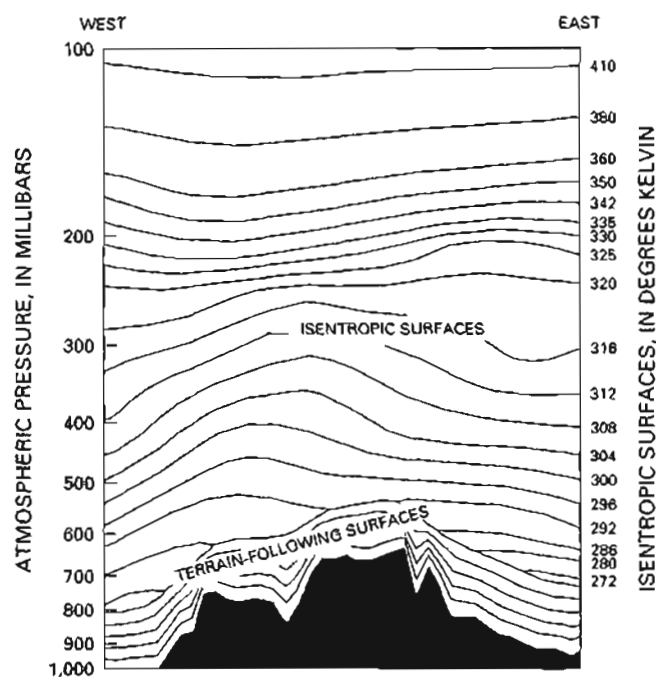


Figure 5. An illustration of the hybrid vertical coordinates used in MAPS. This vertical cross section was taken at 12:00 UTC 1 February 1990. It runs from the Pacific Ocean, off the Oregon coast on the left, to South Dakota, on the right. Terrain is silhouetted in black. Six terrain-following surfaces, each higher one smoother than the one below, occupy, on average, the first 150 mb above ground. In the free atmosphere, up to 19 isentropic surfaces with variable spacing (generally from 4 to 10 degrees Kelvin) are used for computation.

spaced when the lapse rate (decrease of temperature with altitude) is steep. This property gives enhanced spatial resolution where it is needed, such as in the vicinity of atmospheric fronts and jet streams.

One drawback of isentropic coordinates is that they become too widely spaced in deep, well-mixed boundary layers, which develop often on hot summer days and over elevated terrain. To overcome this drawback, terrain-following coordinates are used, spaced about 30 mb (or roughly 300 m) apart, on average, for the lowest six surfaces. This gives reasonable precision in the calculation of vertical fluxes of momentum, heat, and moisture close to the ground. The hybrid coordinate system is illustrated in figure 5. The surfaces move up or down depending upon atmospheric conditions; hence, this depiction is for a specific time and date.

PERFORMANCE: MAPS VERSUS NGM

In a recent comparison between MAPS and NMC's nested grid model, we interpolated wind predictions by

MAPS and the NGM to rawinsonde sites in the United States and southern Canada. We then computed the magnitude of the vector difference between predicted and observed winds. The root-mean-squares of these differences appear in figure 6 as a function of pressure level. The most striking result is that 3-hour and 6-hour MAPS wind forecasts are consistently better than the 12-hour NGM forecasts that are valid at the same time. This is true at all levels, but it is especially true at altitudes between 24,000 and 45,000 ft (or, equivalently, between 400 and 150 mb on fig. 6) where commercial jets provide most of the ACARS data. This demonstrates clearly the advantage of frequent assimilation of off-time data. The choice of isentropic coordinates is also an advantage; these coordinates tend to crowd together and give good vertical resolution in the high troposphere and lower stratosphere in the vicinity of the jet stream.

During 1992, MAPS ran experimentally in real time on NMC's Cray Y-MP supercomputer on a domain covering the lower 48 States. Output stored on disks at NMC was carefully examined for evidence of mistakes in the computer code. By late 1992, the system was running reliably and performing well. Preliminary tests of an Alaskan version of MAPS are scheduled for 1993 at the Forecast Systems Laboratory in Boulder, Colo. If the available data show that a 3-hour assimilation cycle over Alaska is viable, more rigorous testing could begin at NMC.

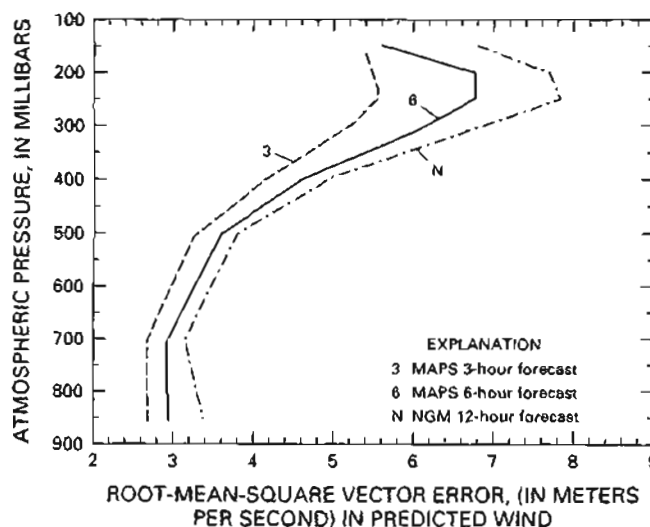


Figure 6. The root-mean-square vector error in wind forecasts produced by MAPS and the NGM. The error was estimated by comparing predicted winds with winds measured by rawinsonde in the United States and southern Canada from 26 November through 29 December 1991. All three forecasts shown are valid at the same time.

ADAPTING MAPS FOR USE OVER ALASKA

Alaska has far greater topographical relief than any of the lower 48 States. It also has a longer, more convoluted shoreline. The terrain-following surfaces used in MAPS conform to the rough topography as closely as the horizontal resolution allows. Our first experiments over Alaska will employ "envelope" topography, obtained from a file of

very high resolution topography in the following way. For each grid box of the prediction model, one adds the standard deviation of altitude to the mean altitude. Envelope topography accounts for the fact that mountain barriers to the wind are higher than the mean altitude. The MAPS domain for Alaska and envelope topography for a 60-km grid are shown in figure 7.

Roughly 50 percent of the domain in figure 7 is covered by ocean. The observation sources currently contributing to

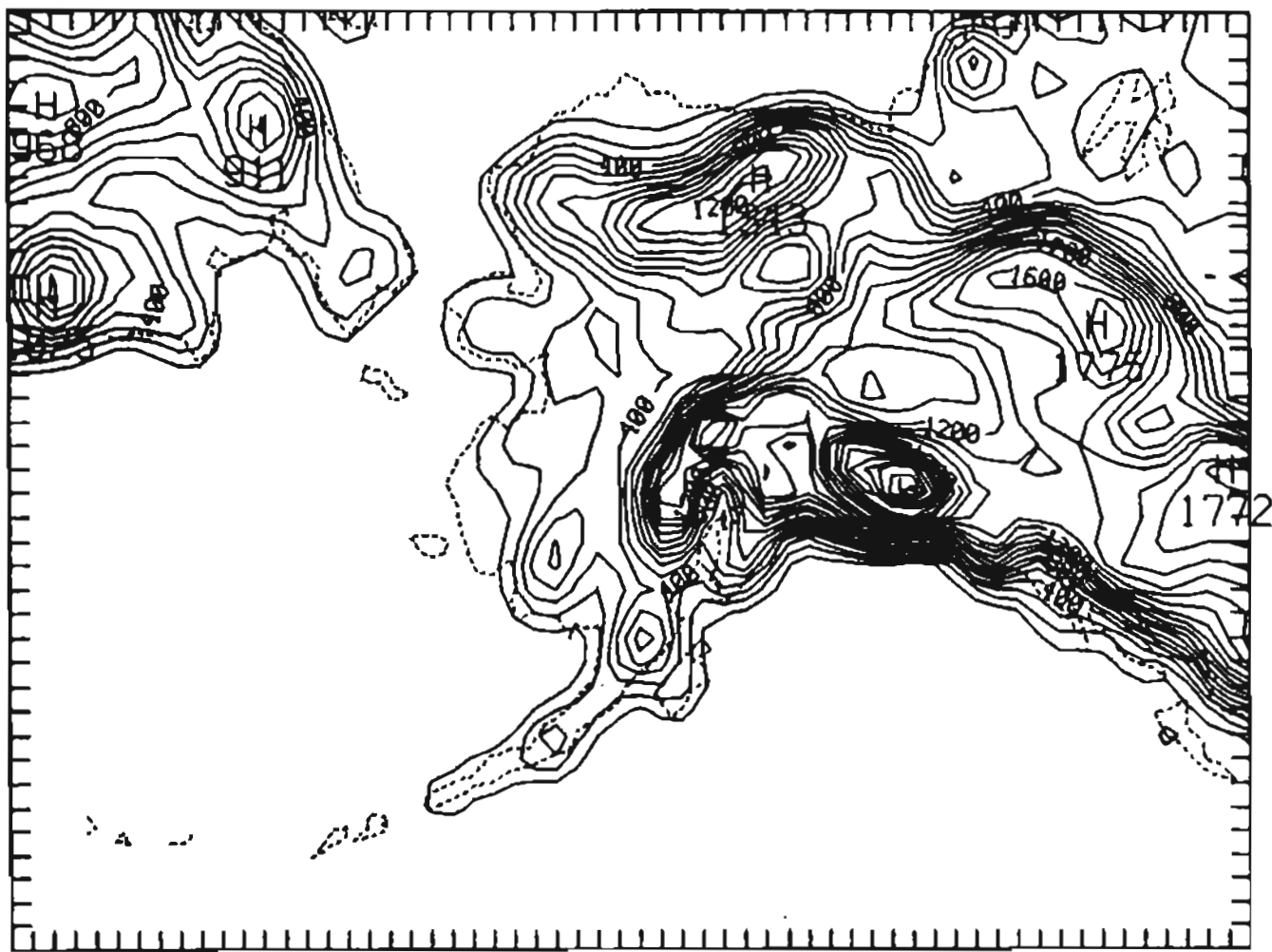


Figure 7. The geographical domain for the Alaska version of MAPS. Tick marks around perimeter are at 60-km spacing. Elevation contours for envelope topography (see text) are at 100-m intervals.

MAPS will supply scant information over the ocean because ACARS data are acquired only within a few hundred kilometers of a ground station. To improve analyses in oceanic regions, it will be necessary to adapt MAPS for assimilation of ship reports and TIROS radiance data. In addition, the western boundary of the NGM is so close to Alaska that the inflow conditions are likely to be poorly defined, thus quickly contaminating the forecast. To correct this problem, we also must replace the time-dependent lateral boundary conditions from the NMC's nested grid model with those from the aviation (global spectral) model.

CONCLUDING REMARKS

MAPS is a system for the frequent assimilation of diverse surface, tropospheric, and lower stratospheric weather data. The system provides frequent updates on atmospheric conditions to aviation and local forecasters. A wealth of wind reports available from wind profilers and commercial jets permits detailed analyses every 3 hours and accurate short-term predictions of winds over the lower 48 States. These 3-hour "snapshots" and corresponding predictions can feed into trajectory calculations for tracking volcanic plumes and predicting their future movement (Stunder and Heffter, this volume).

One major obstacle prevents immediate application of MAPS over Alaska: the lack of data. Many aircraft fly over Alaska, and the Aleutian chain is a major international route. While many of these aircraft are equipped to provide automated reports, as of summer 1991, the only ground station for receipt of these reports was at Anchorage. In the same way that thousands of ACARS reports per day make MAPS a viable system for the lower 48 States, a similar density of reports is required for the Alaskan version.

The Federal Aviation Administration and Aeronautical Radio, Inc. are helping to alleviate this problem. As of January 1993, nine more ground receiving stations are operating in Alaska: at Shemya, Adak, Dutch Harbor, Cold Bay, St. Paul Island, Bethel, King Salmon, McGrath, and Fairbanks. By late 1993, eight more are expected in southeast Alaska and northwest Canada. This will greatly increase the number of reports. Efforts should also be made to obtain over-water reports relayed by satellite. Until about 100 reports can be collected every hour, reasonably distributed over the domain of figure 7, we should not expect that

a rapid-update assimilation cycle will improve upon the operational 12-hour forecasts that are already available.

ACKNOWLEDGMENTS

We thank our colleagues, Patty Miller, Tracy Smith, and Kevin Brundage and long-term visitors Jean-Marie Carriere and Pan Zaitao for their assistance in developing MAPS. We acknowledge the help of the Facilities Division of the Forecast Systems Laboratory in decoding ACARS reports. This project is funded by the National Weather Service.

REFERENCES CITED

- Beget, J.E., Swanson, S.E., and Stone, D., 1991, Frequency and regional extent of ash eruptions from Alaskan volcanoes [abs.], in Casadevall, T.J., ed., *First International Symposium on Volcanic Ash and Aviation Safety*, U.S. Geological Survey Circular 1065, p. 13.
- Benjamin, S.G., 1991, Short-range forecasts from a 3h isentropic-sigma assimilation system using ACARS data: Boston, Mass., American Meteorological Society, Proceedings, Fourth International Conference on Aviation Weather Systems, 24-28 June, Paris, France, p. 329-334.
- Benjamin, S.G., Brewster, K.A., Brummer, R., Jewett, B.F., Schlatter, T.W., Smith, T.L., and Stamus, P.A., 1991, An isentropic three-hourly data assimilation system using ACARS aircraft observations: *Monthly Weather Review*, v. 119, p. 888-906.
- Benjamin, S.G., Smith, T.L., Miller, P.A., Kim, D., Schlatter, T.W., and Bleck, R., 1991, Recent improvements in the MAPS isentropic-sigma data assimilation system: Boston, Mass., American Meteorological Society, Proceedings, Ninth Conference on Numerical Weather Prediction, 14-18 October, Denver, Colo., p. 118-121.
- Bleck, R., 1984, An isentropic coordinate model suitable for lee cyclogenesis simulation: *Estratto dalla Rivista di Meteorologia Aeronautica*, v. 44, p. 189-194.
- Brantley, S.R., ed., 1990, The eruption of Redoubt Volcano, Alaska, December 14, 1989-August 31, 1990. U.S. Geological Survey Circular 1061, 33 p.
- Gandin, L.S., 1963, Objective analyses of meteorological fields: Leningrad, *Gidrometeorologicheskoe Izdatel'stvo*, [original in Russian, translated in 1965 by Israel Program for Scientific Translations], 242 p.
- Simkin, T., Siebert, L., McClelland, L., Bridge, D., Newhall, C., and Latter, J.H., 1981, *Volcanoes of the World*: Stroudsburg, Pa., Hutchinson Ross Publishing Co., Smithsonian Institution, 240 p.

DEVELOPMENT OF A PREDICTION SCHEME FOR VOLCANIC ASH FALL FROM REDOUBT VOLCANO, ALASKA

By Hiroshi L. Tanaka

ABSTRACT

The purpose of this project is to develop a volcanic plume prediction model for volcanoes located in the Cook Inlet area, Alaska. Knowing where the ash plume is and predicting where it will go are important for public health and safety, as well as for flight operations and mitigating economic damage. For near-real-time plume prediction, acquisition of upper-air wind data is the essential part of the prediction scheme.

In this project, near-real-time meteorological data are provided by the National Meteorological Center, transmitted via Unidata. Reading the real-time and forecast wind data, the prediction model computes advection, diffusion, and gravitational fallout for the plume particles from the vertical column over the volcano. Three-dimensional dispersal of plume particles are displayed on the computerized graphic display as a function of time following the eruption. The model predictions appear on the screen about 15 minutes after the eruption report, showing the geographical distributions of plume dispersal for the following several hours. Although the model simulation inevitably has forecast errors owing largely to errors in the forecast wind input, the prediction product offers a useful guide for public safety, especially for the Cook Inlet area, Alaska.

INTRODUCTION

Anchorage, Alaska is one of the focal points of international aviation activities. The city lies close to several active and potentially active volcanoes including Hayes, Spurr, Redoubt, Iliamna, Augustine, and Douglas along the west shore of Cook Inlet, and Wrangell Volcano to the east. In this century Spurr, Redoubt, and Augustine together have had eight significant eruptions that have spread ash over a broad area of south-central Alaska. It is necessary to establish a reliable scheme for predicting the distribution of volcanic ash fall after an eruption in order to avoid unnecessary disruptions of aircraft operations. For the plume prediction to be operational, an immediate eruption report and real-time

upper-air data must be available. A quick response is one of the priorities of the plume-prediction system.

The Alaska Volcano Observatory (AVO) at the Geophysical Institute, University of Alaska, Fairbanks, has direct access to near-real-time satellite imagery and upper-air weather data (Dean and others, this volume). By combining this information with the established eruption-monitoring network provided by AVO, we have established a volcanic plume prediction model that predicts volcanic ash dispersal as a function of time immediately after the eruption. The upper-air wind data are the fundamental input to the plume-prediction model. The National Meteorological Center (NMC), in Washington, D.C., offers daily weather predictions as well as analyzed and initialized meteorological data on three-dimensional (3-D) gridded mesh. Recently, a national program in atmospheric sciences, referred to as Unidata, enables university researchers to use the real-time NMC data through a satellite downlink (Sherretz and Fulker, 1988; Tanaka, 1991a, 1991b). Therefore, the real-time upper-air wind data are available at AVO.

In response to the eruption of Redoubt Volcano at the end of 1989, a volcanic plume prediction model has been developed within the AVO (Tanaka, 1990). This project incorporates wind data from Unidata for predicting the distribution of volcanic ash plumes on a real-time basis after an eruption is reported. Using the real-time and predicted upper-air data, the model computes advection, diffusion, and gravitational fallout of the ash particles. Three-dimensional distributions of the ash plume are displayed on the computerized graphic display, predicting the direction and dispersion of ash clouds for the first several hours after eruption. This report describes the algorithm of the present particle-tracking model in a Lagrangian framework. The results of the demonstrations and the procedure of the information-transfer network are presented.

UNIDATA

Unidata (University data) is a national program for providing near-real-time meteorological data to university

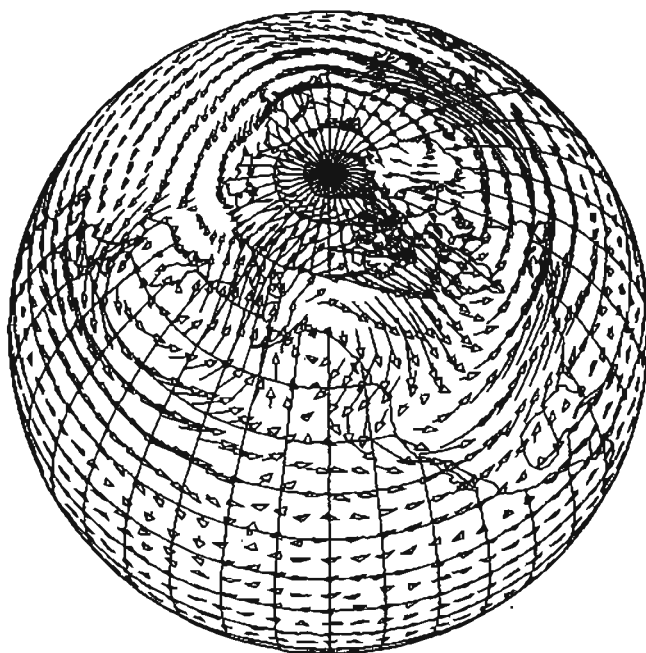


Figure 1. Example of NMC data received at the Alaska Climate Research Center via Unidata showing the global distribution of wind vectors at the 500-mb level, February 3–7, 1989. Length of staff indicates wind speed; pointer indicates wind direction. The horizontal grid interval available for Unidata is 5° for longitude and 2.5° for latitude.

users. The Unidata program center is located in Boulder, Colo., and it is managed by the University Corporation for Atmospheric Research (UCAR). The Unidata program established its own data feed from the National Weather Service operational circuit to distribute the near-real-time and forecast meteorological data for university users. Among the service programs, the NMC provides global analysis data and forecast gridded data. The meteorological data are transmitted by satellite downlink under a contract with Zephyr Weather Information Service.

The NMC meteorological variables of zonal and meridional wind speeds, u and v (m/s); temperature, T (K); geopotential height, ϕ (m); and relative humidity, R (percent) are given at 2.5° latitude and 5.0° longitude grids at 10 mandatory vertical levels of 1,000, 850, 700, 500, 400, 300, 250, 200, 150, and 100 mb over the whole global domain (fig. 1). Those basic meteorological variables are transmitted twice a day, for 00:00 and 12:00 UTC. In every data transmission, the global gridded data include not only the initial conditions for the weather-prediction model (plus 0-hour NMC initial data) but also the data for the forecasting time of 6, 12, 18, 24, 30, 36, 48, and 60 hours, provided by the NMC numerical weather-prediction model. The initialized global data at forecasting time 00:00 may be regarded as observed data.

Figure 2 illustrates a relation between NMC data transmission and the volcanic plume prediction. The twice daily NMC data, including the forecast data, are stored and

continuously updated in the computerized database. The database always consists of past observed data and forecast data for 2 to 3 days ahead. Therefore, when an eruption is reported, the prediction model can use the present and future upper-air data for the computation of plume advection. The forecast upper-air wind data for a 1-day prediction are typically as good as the analyzed wind data (Kalnay and others, 1990), even though the analysis data often contain considerable discrepancy from the real upper-air wind.

As an example, figure 3 compares the analyzed wind field (solid arrows) at the 500-mb level with the corresponding wind field for the 24-hour forecast from 1 day before (dashed arrows). The differences appear to be minor for this example, suggesting that the forecast wind field is useful for real-time plume prediction. However, the accuracy of the predicted wind depends on the weather situation. For example, the prediction is generally good when a persistent, blocking, high-pressure system stays near Alaska, but the prediction is poor when a low-pressure system is passing the Cook Inlet. Moreover, the analyzed wind field, interpolated from the upper-air observations onto the longitude-latitude grids, often contains considerable errors due to the imperfect interpolation technique. Yet, knowing the degree of the analysis error, the NMC upper-air data is still useful for plume prediction when no alternative exists.

DESCRIPTION OF THE MODEL

The volcanic plume prediction model is constructed by an application of pollutant dispersion models (e.g., Prahm and Christensen, 1977; Suck and others, 1978; Kai and oth-

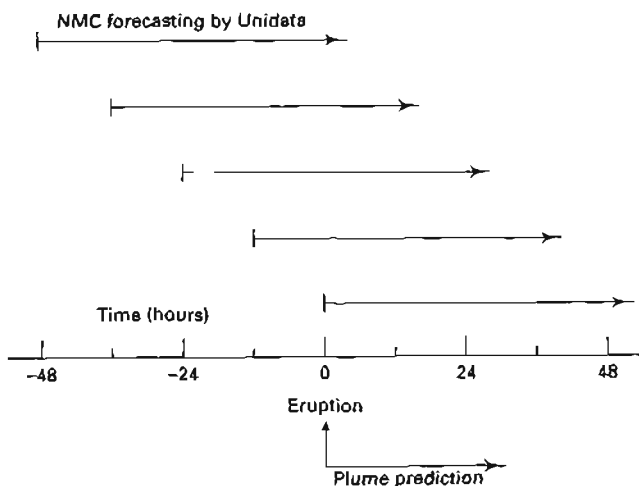


Figure 2. Schematic diagram showing the relation between the twice-daily NMC data transmitted by Unidata and the volcanic plume prediction. Arrow for NMC data describes a data span for the forecasting time from 0 to 48 hours. In response to an eruption report, the volcanic plume prediction model reads the archived NMC database to run the model using real-time wind data.

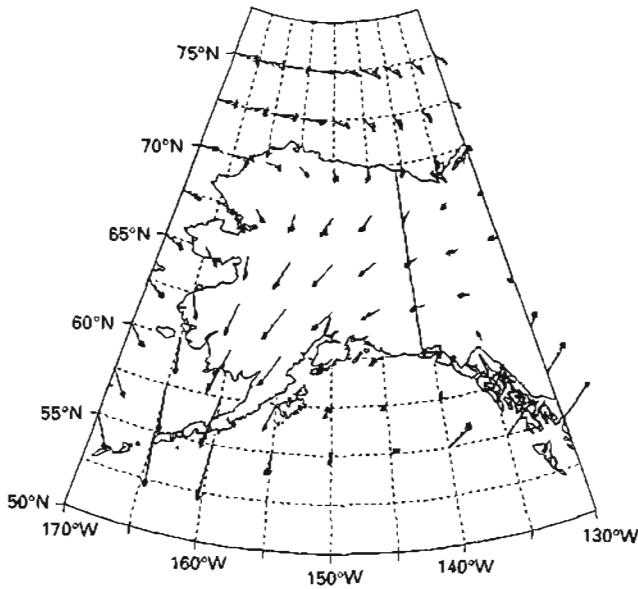


Figure 3. Comparison of analyzed wind vectors (solid arrows) at the 500-mb level and corresponding wind vector of the 24-hour forecast from 1 day before (dashed arrows), the State of Alaska, November 11, 1990. This example indicates the usefulness of the 1-day forecast data, although the wind error can be large depending on the weather situation (see text).

ers, 1988). The model is based on the three-dimensional (3-D) Lagrangian form of the diffusion equation. We assume a vertical column of pollutant source that diffuses along with the Gaussian distribution in the 3-D space. A diffusion approximation of the pollutant turbulent mixing is used with 3-D diffusion coefficients to evaluate the dispersion of pollutant concentration. In the Lagrangian framework, diffusion of plume particles may be described by a random walk process (Chatfield, 1984). Here, the diffusion is simulated by a sufficiently large number of random variables $r_i(t)$, ($i = 1 \equiv M$), representing position vectors of M particles from the origin (the volcanic crater). The diffusion is superimposed on advection and gravitational fallout.

With a discrete time increment, Δt , the Lagrangian form of the governing equation may be written as:

$$r_i(t + \Delta t) = r_i(t) + V\Delta t + Z\Delta t + G\Delta t, \quad i=1 \equiv M \quad (1)$$

where

$r_i(t)$ is a position vector of an i th particle at time t ,

V is the local wind velocity to advect the particle,

$Z = (z_h, z_h, z_v)$ is a vector containing three Gaussian random numbers with its standard deviation (c_h, c_h, c_v) for horizontal and vertical directions, and

G is the gravitational fallout speed approximated by Stokes' law.

Note that the diffusion, $Z\Delta t$, is direction dependent, and the gravity settling, $G\Delta t$, depends on particle size.

For the computation of advection, the wind velocity, V , is obtained from NMC via Unidata. The gridded data are first interpolated in time onto the model's time step. The cubic spline method (Burden and others, 1981) is used up to the 3-hour interval, then a linear interpolation is applied for the 5-minute time steps. The wind velocity at an arbitrary spatial point is evaluated using the 3-D B-splines (Burden and others, 1981) from the nearby gridded data.

For the computation of diffusion, we consider the following diffusion equation in Eulerian form:

$$\frac{\partial q}{\partial t} = K\nabla^2 q \quad (2)$$

where

q is the plume mass density,

∇^2 denotes a Laplacian operator, and

K denotes the diffusion coefficient.

For simplicity in derivation and for uncertainty in the magnitude of K , we consider a one-dimensional case in space along the x -axis. The solution of the diffusion equation for a point source at the origin is given by:

$$q(x, t) = \frac{1}{2\sqrt{\pi Kt}} \exp\left(-\frac{x^2}{4Kt}\right) \quad (3)$$

which may be regarded as a Gaussian distribution with its standard deviation

$$\sigma = \sqrt{2Kt} \quad (4)$$

It is found that the plume dispersal, represented by σ , expands in proportion to \sqrt{t} .

On the other hand, a random walk process in Lagrangian form is defined as:

$$\begin{cases} r(0) &= 0, \\ r(t + \Delta t) &= r(t) + z(t)\Delta t \end{cases} \quad (5)$$

where

$r(t)$ is the position of a particle along the x -axis,

$t = n\Delta t$, ($n = 0, 1, 2, \dots, N$), and

$z(t)$ is the zero-mean Gaussian random number with its standard deviation, c .

For this random walk process, the standard deviation of $r(t)$ is given by:

$$\sigma = c\sqrt{t\Delta t} \quad (6)$$

Comparing these standard deviations in Eulerian form and in Lagrangian form, we obtain a relation between the diffusion coefficient, K , and the diffusion speed, c , as:

$$c = \sqrt{\frac{2K}{\Delta t}} \quad (7)$$

The diffusion velocity depends on the time increment of the discrete time integration. We use $\Delta t = 5$ minutes in this study. We have repeated diffusion tests with various values of K , and the resulting dispersals are compared with satellite images of actual dispersals from Redoubt Volcano. With these diffusion tests, we find that the appropriate diffusion coefficients are $K_h = 10^4$ (m^2/s) and $K_v = 10$ (m^2/s) for the horizontal and vertical directions, respectively. Note that values may be different for other volcanoes.

The diffusion speed may be sensitive to the scale in consideration. For example, the present value of the diffusion coefficient varies as the horizontal scale, which ranges from several hundreds of kilometers to 1,000 km in length. Figure 4 illustrates a result of the diffusion test. The steady plume at the origin spreads downstream of the source under the influence of constant wind. The theoretical standard deviation of the plume dispersal is indicated by the parabolic solid line in the figure.

The gravitational settling is based on Stokes' law as a function of the particle size, d_i . The fallout speed $|G|$ is approximated by the terminal velocity below:

$$|G| = \frac{2\rho g d_i^2}{9\eta} \quad (8)$$

where

ρ is the density of plume particles,

η is the dynamic viscosity coefficient, and

g is the acceleration due to gravity.

We have assumed a constant for $\rho g/\eta = 1.08 \times 10^9 \text{ m}^{-1}\text{s}^{-1}$ for simplicity. The actual eruption contains large fragments, up to few centimeters in diameter, as well as fine ash, which occupies a continuous particle-size range to less than $1 \mu\text{m}$. Large particles typically settle out within a short time, and the particle-size spectrum in the air shifts toward smaller

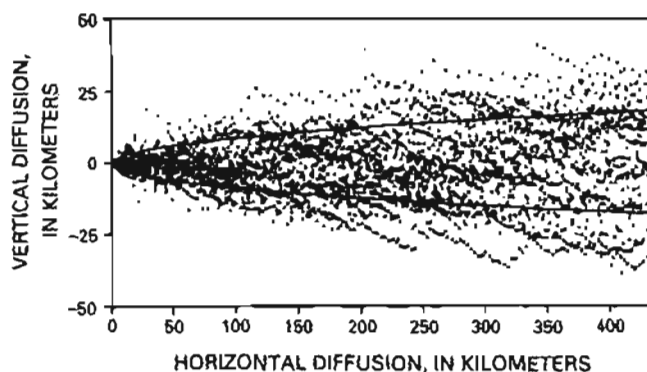


Figure 4. Plan view showing a 12-hour particle diffusion test for a steady plume at a constant zonal wind of 10 m/s. The parabolic line in the figure indicates a theoretical standard deviation of the plume distribution.

particles. Because we are interested in particles that can travel for several hours, we have assumed that the initial particle-size distribution is centered at $100 \mu\text{m}$. It is assumed that the size distribution in logarithmic axis has a Gaussian distribution. Thus, about 95 percent of the particles are supposed to have diameters between $1 \mu\text{m}$ and 1 cm . Using Gaussian random numbers, every particle is assigned with its own diameter, between $1 \mu\text{m}$ and 1 cm , when it appears at the volcanic crater. In practice, particles larger than $100 \mu\text{m}$ drop quickly, within a few steps of time integration. Particles that are less than $100 \mu\text{m}$ in diameter can travel far from the source, providing important information on plume dispersion.

The initial particles are modeled to be uniformly distributed in the vertical column, between the top of the erupting volcano and the specified plume top, using a uniform random-number generator. The altitude of the plume top is assumed to have been reported to AVO by visual observers, which may include pilot reports and reports from ground-based observers. In a case of a short-lived explosive eruption, ash particles are generated only for the initial time of the time integration. When the eruption continues for a period of more than a few minutes, the model generates new particles over the same vertical column for every time step during the specified eruption period. For a steady eruption, the particle number tends to increase in the model atmosphere before the plume particles have dropped out. Therefore, the number of particles released at every time step is adjusted to draw optimal statistical information from the model products.

The total number of particles in the model atmosphere is kept at less than 1,000. Although it is possible to increase the number toward the limit of computer capability, the time integration will then be considerably slower, which is a disadvantage for the urgent prediction requirement. Likewise, excessive complication and sophistication are not recommended in the present application for urgent operational prediction. For comprehensive numerical predictions, refer to Sullivan and Ellis (this volume), Heffter and others (1990), Kai and others (1988), and Draxler (1988).

The plume-prediction model is tested first with a sheared flow in the vertical. Advective wind in the atmosphere has vertical shear with larger velocity, in general, at higher altitude. Figure 5 illustrates the result of the vertical cross sections of a plume-puff simulation for 1 through 6 hours after the eruption. Concentrated ash particles are released uniformly over the vertical column up to an altitude of 10 km at the origin. The plume clouds drift downstream by sheared flow. They diffuse and become thinner due to removal of larger particles. The result simulates reasonably well the transport of the ash plume.

The plume-prediction model is tuned by comparison with actual eruption records of Redoubt Volcano (Brantley, 1990). Model simulations are conducted for about 30 major and minor eruptions during December 1989 through April

1990, and the resulting plume-cloud distributions are compared with satellite images (K. Dean, University of Alaska, oral commun., 1991). Unfortunately, for this period, the Cook Inlet area is mostly covered by dense weather clouds, and there were not many satellite images that captured the ash plume immediately after the eruption.

Figure 6 illustrates a steady plume cloud for December 16, 1989, simulated by this model. Because Redoubt was in near-continuous ash emission on this date, we started the simulation assuming the eruption occurred at 10:00 UTC. A linear cloud extends from Redoubt Volcano toward the northern part of the Kenai Peninsula at 12:30 UTC. In the figure, open circles represent particles higher than 1,800 ft and solid circles represent particles lower than 1,800 ft. The

simulation result is compared with satellite images from the NOAA-11 advanced very high resolution radiometer (AVHRR) at 12:18 UTC (see fig. 7). In figure 7, the black area over Cook Inlet describes a relatively dense ash cloud and the shaded area over the Kenai Peninsula represents a thin ash cloud. The satellite image describes the detailed structure of the cloud, which is beyond the model's resolution. Nevertheless, the overall agreement between the simulated and observed plume distributions is encouraging.

Figure 8 (A–D) illustrates a sequence of graphic products simulated for the eruption on January 8, 1990. The eruption started at 19:09 UTC and continued for 30 minutes. At 20:00, a cellular ash cloud is located near Redoubt Volcano (fig. 8A). The cloud crossed over the Cook Inlet and reached

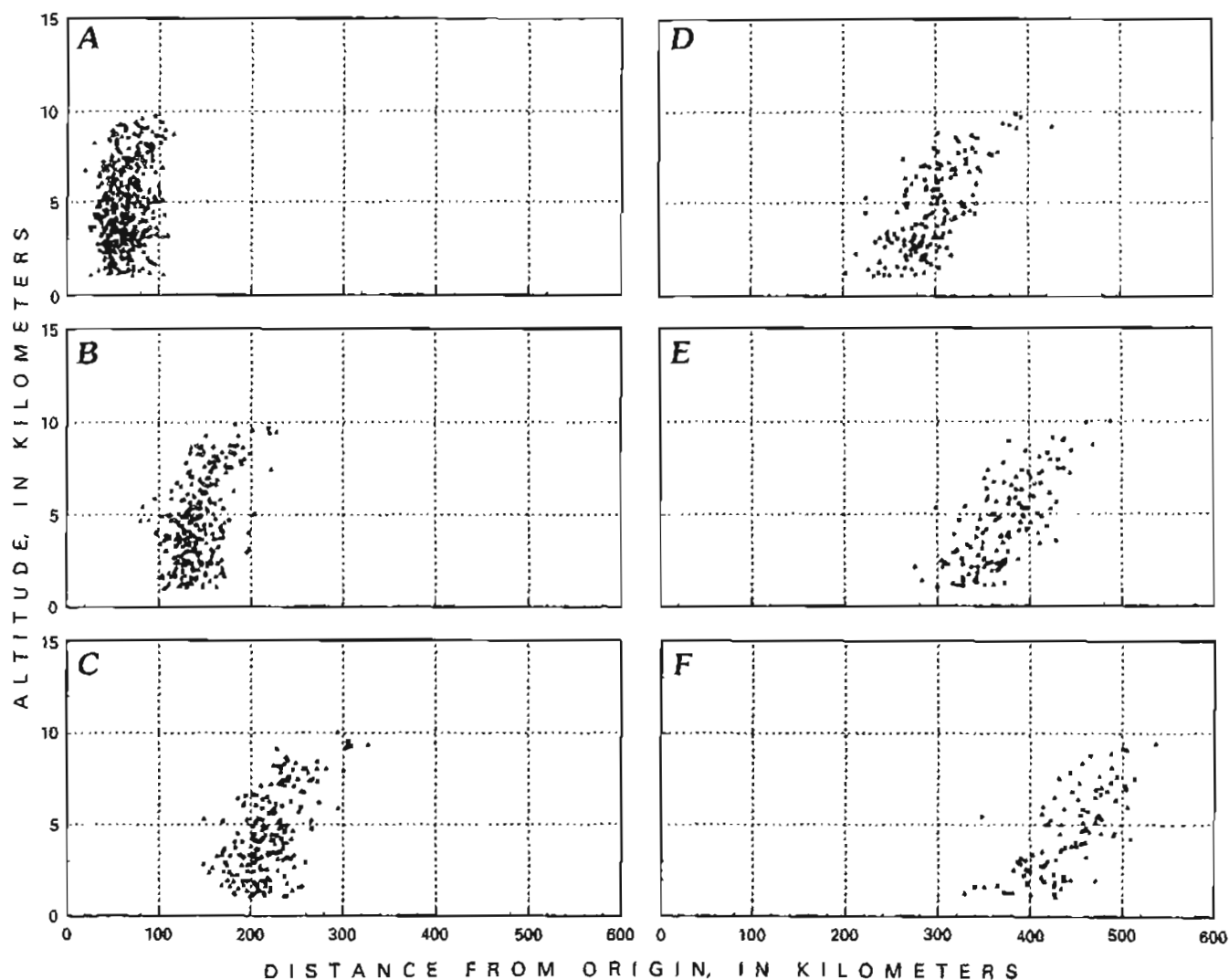


Figure 5. Vertical cross sections of a puff plume simulated for 1 through 6 hours after an eruption. In this test run, the initial ash particles are released uniformly over the vertical column up to an altitude of 10 km at the origin. *A*, plume simulation 1 hour after eruption; *B*, plume simulation 2 hours after eruption; *C*, plume simulation 3 hours after eruption; *D*, plume simulation 4 hours after eruption; *E*, plume simulation 5 hours after eruption; *F*, plume simulation 6 hours after eruption.

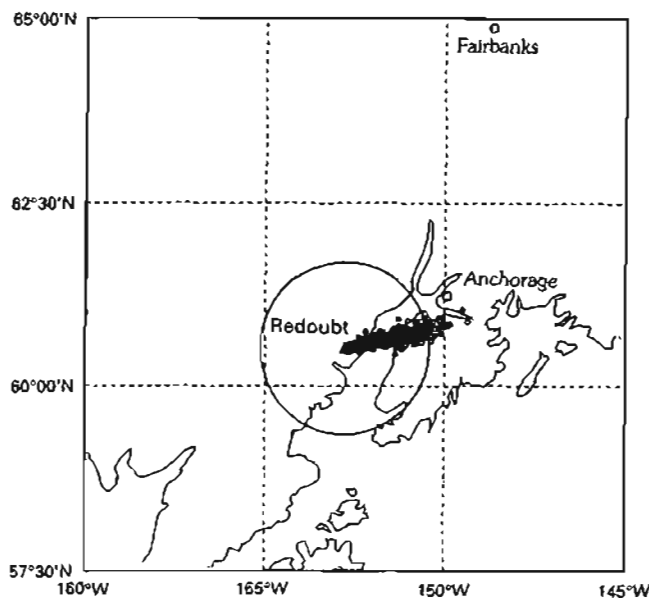


Figure 6. Simulated geographical distribution of particles from a steady plume for eruption of Redoubt Volcano, which started at 10:00 UTC, December 16, 1989. Illustration shows the model result at 12:30 UTC. Open circles, particles higher than 1,800 ft; solid circles, particles lower than 1,800 ft.

the Kenai Peninsula at 21:00 (fig. 8B). The cloud traveled over the Kenai Peninsula, indicating north-south elongation at 22:00 UTC (fig. 8C). A witness report describes that a dense volcanic ash cloud passed the western shore of the Kenai Peninsula at this time (Brantley, 1990), and, in downtown Soldotna, day time turned into darkness during the passage of the dense ash cloud. At 23:00, the northern edge of the elongated cloud reached just the south of Anchorage, and the southern edge of the cloud passed the Alaska coastline (fig. 8D). The simulation results are compared with a satellite image at 23:13 (fig. 9), which clearly shows a linear plume extending from the northern Kenai Peninsula to the Pacific coast near Seward. The satellite observation agrees well with the model simulation.

The graphic outputs (fig. 8) are stored in computer memory, which is connected with other systems through computer networks. The final stage of plume prediction is to distribute the graphic product to various users, including the Federal Aviation Administration (FAA), the National Weather Service (NWS), and the response center of the Alaska Volcano Observatory in Anchorage. In principle, any system connected with the ethernet electronic mail network can receive the graphic product through the network, and users in Anchorage can access the graphic product by telephone modem. For users without any computer facility, the graphic product is distributed by telephone facsimile.

This study demonstrates that the prediction model can provide useful information when it is applied for a real

eruption. We have repeated similar demonstrations for each of the eruptions of Redoubt Volcano in 1989–90 and for Mt. Spurr in 1992. The results are compared with available satellite observations in order to increase the reliability of the prediction model. The model output will be especially useful when Cook Inlet is covered by dense cloud when neither satellite observations nor pilot's visual reports are available.

SUMMARY AND REMARKS

A volcanic plume prediction model has been developed for Cook Inlet volcanoes in Alaska. Reading the real-time upper-air data provided by NMC via Unidata, the prediction model computes advection, diffusion, and gravitational settling for plume particles released from the vertical column over the volcano. Three-dimensional distributions of the simulated plume particles are displayed on computerized graphic display. Hence, we can have important information on the predicted location of the ash plume in a real-time basis.

The model predictions, showing the projected geographical location of the plume clouds for several hours after the eruption, can appear on the computer screen about 15 minutes after eruption reports are received. This prediction is immediately available for users through existing computer networks. The graphical model output is distributed to related organizations using ordinary telephone facsimile. The present model simulation will have forecast errors owing, in part, to the errors in the forecast wind input.

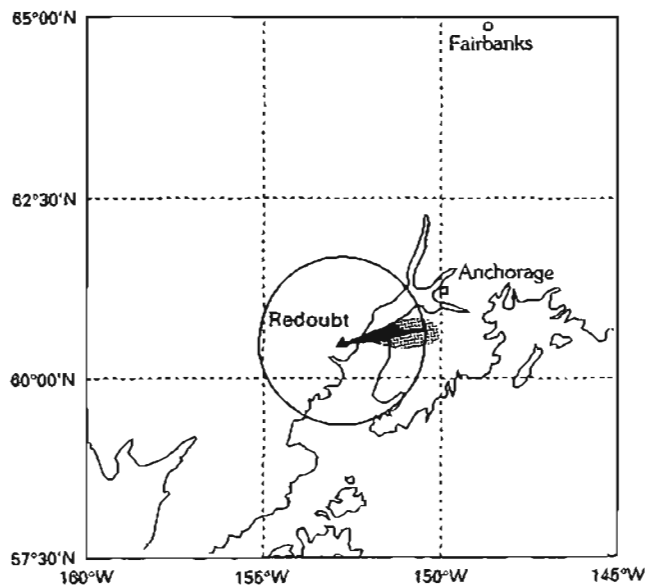


Figure 7. Sketch of satellite image of the steady plume at 12:18 UTC, December 16, 1989, derived by analysis of NOAA-II data. Figure has been scaled to permit comparison with figure 6. Black area shows dense core of the ash cloud. Stippled area shows diffuse margin of the ash cloud (Kienle and others, 1990).

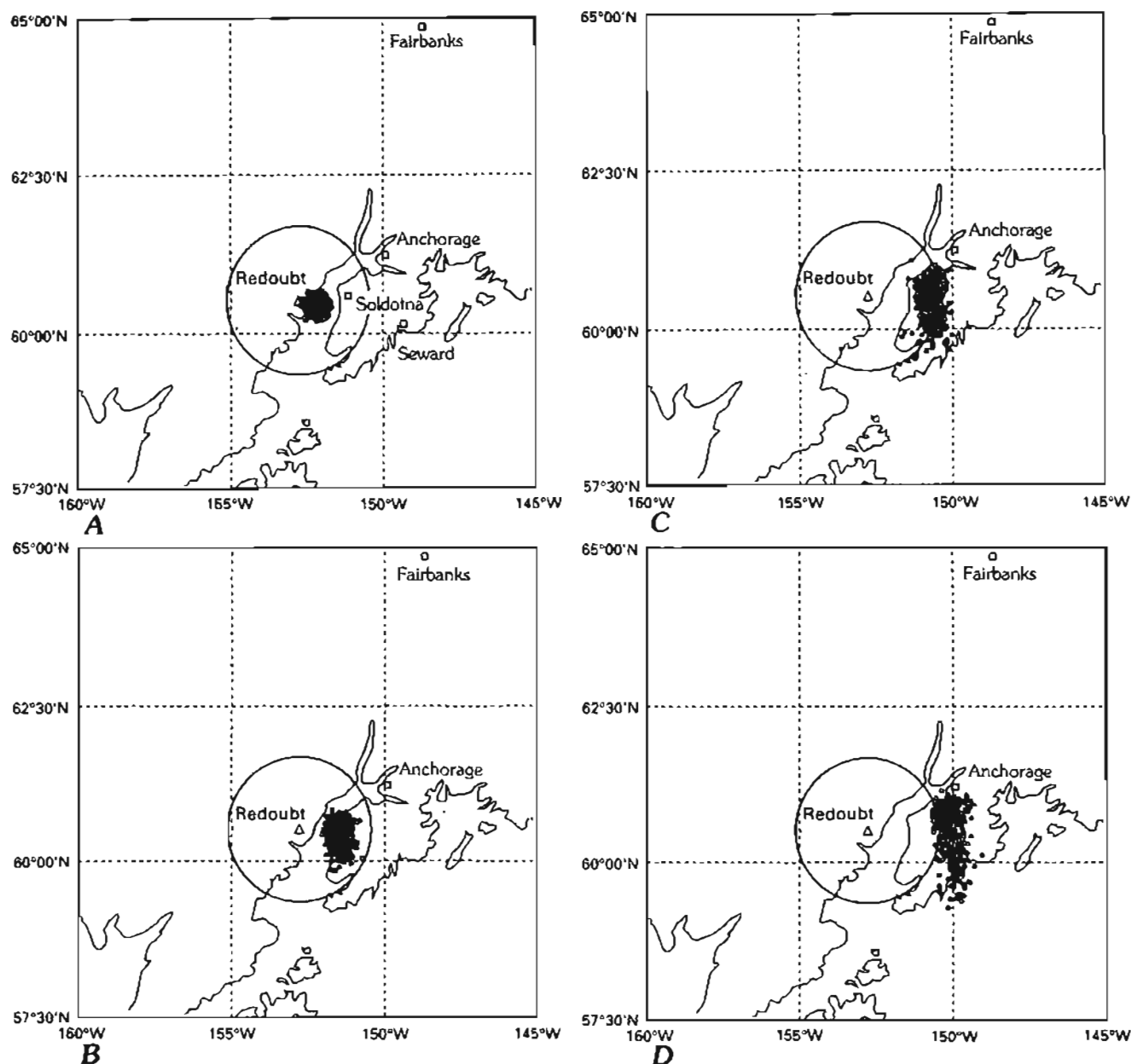


Figure 8. Simulated geographical distribution of a puff plume for the eruption of Redoubt Volcano on January 8, 1990, at 19:09 UTC. Model results are shown for A, 20:00 UTC; B, 21:00 UTC; C, 22:00 UTC; D, 23:00 UTC.

According to the latest statistics, upper-air wind has about 8 m/s root-mean-square (RMS) error on average for the Northern Hemisphere (Kalnay and others, 1990). Nevertheless, the prediction product, knowing the possible prediction errors, can offer a useful guide for public safety. The use of gridded data from a finer mesh weather prediction model would improve the advection computation. Because the NMC gridded data used in this project cover the whole globe, this prediction model can be applied for other volcanoes around the world.

ACKNOWLEDGMENTS

This project was supported by ASTF grant agreement 90-2-058 with matching funds from National Science Foundation grant ATM-8923064, AVO/USGS, Anchorage International Airport, Municipality of Anchorage, Japan Airlines, Nippon Cargo Airlines, China Airway, Scandinavian Airways System, British Airways, Swissair, and Reeve Aleutian Airways. The author appreciates various suggestions from S.-I. Akasofu and Thomas J. Casadevall.

- dispersion model: *Journal of Applied Meteorology*, v. 16, p. 896–910.
- Sherretz, L.A., and Fulker, D.W., 1988, Unidata: Enabling universities to acquire and analyze scientific data: *Bulletin of the American Meteorological Society*, v. 69, p. 373–376.
- Suck, S.H., Upchurch, E.C., and Brock, J.R., 1978, Dust transport in Maricopa county, Arizona: *Atmospheric Environment*, v. 12, p. 2265–2271.
- Tanaka, H.L., 1990, Model used to track volcanic plume: *Geophysical Institute Quarterly*, University of Alaska, Fairbanks, Fall 1990, p. 7–8.
- 1991a, Unidata at Alaska.: *Unidata Newsletter*, Summer 1991, p. 10–11.
- 1991b, Weather data access improved: *Geophysical Institute Quarterly*, University of Alaska, Fairbanks, Summer 1991, p. 1–3.

THE AERONAUTICAL VOLCANIC ASH PROBLEM

By Jerald Uecker

ABSTRACT

The International Civil Aviation Organization (ICAO) requires warnings and flight-planning information about one of the most potentially hazardous but non-meteorological aeronautical phenomena that exists, volcanic ash. This paper discusses the provision of required information based on the experiences gained from eruptions of Mount St. Helens and Redoubt Volcano in the United States. The frequency and duration of these eruptions, as well as the lack of guidelines about ash concentrations and their affect on aircraft, have made it difficult to meet the requirements for supporting safe and efficient aeronautical operations with available information messages. While progress has been achieved with warnings and flight-planning data, efficient dissemination has not been achieved for graphical representations of ash clouds. Meeting aeronautical information requirements for this non-meteorological phenomenon requires cooperation, research, and development among people in various disciplines to attain safe and efficient operations.

INTRODUCTION

The experience gained in providing meteorological information on volcanic ash clouds to those in aeronautical operations has resulted in adjusting some procedures to accommodate requirements. This paper briefly discusses the requirements and challenges and how support will be improved, primarily through communications, in the near future.

During the past decade, a number of aircraft have encountered volcanic ash clouds while in flight. Three incidents involved loss of engine power and posed potential disaster for passengers and crew; these encounters caused extensive damage to the aircraft. Fortunately, such incidents have been rare, and disaster has been averted because of good crews and equipment. These incidents have, however, instilled a healthy awareness of and respect for the problem of volcanic ash.

The relative infrequency of large volcanic eruptions and the inability to predict the onset of eruptions in an

aeronautically timely manner increases the potential danger faced by crews and operators. In spite of the non-meteorological nature of volcanic eruptions and ash, the responsibility rests with meteorologists for: (1) the issuance of alphanumeric significant meteorological (SIGMET) information to warn of the hazard, and (2) the inclusion of ash-cloud information in abbreviated, plain-language, area forecasts and on significant weather charts used for flight planning.

Satellite images, radar data, aircraft reports, and cooperation and information coordination with volcanologists are all essential for early detection of eruptions and for tracking ash clouds. However, there are considerable limitations inherent in the system that provides SIGMET information. Two limitations are: (1) forecasting the onset of eruption with the timeliness required for aeronautical operations—this goal will certainly elude meteorologists, and (2) determining the concentration of erupted ash particles and (or) gases that may or may not affect aircraft. Hopefully, studies that address these limitations will also provide guidance as to when ash concentrations are sufficiently low so that the ash no longer threatens aircraft.

Wind data in the form of particle-trajectory and dispersion-model forecasts for flight planning are essentially the only aspect of the volcanic eruption and ash problem that adheres to meteorological prediction principles (Murray and others, this volume; Stunder and Heffter, this volume). This means that meteorologists need help in providing the best ash-cloud-warning service for the aeronautical community.

The experience in the United States for issuing ash cloud warnings and SIGMET's began with the eruption of Mount St. Helens in 1980. The St. Helens experience differed considerably from the more than 25 eruptions at Redoubt Volcano, which is 177 km southwest of Anchorage, Alaska, and to which meteorologists responded beginning in December 1989. Mount St. Helens eruptions were longer in duration and less frequent than those of Redoubt Volcano. Initially, each Redoubt eruption lasted several hours, and subsequent eruptions, some consisting primarily of steam, lasted less than 30 minutes (Brantley, 1990).

ALPHANUMERIC INFORMATION REQUIREMENTS

The international requirements for reports, warnings, and forecasts about volcanic ash are contained in the ICAO publication entitled "Meteorological Service for International Air Navigation, Annex 3," (ICAO, 1992)—this publication is hereinafter referred to as "ICAO Annex 3." United States domestic and international procedures and policies meeting these requirements are detailed in National Oceanic and Atmospheric Administration (NOAA) and National Weather Service (NWS) operations manuals. Within the United States, additional measures are taken both from a warning and flight-planning point of view. For warnings, NWS meteorologists assigned to air route traffic control centers (ARTCC) provide center weather advisories (CWA's) as a quick response to new or quickly changing conditions that may not be detailed in SIGMET's prepared by meteorological watch offices (MWO's). For flight planning, trajectory information (see Recent Developments section in this paper) is provided to aeronautical and meteorological facilities in accordance with existing agreements. Currently, this information is distributed on a limited basis, but extensive distribution of flight-planning information through meteorological graphics communications systems within the United States and internationally are planned and are nearing fruition. This will result in extensive distribution of this information to the aeronautical community and to information providers.

REPORTS

Recommended practices concerning observations and reports of volcanic activity by meteorological stations are described in the ICAO Annex 3 (chap. 4, p. 20): "The occurrence of pre-eruption volcanic activity, volcanic eruptions, and volcanic ash clouds should be reported without delay to the associated air traffic services unit, aeronautical information services unit, and meteorological watch office. The report should be made in the form of a volcanic activity report [VAR—see Fox, this volume] comprising the following information in the order indicated:

- Message type: volcanic activity report,
- Station identifier: location indicator or name of station,
- Date and time of message,
- Location of volcano and name if known,
- Concise description of event, including, as appropriate, level of intensity of volcanic activity, occurrence of an eruption and its date and time and the existence of a volcanic ash cloud in the area together with direction of ash cloud movement and height."

The standard concerning aircraft observations and reports that is cited in ICAO Annex 3 (chap. 5, p. 24) is that "special observations shall be made by all aircraft whenever...

- Volcanic ash is observed or encountered,...
- Pre-eruption volcanic activity or a volcanic eruption is observed."

Note—Pre-eruption volcanic activity, as used in both contexts cited above, means unusual and (or) increasing volcanic activity that could presage a volcanic eruption.

The ICAO standard for the contents of special air reports of pre-eruption volcanic activity, a volcanic eruption, or volcanic ash cloud and their order in the volcanic activity report (VAR) (Fox, this volume) is:

- Aircraft identification,
- Position,
- Time,
- Flight level or altitude,
- Volcanic activity observed,
- Air temperature,
- Wind, and
- Supplementary information.

SIGMET INFORMATION

SIGMET's are aeronautical meteorological warnings, and they are issued in alphanumeric form. The ICAO Annex 3 (chap. 7, p. 34–36) standard on the issuance of SIGMET information includes the occurrence and (or) expected occurrence of volcanic ash cloud at subsonic, transonic, and supersonic cruising levels. The recommended issuance of "SIGMET messages concerning volcanic ash cloud... expected to affect a flight-information region (FIR) should be issued at least 12 hours before the commencement of the period of validity and should be updated at least every 6 hours."

This requirement combined the short-term requirement for hazardous SIGMET information and the longer term requirement for flight-planning data. However, at the ICAO communications-meteorology-operations divisions and the World Meteorological Organization (WMO) commission on aeronautical meteorology meeting (September 1990, held in Montreal, Canada), several states that have had experience with volcanic activity SIGMET's indicated that permitting the period of validity of SIGMET's for volcanic ash to be extended up to 12 hours, in their opinion, was quite impossible given current volcanic-activity-observing techniques, especially concerning ash particle size and density.

Even though the requirement does state "up to 12 hours," local user requirements during the Redoubt Volcano eruptions led to SIGMET updates as often as every 2 hours. This implied a dichotomy of purpose for the SIGMET (i.e., updates every 2 hours and the requirement for an outlook for up to 12 hours).

A few initial Redoubt Volcano eruptions in December 1989 and January 1990 lasted up to several hours; subsequent eruptions lasted usually less than 30 minutes (Brantley, 1990). With the frequency and duration of Redoubt Volcano eruptions, the MWO issuing SIGMET's would not have been able to comply with the spirit of the long-term requirement at the volcano or for flight-information regions (FIR's) affected downstream by the ash cloud.

Another significant aspect of SIGMET's being valid essentially from 12 to 24 hours is that the area encompassing volcanic ash could be very large. Situations did occur at Redoubt Volcano whereby ash was spread at high levels far to the southeast and at low levels to the north and northwest. In this case, the area was already quite large. However, consider the area that would be covered by ash with the wind directions indicated above and with a speed of 100 knots at high levels and 25 knots at low levels for a period of 12 to 24 hours. A SIGMET encompassing such an ash cloud would be meteorologically supportable but operationally difficult to implement. Even the 4-hour-valid-period SIGMET's issued for the initial Redoubt Volcano ash clouds resulted in large areas that unnecessarily restricted air traffic—this is a considerable impact at or near high-density routes and aerodromes, such as Anchorage International Airport.

Ash dispersion can quickly become complicated and can cover extensive areas with ash that is emanating only from the source. However, rapidly transported ash at high levels that falls into lower levels with different wind directions essentially results in multiple, albeit less concentrated, sources and an extremely complicated ash-cloud pattern.

SIGMET DISSEMINATION

SIGMET's are disseminated over teletypewriter or computer networks in alphanumeric, abbreviated, plain language. ICAO Annex 3 (p. 36) recommends that "SIGMET messages should be disseminated to meteorological watch offices,... and to other meteorological offices, in accordance with regional air navigation agreement."

GRAPHICS REQUIREMENTS

The requirements for graphical information (i.e., charts for flight documentation) reside in ICAO Annex 3, chapter 9, and is entitled "Service for Operators and Flight Crew Members." Flight documentation, usually in the form of charts, is provided "to operators and flight crew members for:

- a. Pre-flight planning by operators,
- b. Use by flight crew members before departure,
- c. Aircraft in flight."

For pre-flight planning purposes by the operator, the ICAO recommendation for significant en-route weather

information is that the information should normally be supplied as soon as available, but not later than 3 hours before departure.

Prior to the ICAO/WMO meeting in 1990, different ways to portray volcanic ash on significant weather charts were tried in the United States for the Redoubt Volcano eruptions. However, the inclusion of ash clouds on significant weather forecast charts caused concern among aeronautical operators. One of the early Redoubt eruptions occurred before the significant weather chart was disseminated, and the projected ash cloud area was determined by trajectory information. This area was enclosed by a scalloped line and identified with a plain-language note. Unfortunately, the area enclosed was larger than it might have been under those meteorological conditions, and it caused some anguish among users. It should be noted, however, that large areas can be expected under certain meteorological conditions.

Experience with these charts showed that:

1. Inclusion of ash clouds on significant weather forecast charts is consistently possible only if the volcano erupts shortly before or during the preparation of a chart and, of course, if the meteorologist is notified in time,
2. Providing long-term (up to 12 hours and beyond) volcanic ash information by outlining the ash cloud on significant weather charts, while possible, may be confusing and may be a disservice to the aeronautical user when the area delineated is significantly larger than it might be or if the chart is prepared for an eruption that turns out to be mostly steam (hence, posing little or no hazard), and
3. The lead time that must exist so that the charts are available to the operator, in addition to the time required to prepare the chart, makes it an extremely difficult task to include the information as precisely as desirable.

The Redoubt Volcano experience led the United States to suggest at the September 1990 ICAO/WMO meeting that the best way to inform flight planners about volcanic ash was to include a statement such as "see potential SIGMET's for volcanic ash" near the volcano on the significant weather chart—this statement would be included on all significant weather charts until the volcano becomes inactive again. Discussions pointed out that longer term, precise information on the occurrence and location of volcanic ash cannot be adequately depicted on significant weather charts. The reason for this is that these charts should be in the users' hands some 9 hours before the valid time—this time corresponds approximately to the midpoint of the flight. Also, these charts are prepared up to 6 hours before being disseminated. The net result is that a volcanic eruption and ash cloud may have occurred at any time during a period of 15 hours and may not be depicted on the significant weather chart that the air crew receives. It was agreed at the meeting that an ash

cloud could not be included reliably for short-term eruptions because of timing and dissemination requirements.

The participants at the ICAO/WMO meeting in 1990 felt that WMO should be requested to develop, in consultation with ICAO, appropriate symbology to represent the volcanic ash phenomenon on significant weather charts—this resulted in the recommendation that WMO, in consultation with ICAO, develop appropriate symbology to represent the occurrence of volcanic eruptions on world-area forecast system significant weather charts. Subsequently, it was agreed that symbology would be added to the significant weather chart at the location of the volcano and that adequate information would be added to the legend of the chart, including a statement advising concerned air crews to inquire about SIGMET's in an area where a volcanic eruption or ash contamination is suspected.

RECENT DEVELOPMENTS

Since the First International Symposium on Volcanic Ash and Aviation Safety in 1991, graphic information has been developed. The volcanic ash forecast transport and dispersion (VAFTAD) model, developed by National Oceanic and Atmospheric Administration (NOAA) Air Resources Laboratory, is a three-dimensional, time-dependent depiction of the volcanic ash cloud (Stunder and Heffter, this volume). Eruption input includes volcano name and location, eruption time, and ash-cloud-top height. The model assumes a given particle-size distribution throughout the initial ash cloud. Ash is advected horizontally and vertically as it falls through the atmosphere, using either the Washington World

Area Forecast Center global wind and temperature computer model data or a U.S. regional model.

This graphic information, produced automatically and shortly after notification of an eruption, will be disseminated internationally in addition to significant weather charts on ICAO world-area forecast system satellite broadcasts. Broadcasts operated by the United States are expected to begin in late 1993 or early 1994 over the Americas and in late 1994 over the Pacific Ocean—eastern Asia area. In the United States, the graphic will be disseminated on meteorological computer and graphic-dissemination systems.

SUMMARY

Problems faced by meteorologists and operators concerning: (1) when and where an eruption may occur, (2) the timely notification of an eruption in the aeronautical sense, and (3) what concentrations of volcanic ash threaten life and property, contribute to the difficulty in providing useful volcanic ash information. However, improved dissemination of information will significantly assist in planning for efficient flight and will contribute to safe operations.

REFERENCES CITED

- Brantley, S.R., ed., 1990, The eruption of Redoubt Volcano, Alaska, December 14, 1989–August 31, 1990: U.S. Geological Survey Circular 1061, 33 p.
- International Civil Aviation Organization (ICAO), 1992, Meteorological Service for International Air Navigation, Annex 3 (11th ed.): International Civil Aviation Organization.

AN AIRCRAFT ENCOUNTER WITH A REDOUBT ASH CLOUD (A SATELLITE VIEW)

By Kenneson G. Dean, Lawrence Whiting, and Haitao Jiao

ABSTRACT

Satellite images, wind measurements, and ground observations were used to track and map gas clouds and ash clouds emitted by Redoubt Volcano, Alaska, on 15 December 1989. This eruption resulted in a nearly catastrophic encounter between airborne ash and a Boeing 747 jet aircraft (most of southern Alaska was completely covered by clouds on that day). Four satellite images were analyzed using complex digital-processing techniques to locate geographic features and to distinguish eruption-related gas clouds from meteorological clouds. The technique of subtracting thermal infrared bands to detect ash clouds was applied to three images but was only successful on the 13:42 Alaska Standard Time (AST) image. The 13:42 image revealed the presence of two ash clouds near Fairbanks and Delta Junction that may have been involved in the encounter with the 747 aircraft earlier that morning. Ground samples from the two ash clouds help quantify the characteristics of ash clouds detected by satellite sensors. The eruption at 10:15 AST appears to be the origin of the ash involved in the aircraft encounter.

INTRODUCTION

On 14 December 1989, Redoubt Volcano, located 177 km southwest of Anchorage, Alaska (fig. 1), erupted and expelled a huge eruption cloud composed of ash and gas to altitudes greater than 10 km (Brantley, 1990). For the next 4 months, 24 additional eruptions resulted in the deposition of ash throughout southern Alaska (Scott and McGimsey, 1991). Clouds of ash and gas from Redoubt Volcano drifted hundreds of kilometers to locations beyond Fairbanks, Delta Junction, and Glennallen.

The danger to airline traffic posed by airborne ash was exemplified on 15 December at 11:45 Alaska Standard Time, when a Boeing 747 jet flew into an ash cloud at an altitude of 7,600 m (25,000 ft) northeast of Talkeetna, Alaska. All four engines shutdown within minutes after the aircraft entered the cloud but were restarted about 8 minutes later,

narrowly averting a catastrophe (Brantley, 1990; Casadevall, in press). The ability to detect, monitor, and predict the movement of volcanic plumes and ash clouds would help to minimize the possibility of aircraft encounters with ash. Satellite images are one potential source of this information. The 15 December 1989 chronology of events and National Oceanographic and Atmospheric Administration (NOAA) advanced very high resolution radiometer (AVHRR) satellite images used in our analysis are given in table 1.

NOAA AVHRR satellite images have been used to monitor and analyze eruption clouds from Redoubt (Dean and others, 1990; Kienle and others, 1990); from Augustine (Holasek and Rose, 1991); from Colo, Indonesia (Maligreau and Kaswanda, 1986); from Mt. Galunggung, Indonesia (Hanstrum and Watson, 1983); from El Chichón, Mexico (Matson, 1984); and from Mount St. Helens (Matson and Staggs, 1981). Techniques have been developed to distinguish ash clouds from meteorological clouds and other airborne volcanic constituents (Prata, 1989; Holasek and Rose, 1991). Images from the Earth observing system (EOS) spacecraft will become an additional source of data for analyzing volcanoes in the near future (Mouginis-Mark and others, 1991).

Images from the AVHRR sensor aboard the polar-orbiting NOAA-10 and NOAA-11 (N-10, N-11) satellites are recorded for the Cook Inlet region more than 10 times per 24-hour period. This high temporal resolution is unique to high latitudes due to extensive overlap on each image swath from adjacent orbits. The data have a spatial resolution of 1 km and a swath width greater than 2,000 km. The images are recorded in five wavelengths: visible band 1 (0.58–0.68 μm), near-infrared band 2 (0.72–1.1 μm), thermal-infrared band 3 (3.55–3.93 μm), thermal-infrared band 4 (10.3–11.3 μm), and thermal-infrared band 5 (11.5–12.5 μm). However, on even-numbered NOAA satellites up to but not including N-12, band 5 is a duplicate of band 4. The five-band coverage can detect both volcanic and non-volcanic cloud formations during both day and night.

In this paper, clouds composed of gas and ash emitted by a volcano are referred to as eruption clouds. Eruption clouds may have a conical shape with an apex ending at the

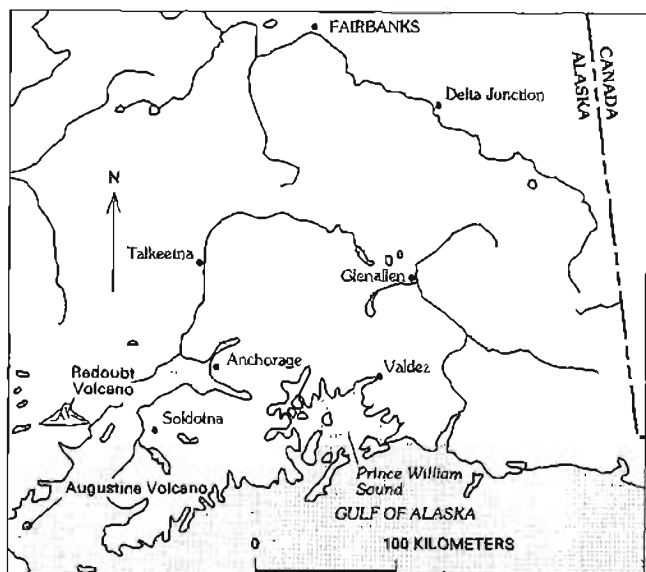


Figure 1. Location map of south-central Alaska.

volcano indicating that it is still being emitted, or the apex may be adrift and not connected to the volcano. An ash cloud is that portion of an eruption cloud containing volcanic ash that damages aircraft and other mechanical devices. Both ash and gas components of eruption clouds can be detected on satellite images, but they may not always be distinguishable from each other.

OBJECTIVES

The objective of this analysis is to use satellite images to identify and monitor eruption clouds, including the ash clouds responsible for the near-downing of an aircraft on 15 December 1989. AVHRR images are used to distinguish eruption clouds from surrounding meteorological clouds, to map the trajectory and distribution of eruption clouds, and to detect and track the movement of the ash cloud that the aircraft encountered.

METHODS

SATELLITE ANALYSIS

Three eruptions occurred on the morning of 15 December: at 01:40, 03:48, and 10:15 AST. Four satellite images were recorded at 03:28, 05:09, 09:28, and 13:27 AST (table 1) and show that most of southern Alaska was completely covered by clouds. To relate cloud structures to ground locations, the images were registered to an Albers equal-area map projection, and geographic features were digitally superimposed. The values of individual pixels were

Table 1. Chronology of Events on 15 December 1989.

(AST, Alaska Standard Time)

Time (AST)	Event
01:40	Eruption, 12 minutes duration
03:28	Image: NOAA-11; orbit no. 6305
03:48	Eruption, 10 minutes duration
05:09	Image: NOAA-11; orbit no. 6306
09:28	Image: NOAA-10; orbit no. 16851
10:15	Eruption, 40 minutes duration
11:45	Aircraft-ash cloud encounter
13:27	Image: NOAA-11; orbit no. 6311

transformed to temperature and albedo using coefficients provided with the data as described in the NOAA polar orbiter data users guide (Kidwell, 1991). Contrast was enhanced to optimize the detection of eruption-related gas clouds and ash clouds. Individual bands of satellite data were combined to distinguish gas clouds, ash clouds, and other plume constituents from meteorological clouds using established experimental techniques. These included:

- Subtraction between bands 5 and 4 to distinguish ash clouds from meteorological clouds,
- Subtraction between bands 2 and 1 to help distinguish the water-vapor portion of eruption clouds from other plume constituents, and
- Principal-component analysis to distinguish eruption clouds from meteorological clouds.

Color composite images were generated using various combinations of raw images, band subtractions, and principal component images.

Images that result from the subtraction of two bands of data may detect distinct properties of eruption clouds. The image that results from subtracting the two thermal infrared bands on AVHRR data (bands 4 and 5 on NOAA-9, 11, and 12 satellites) detects ash clouds (Prata, 1989; Holasek and Rose, 1991). The image that results from subtracting visible and near-infrared bands may help to distinguish water vapor from other plume constituents (Dean and others, in press). These band-subtraction techniques were used in this analysis to help distinguish plume components.

The principal-component-analysis technique creates new images by performing coordinate transformations that recognize the maximum variance in multispectral data. This technique generates new images referred to as "principal-component images" (PC1, PC2, PC3, etc.). The first principal-component image is a weighted-average picture: the remaining principal-component images are similar to pairwise differences between bands (Sabins, 1987; Siegal and Gillespie, 1980). The principal-component images were used to help distinguish subtle eruption-cloud signatures from meteorological clouds.

Altitudes of the eruption clouds were estimated by comparing their temperatures with the temperature profile of the

central Alaska, eruption clouds were observed on several satellite images. However, the position of the clouds seen on the images did not always agree with ground observations of fallen ash, probably due to height differences between the ash component and gas component of the eruption cloud (and the air masses that transported those parts). A technique of using multiple thermal bands to distinguish ash clouds from other clouds was successful on only one out of three possible images (fig. 6). This image, recorded at 13:27 AST, detected ash clouds near Fairbanks and Delta Junction. One or both of these ash clouds were very likely involved in the aircraft encounter at 11:45 AST.

Validation analyses of eruption clouds observed on satellite images have been minimal. It is not known how opacity, plume composition, particle size, and particle density affect the signatures observed on the satellite images. A thorough understanding of these factors would significantly improve the utility of satellite images for tracking and monitoring eruption clouds.

REFERENCES CITED

- Brantley, S.R., ed., 1990, The eruption of Redoubt Volcano, Alaska, December 14, 1989–August 31, 1990: U.S. Geological Survey Circular 1061, 33 p.
- Casadevall, T. J., in press, The 1989–1990 eruption of Redoubt Volcano, Alaska: Impacts on aircraft operations: *Journal of Volcanology and Geothermal Research*.
- Dean, K.G., Bowling, S.A., Shaw, G., and Tanaka, H., in press, Satellite analysis of movement and characteristics of the Redoubt Volcano plume: *Journal of Volcanology and Geothermal Research*.
- Dean, K.G., Guritz, R., and Garbeil, H., 1990, Near-real time acquisition and analysis of satellite images of Redoubt Volcano [abs.]: *Eos, Transactions, American Geophysical Union*, v. 71, p. 1701.
- Hanstrum, B.N., and Watson, A.S., 1983, A case study of two eruptions of Mount Galunggung and an investigation of volcanic cloud characteristics using remote sensing techniques: *Australian Meteorological Magazine*, v. 31, p. 171–177.
- Holasek, R.E., and Rose, W.I., 1991, Anatomy of 1986 Augustine Volcano eruptions as recorded by multispectral image processing of digital AVHRR satellite data: *Bulletin of Volcanology*, v. 53, p. 420–425.
- Kidwell, K.B., ed., 1991, NOAA polar orbiter data users guide (TIROS-N, NOAA-6, NOAA-7, NOAA-8, NOAA-9, NOAA-10, NOAA-11, and NOAA-12): Washington D.C., National Oceanic and Atmospheric Administration, National Environmental Satellite Data and Information Service, National Climatic Data Center, Satellite Data Services Division.
- Kienle, J., Dean, K.G., Garbeil, H., and Rose, W.I., 1990, Satellite surveillance of volcanic ash plumes; application to aircraft safety: *Eos, Transactions, American Geophysical Union*, v. 71, p. 266.
- Malgouyres, J.-P., and Kaswanda, O., 1986, Monitoring volcanic eruptions in Indonesia using weather satellite data: The Colo eruption of July 28, 1983: *Journal of Volcanology and Geothermal Research*, v. 27, p. 179–194.
- Matson, M., 1984, The 1982 El Chichón eruptions—A satellite perspective: *Journal of Volcanology and Geothermal Research*, v. 23, p. 1–10.
- Matson, M., and Staggs, S.J., 1981, The Mount St. Helens ash cloud: *Bulletin of the American Meteorological Society*, v. 62, p. 1486.
- Mouginis-Mark, P., Rowland, S., Francis, P., Friedman, T., Garbeil, H., Gradie, J., Self, S., and Wilson, L., 1991, Analysis of active volcanoes from the Earth observation system: *Remote Sensing of the Environment*, v. 36, p. 1–12.
- Prata, A.J., 1989, Observations of volcanic ash clouds in the 10–12 μm window using AVHRR/2 data: *International Journal of Remote Sensing*, v. 10, p. 751–761.
- Sabins F.F., 1987, *Remote Sensing: Principles and Interpretations* (2nd ed.): New York, W.H. Freeman and Company, 449 p.
- Scott, W.E., and McGimsey, R.G., 1991, Mass, distribution, grain size, and origin of 1989–1990 tephra-fall deposits of Redoubt Volcano, Alaska [abs.], in Casadevall, T.J., ed., *First International Symposium on Volcanic Ash and Aviation Safety*, U.S. Geological Survey Circular 1065, p. 39.
- Siegal, B.S., and Gillespie, A.R., 1980, *Remote Sensing in Geology*: New York, John Wiley and Sons, 702 p.
- Woods, A.W., and Self, S., 1992, Thermal disequilibrium at the top of volcanic clouds and its effect on estimates of the column heights: *Nature*, v. 355, p. 628–630.

OBSERVATIONS OF THE 1989–90 REDOUBT VOLCANO ERUPTION CLOUDS USING AVHRR SATELLITE IMAGERY

By David J. Schneider and William I. Rose

ABSTRACT

The 1989–90 eruptions of Redoubt Volcano, Alaska, generated ash clouds that reached altitudes of as much as 12 km and provided an opportunity to test and refine the use of the advanced very high resolution radiometer (AVHRR) for satellite remote sensing of volcanic eruption clouds. Several aircraft encountered dispersed volcanic clouds, including a Boeing-747 that temporarily lost power from all four engines. Such near-tragic incidents highlighted the need for improved methods of discriminating and tracking volcanic clouds.

Thirty-one AVHRR images from various stages of the Redoubt eruption were examined. In the early, more energetic phases of the eruption, the Redoubt volcanic clouds could be discriminated by a technique that employs an apparent temperature difference between bands 4 and 5 of AVHRR. This method was particularly successful in clouds that were older than 1 hour, demonstrating that slight aging of the cloud during dispersal enhances its discrimination by this method. In the later stages of Redoubt activity, this method fails, probably because of environmental variables associated with the changing character of the eruption. The ash clouds associated with dome collapses that marked the later Redoubt clouds were of small volume and may not have contained as high a proportion of fine ash particles.

Laboratory biconical reflectance measurements were conducted to determine the spectral variability of ash that fell out of the Redoubt clouds. The results show that ash reflectance is controlled more by particle size than by particle composition, but these alone do not explain the variability we observed in the satellite data.

INTRODUCTION

Satellite remote sensing of volcanic clouds is an important tool for scientists and those engaged in mitigating natural hazards. The total ozone mapping spectrometer (TOMS) has been used to measure the SO₂ released by eruptions (Krueger, 1983; Krueger and others, this volume), and

multispectral image processing of advanced very high resolution radiometer (AVHRR) data has succeeded in discriminating volcanic clouds from weather clouds (Hanstrum and Watson, 1983; Prata, 1989a; Holasek and Rose, 1991). Perfection of image-processing algorithms and identification of primary physical parameters controlling success of the algorithms could lead to operational use of AVHRR data in reducing dangerous encounters between aircraft and volcanic clouds (Rose, 1987; Casadevall, 1990; Steenblik, 1990) and for monitoring the global dispersion of large atmospheric injections by volcanoes.

This paper attempts to advance satellite-based volcanic-cloud sensing through analysis of AVHRR data collected during the Redoubt eruptions of 1989–90. In particular, it tests a volcanic-cloud-discrimination algorithm developed by Holasek and Rose (1991) for the 1986 eruption of Augustine Volcano. Redoubt and Augustine Volcanoes, located in the Cook Inlet area of Alaska (Kienle, this volume), both erupted during the winter and early spring and have similar chemical compositions.

AVHRR satellite images collected during various stages of the Redoubt eruption were analyzed to test the utility of cloud-discrimination algorithms. In addition, the spectral variability of the Redoubt volcanic clouds were investigated through analysis of biconical reflectance measurements of samples of ash fallout and crushed pumice, glass, and minerals separated from Redoubt Volcano.

AVHRR SENSOR

The AVHRR sensor, aboard the National Oceanic and Aeronautics Administration (NOAA) polar-orbiting weather satellites since 1978, has been used in the study of several eruptions (Kienle and Shaw, 1979; Hanstrum and Watson, 1983; Matson, 1984; Malingreau and Kaswanda, 1986; Glaze and others, 1989; Holasek and Rose, 1991). AVHRR data from NOAA-10 and NOAA-11 were used to study the Redoubt eruptions. This sensor images a 2,800-km-wide swath with a spatial resolution of 1.1 km at the nadir. The AVHRR sensor aboard NOAA-10 has four bands: band 1,

visible (0.58–0.68 μm); band 2, near-infrared (0.73–1.10 μm); band 3, mid-infrared (3.55–3.93 μm); and band 4, thermal-infrared (10.3–11.3 μm), whereas the AVHRR sensor aboard NOAA-11 contains the previous bands plus band 5, thermal-infrared (11.5–12.5 μm). Each satellite passes over a point on the ground twice per day, with more frequent coverage occurring at high latitudes where the orbits converge at the poles. The large swath width, frequent coverage, and multispectral capability make the AVHRR sensor a useful instrument for studying volcanic clouds.

THE 1989–90 ERUPTION OF REDOUBT VOLCANO

Redoubt Volcano is an andesitic composite volcano located in the Cook Inlet region of Alaska, approximately 200 km southwest of Anchorage (fig. 1). In mid-December 1989, Redoubt erupted for the first time since 1966. During the next 5 months, there were more than 20 eruptive episodes, which produced ash clouds reaching greater than 12-km altitude (table 1) (Brantley, 1990). Scott and McGimsey (in press) estimate the total tephra-fall volume to be 2×10^7 – 4×10^7 m^3 , dense-rock equivalent, and note that two different tephra types were produced. Pumiceous tephra was generated by magmatically driven explosions on December 14 and 15, and fine-grained lithic-crystal tephra was erupted starting on December 16 and during all later events. The lithic-crystal tephra was generated by two processes: hydro-volcanic explosions dominated from December 16 to 19, and pyroclastic flows, resulting from dome collapse, became an increasingly important process from January 2, 1990, to the end of eruptive activity in April. Pyroclastic flows were the only mechanism generating tephra during the last five eruptive episodes (Scott and McGimsey, in press).

More than 60 percent of Alaska's population lives in the Cook Inlet region. Major oil facilities are also located in this region, and Anchorage is a major hub of air traffic between Asia and Europe. There were four incidents of commercial aircraft encountering volcanic clouds, including one incident in which a Boeing 747 carrying 246 people lost power from all four engines after flying through a cloud (Casadevall, 1990). The aircraft lost more than 4 km of altitude before two engines were restarted at 5.2 km—the remaining engines were restarted at about 4.1 km (Przedpelski and Casadevall, this volume). The aircraft was extensively damaged (Steenblik, 1990), and the incident highlighted the need for new techniques to detect and track volcanic clouds.

MULTISPECTRAL IMAGE PROCESSING OF THE AVHRR IMAGES

More than 30 images of the Redoubt region were collected from the archive at the NOAA National Environmental

Table 1. Chronology of the 1989–90 eruption of Redoubt Volcano.

[Modified from Brantley (1990). X, volcanic activity occurred; na, not applicable; ?, volcanic activity uncertain; cont., continuous; fr., from]

Day	Time ¹	Type of volcanic activity		
		Explosion ²	Dome collapse	Plume height
December 1989				
14	9:47	X(17)	na	>10 km
15	1:40	X(12)	na	?
	3:48	X(10)	na	?
	10:15	X(40)	na	>12 km
16-18	(Nearly cont. ejection of tephra fr. crater)			<7 km
19	6:30	X(9)	na	>9 km
January 1990				
2	17:48	X(26)	X	>12 km
	19:27	X(61)	X	>12 km
8	10:09	X(15)	X	>12 km
11	10:01	X(5)	?	>9 km
	13:42	X(12)	?	?
16	22:48	X(13)	?	>11 km
February 1990				
15	4:10	X(20)	X	>10 km
21	12:32	X(6)	X	9 km
24	5:05	X(4)	X	9 km
28	9:47	X(5)	X	8 km
March 1990				
4	20:39	X(8)	X	12 km
9	9:51	X(10)	X	10 km
14	9:47	X(14)	X	12 km
23	4:04	X(8)	X	>10 km
29	10:33	X(7)	X	?
April 1990				
6	17:23	X(7)	X	9 km
15	14:49	X(8)	X	>10 km
21	18:11	X(4)	X	>8 km

¹ Alaska Standard Time.

² Numbers in parentheses indicate duration of explosive activity in minutes, based on seismicity.

Satellite Data and Information Service (NESDIS) and from the University of Alaska's Geophysical Institute following the eruption; 11 images are described in detail in this paper (table 2). In several cases, eruptive episodes are recorded in multiple images, providing an opportunity to track the ash clouds from the initial eruption through the dispersion of the volcanic clouds.

Image processing of the AVHRR scenes was conducted using Erdas and Terascan on a Sparc-1+ workstation. Images of the Redoubt region were extracted from the full scene; the thermal channels were calibrated using the procedure of Kidwell (1991); and the images were georeferenced to a common projection. Following the technique of Prata (1989a) and Holasek and Rose (1991), algebraic manipulations were

Table 2. Satellite images of Redoubt volcanic clouds used in this study.

[LUT (look-up table) represents image channel color rendition in red (R), green (G), and blue (B)]

Date and start time (GMT) ¹	Color, LUT			Satellite	Cloud type ²
	R	G	B		
12/16/89 12:18	4m5	3	4	NOAA-11	1
12/16/89 13:59	4m5	3	4	NOAA-11	1
12/18/89 21:55	4m5	3	4	NOAA-11	1
12/18/89 23:37	4m5	3	4	NOAA-11	1
01/08/90 19:28	4	4	4	NOAA-10	2
01/08/90 23:13	3m4	3	4	NOAA-11	3
02/15/90 13:17	4	4	4	NOAA-11	2
02/15/90 18:26	3m4	2	1	NOAA-10	3
03/23/90 13:25	4	4	4	NOAA-11	2
03/23/90 18:11	3m4	2	1	NOAA-10	3
03/23/90 23:24	3m4	2	1	NOAA-11	3

¹ Greenwich Mean Time. Local time is GMT minus 9 hours.

² See text for discussion of cloud types.

performed on AVHRR bands 4 and 5 to enhance the volcanic clouds and distinguish them from weather clouds. Ratios of band 4 to band 5 and differences between band 4 and band 5 were calculated and evaluated. The subtraction process results in an "apparent temperature difference," which we find particularly useful. The term "apparent temperature difference" is defined as the difference between temperature values derived from emitted energy measured at 10.5–11.3 μm (band 4) and 11.5–12.5 μm (band 5). The temperature difference is not real, but rather it is the result of differential emission of energy at these two wavelengths. When the emittance is converted to a temperature value, it produces an apparent temperature difference. An example of the band-4-minus-band-5 operation is shown in figure 2. In figure 2A–B, the single-band images are quite similar, and the volcanic plume is not very distinct. The plume is greatly enhanced by the band subtraction operation (fig. 2C), which generally produced better results, in terms of plume discrimination, than the ratio operation. When these operations were not successful, or when using data from NOAA-10 (which does not contain band 5), ratios and differences of band 3 and band 4 were calculated.

The results of these mathematical operations were visually evaluated to determine their ability to enhance volcanic clouds. False-color composites were generated on 24-bit graphic monitors by displaying algebraic enhancements along with several of the AVHRR bands in the red, green, and blue image planes of the monitor. False-color composites are helpful in interpreting the extent of the volcanic cloud because data from the individual bands interact to increase enhancement of the cloud. The various band combinations used to produce the false-color composites are shown in table 2.

OBSERVATIONS OF THE AVHRR IMAGES

For the purpose of description and discussion, the Redoubt volcanic clouds shown in the satellite images are divided into three classes that are chosen on the basis of cloud spectral properties, morphology, and size. It is not implied that these cloud types will be produced by eruptions of other volcanoes or that they are the only type that will be produced. The classes include:

Type-1 volcanic clouds.—Clouds generated by magmatic explosions during the first week of activity (while there was a nearly continuous ejection of tephra from the crater). These clouds were low (< 7 km) and extended for hundreds of kilometers from the vent. Examples of this cloud type are shown in figure 3.

Type-2 volcanic clouds.—Clouds generated in part by dome collapse and subsequent pyroclastic flows (Scott and McGimsey, in press). These short-duration, discrete eruptive events were imaged within minutes of the onset of eruption. The type-2 clouds are higher (>10–12 km) than type-1 clouds and have a distinctive, circular morphology. Examples of these clouds are shown in figure 4.

Type-3 volcanic clouds.—Dispersed type-2 clouds. These clouds were imaged several hours after the initial eruptive event and show the dispersion of clouds produced by a single eruptive pulse. Examples of these clouds are shown in figure 5.

Although volcanic clouds were discriminated from weather clouds in many cases, no single algorithm was successful in enhancing all three cloud types. For the type-1 clouds, the band-4-minus-band-5 operation of Prata (1989a) and Holasek and Rose (1991) worked to discriminate portions of the volcanic cloud from the weather clouds (fig. 3A–D). This operation was successful for both daytime and nighttime images, but the discrimination is enhanced in the daytime images when band 3 data are included. All of the false-color composites in figure 3 were produced using identical band combinations (table 2), but a dramatic difference can be seen between the nighttime images from December 16 (fig. 3A–B) and the daytime images from December 18 (fig. 3C–D). Band 3 of the AVHRR sensor (3.53–3.93 μm) is a hybrid band, measuring thermal emittance at night and a combination of reflectance and emittance during the day. In the nighttime images, the enhanced portion of the volcanic cloud is red, indicating that the enhancement is solely caused by the band-4-minus-band-5 subtraction operation. By contrast, the volcanic cloud in the daytime images is yellow, indicating that the enhancement is a result of both the subtraction operation and high band 3 reflectance of the volcanic cloud with respect to the weather clouds.

The distal portions of two of the type-1 volcanic clouds were enhanced more than the proximal portions (fig. 3A–B). Near the vent, the volcanic cloud is spectrally similar to the weather clouds seen at the bottom of the image—the

Table 2. Satellite images of Redoubt volcanic clouds used in this study.

[LUT (look-up table) represents image channel color rendition in red (R), green (G), and blue (B)]

Date and start time (GMT) ¹	Color, LUT			Satellite	Cloud type ²
	R	G	B		
12/16/89 12:18	4m5	3	4	NOAA-11	1
12/16/89 13:59	4m5	3	4	NOAA-11	1
12/18/89 21:55	4m5	3	4	NOAA-11	1
12/18/89 23:37	4m5	3	4	NOAA-11	1
01/08/90 19:28	4	4	4	NOAA-10	2
01/08/90 23:13	3m4	3	4	NOAA-11	3
02/15/90 13:17	4	4	4	NOAA-11	2
02/15/90 18:26	3m4	2	1	NOAA-10	3
03/23/90 13:25	4	4	4	NOAA-11	2
03/23/90 18:11	3m4	2	1	NOAA-10	3
03/23/90 23:24	3m4	2	1	NOAA-11	3

¹ Greenwich Mean Time. Local time is GMT minus 9 hours.

² See text for discussion of cloud types.

performed on AVHRR bands 4 and 5 to enhance the volcanic clouds and distinguish them from weather clouds. Ratios of band 4 to band 5 and differences between band 4 and band 5 were calculated and evaluated. The subtraction process results in an "apparent temperature difference," which we find particularly useful. The term "apparent temperature difference" is defined as the difference between temperature values derived from emitted energy measured at 10.5–11.3 μm (band 4) and 11.5–12.5 μm (band 5). The temperature difference is not real, but rather it is the result of differential emission of energy at these two wavelengths. When the emittance is converted to a temperature value, it produces an apparent temperature difference. An example of the band-4-minus-band-5 operation is shown in figure 2. In figure 2A–B, the single-band images are quite similar, and the volcanic plume is not very distinct. The plume is greatly enhanced by the band subtraction operation (fig. 2C), which generally produced better results, in terms of plume discrimination, than the ratio operation. When these operations were not successful, or when using data from NOAA-10 (which does not contain band 5), ratios and differences of band 3 and band 4 were calculated.

The results of these mathematical operations were visually evaluated to determine their ability to enhance volcanic clouds. False-color composites were generated on 24-bit graphic monitors by displaying algebraic enhancements along with several of the AVHRR bands in the red, green, and blue image planes of the monitor. False-color composites are helpful in interpreting the extent of the volcanic cloud because data from the individual bands interact to increase enhancement of the cloud. The various band combinations used to produce the false-color composites are shown in table 2.

OBSERVATIONS OF THE AVHRR IMAGES

For the purpose of description and discussion, the Redoubt volcanic clouds shown in the satellite images are divided into three classes that are chosen on the basis of cloud spectral properties, morphology, and size. It is not implied that these cloud types will be produced by eruptions of other volcanoes or that they are the only type that will be produced. The classes include:

Type-1 volcanic clouds.—Clouds generated by magmatic explosions during the first week of activity (while there was a nearly continuous ejection of tephra from the crater). These clouds were low (< 7 km) and extended for hundreds of kilometers from the vent. Examples of this cloud type are shown in figure 3.

Type-2 volcanic clouds.—Clouds generated in part by dome collapse and subsequent pyroclastic flows (Scott and McGimsey, in press). These short-duration, discrete eruptive events were imaged within minutes of the onset of eruption. The type-2 clouds are higher (>10–12 km) than type-1 clouds and have a distinctive, circular morphology. Examples of these clouds are shown in figure 4.

Type-3 volcanic clouds.—Dispersed type-2 clouds. These clouds were imaged several hours after the initial eruptive event and show the dispersion of clouds produced by a single eruptive pulse. Examples of these clouds are shown in figure 5.

Although volcanic clouds were discriminated from weather clouds in many cases, no single algorithm was successful in enhancing all three cloud types. For the type-1 clouds, the band-4-minus-band-5 operation of Prata (1989a) and Holasek and Rose (1991) worked to discriminate portions of the volcanic cloud from the weather clouds (fig. 3A–D). This operation was successful for both daytime and nighttime images, but the discrimination is enhanced in the daytime images when band 3 data are included. All of the false-color composites in figure 3 were produced using identical band combinations (table 2), but a dramatic difference can be seen between the nighttime images from December 16 (fig. 3A–B) and the daytime images from December 18 (fig. 3C–D). Band 3 of the AVHRR sensor (3.53–3.93 μm) is a hybrid band, measuring thermal emittance at night and a combination of reflectance and emittance during the day. In the nighttime images, the enhanced portion of the volcanic cloud is red, indicating that the enhancement is solely caused by the band-4-minus-band-5 subtraction operation. By contrast, the volcanic cloud in the daytime images is yellow, indicating that the enhancement is a result of both the subtraction operation and high band 3 reflectance of the volcanic cloud with respect to the weather clouds.

The distal portions of two of the type-1 volcanic clouds were enhanced more than the proximal portions (fig. 3A–B). Near the vent, the volcanic cloud is spectrally similar to the weather clouds seen at the bottom of the image—the

subtraction operation is successful once the cloud disperses. Note that, in both cases, the subtraction operation is successful once the cloud has been transported approximately 100 km, or about 1 hour, from the vent. A z-shaped bend in the unenhanced portion of the volcanic cloud (east of Kenai) seen in figure 3A can be seen in figure 3B as an enhanced portion of the volcanic cloud. This image was collected about 1 hour after the previous image (fig. 3A) and shows that the discrimination becomes more distinctive as the volcanic cloud disperses.

In some cases, the effectiveness of the band-4-minus-band-5 operation in discriminating dispersed volcanic clouds is influenced by the underlying surface. Holasek and Rose (1991) found that their algorithm was more successful in discriminating volcanic clouds over water than over land, and effects of the underlying surface are observed in several images from Redoubt. In figure 3A, the discrimination of the volcanic cloud is distinct where the cloud passes over the western Kenai Peninsula and over the water of Prince William Sound, but the cloud is not apparent where it passes over the snow-covered mountains. In figure 3C, the discrimination of the cloud is reduced where it overlies low clouds over land.

Whereas the band-4-minus-band-5 difference was successful in discriminating type-1 volcanic clouds, this operation was not successful with type-2 clouds. These clouds are shown in figure 4 as band-4 thermal images, and they were identified by their anomalously low temperature (220° – 230° K), their circular morphology, and their location relative to the vent. An inverted grayscale has been applied to the images in figure 4 so that details of the cold volcanic clouds are discernible.

These images were collected between 7 and 21 minutes after the onset of the eruption, as determined by seismicity (Brantley, 1990), and show that the cloud is detached from the vent, supporting the interpretation of Scott and McGimsey (in press) that these volcanic clouds were generated by

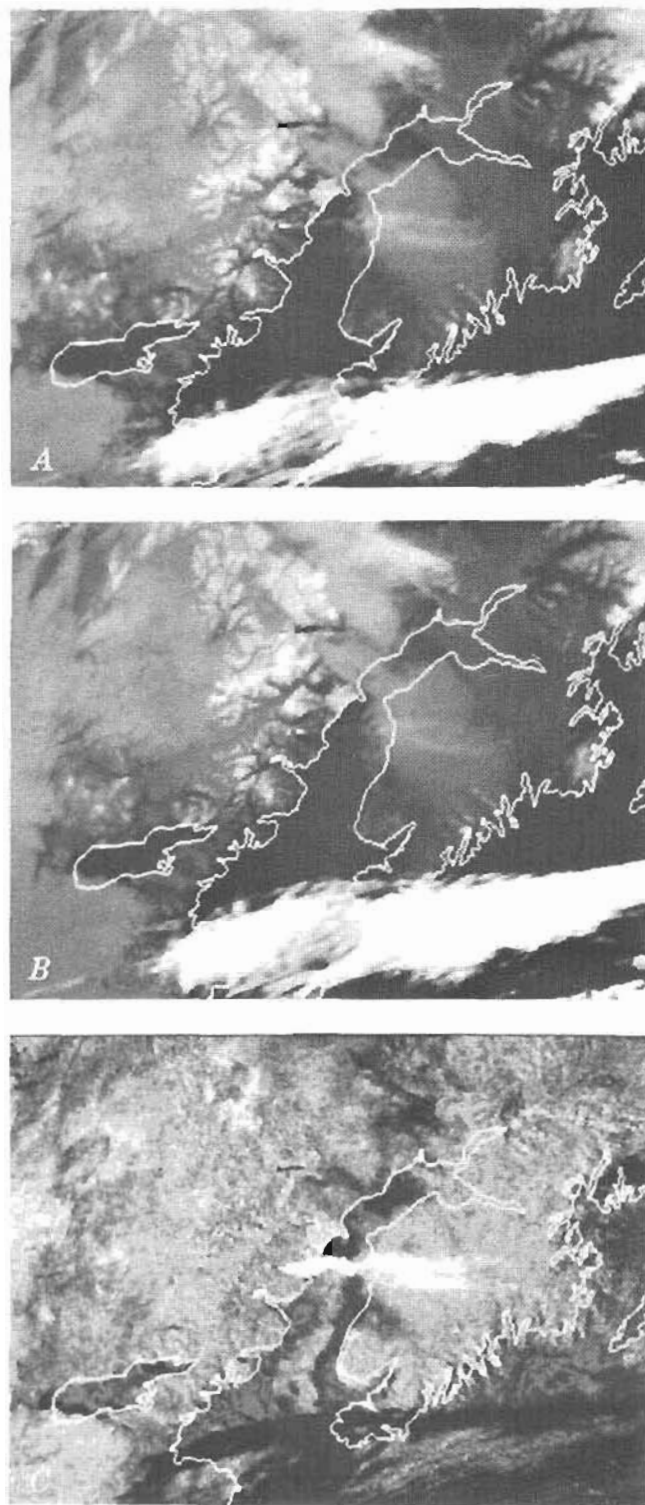


Figure 2 (right). NOAA-11 AVHRR images demonstrating the discrimination of a volcanic eruption cloud from weather clouds. Image was collected on December 18, 1989, at 23:37 GMT. All images are shown with an inverted grayscale, so that cold objects are bright and warm objects are dark. *A*, AVHRR band-4 image showing an indistinct plume from Redoubt and weather clouds throughout the scene. *B*, AVHRR band-5 image. *C*, The result of a band-4-minus-band-5 operation. Note that the volcanic plume is a bright feature and that the weather clouds appear gray to black.

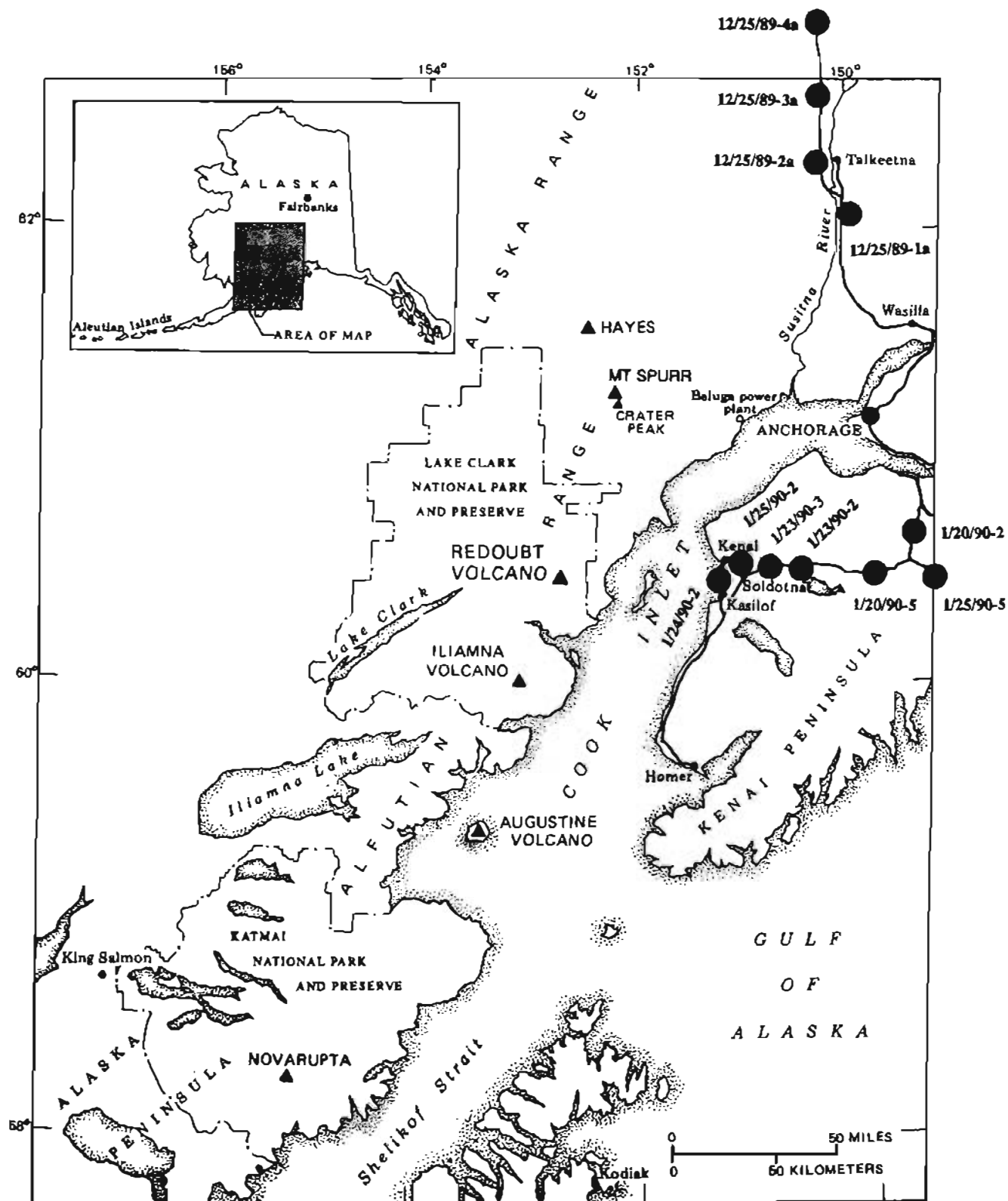


Figure 1. Index map of the Cook Inlet Region of Alaska. Sample locations of the ash spectra shown in figure 6 are indicated by solid circles. Figure modified from Brantley (1990).



The band-4-minus-band-5 operation was not successful in discriminating this cloud, and theories regarding the failure of this operation are included in the discussion.

Another type-3 cloud, from the February 15, 1990, eruptive episode, is seen in figure 5B. The image was collected about 5 hours after the initial eruption seen in figure 4B and consists of a linear, light-red cloud extending from the bottom of the image back toward the volcano, in the upper left of the image. At this time, the cloud front had traveled more than 800 km to the southeast over the Gulf of Alaska. Even though the band-3-minus-band-4 operation was useful in enhancing the volcanic cloud, some of the weather clouds have a similar spectral signal. In this case, manual image interpretation is needed to define the limits of the volcanic cloud. This image was collected by NOAA-10, which contains one thermal band, so it was not possible to attempt the band-4-minus-band-5 operation.

A third type-3 volcanic cloud, from the March 23, 1990, eruption, is seen in two successive images, one NOAA-10 image collected 5 hours after the initial eruption (fig. 5C) and a NOAA-11 image collected 5 hours later (fig. 5D). In figure 5C, the circular volcanic cloud front has traveled about 450 km, and a tail trails back toward the vent. The band-3-minus-band-4 operation was used to enhance the volcanic cloud, but the clarity of the enhancement is diminished by multiple data line dropout along the northern boundary of the volcanic cloud.

In the NOAA-11 image acquired 5 hours later (fig. 5D), the continued dispersal of the volcanic cloud can be seen. The cloud front now extends for more than 825 km, from near the vent to the Bering Sea. Once again, the band-3-minus-band-4 operation helped to enhance the volcanic cloud, but it did not discriminate it from the weather clouds along the top of the scene. The northward bend in the cloud seen in this image is also apparent in the previous image (fig. 5C) and may be due to wind shear. Ash fallout from this eruption is visible as a dark band that trends west for about 300 km and is correlated to the distribution of ash on the ground as mapped by Scott and McGimsey (in press).

REFLECTANCE SPECTRA OF VOLCANIC ASH

The reflectance properties of 19 volcanic ash samples from Redoubt were investigated to see how they varied with transport, and how they varied throughout the eruption. These samples were collected by personnel of the Alaska Volcano Observatory in the weeks to months following the eruption. All of the ash samples used in this study were collected from snowpits throughout Alaska (fig. 1) and were correlated by Scott and McGimsey (in press) to eruptive events by their stratigraphic position. The ash was separated from the snow by melting and filtration, eliminating any sulfuric-acid coatings that may have been present.

To aid in interpretation of the ash reflectance spectra, glass and mineral separates were also prepared. Pumice fragments from the December 15, 1989, eruptive event were crushed mechanically, and glass and crystals were separated using heavy-liquid-separation techniques. The pumice, crystal, and glass separates were sieved to produce a 0.25-mm to 0.088-mm sample, and subsets of these samples were crushed to produce a sample of less than 0.088 mm. This was done to reflect the reduction in grain size and the fractionation of the crystals with respect to glass that occurs as volcanic clouds age and are transported. The crystal separates were composed primarily of plagioclase, with lesser amounts of hornblende and pyroxene.

Laboratory biconical reflectance measurements were conducted on the ash samples and mineral separates by the Jet Propulsion Laboratory (JPL) (J. Crisp, JPL, oral commun., 1991). Although the AVHRR sensor measures emitted energy, reflectance measurements can be related to emittance, which is difficult to measure in the laboratory (Bartholomew and others, 1989). Kirchoff's law states that, for a given temperature and wavelength, emittance and reflectance are complementary. This law only applies to solid objects because scattering is ignored. Although this is a major simplification, we use it to correlate reflectance measurements to the emittance recorded by the satellite sensor.

Biconical reflectance spectra of ash fallout from eruptions on December 15, 1989, December 16, 1989, and from January 8, 1990, are shown in figure 6A-C. These reflectance spectra are typical of the 19 ash samples that were measured and show two reflectance peaks of interest to this study. The first peak extends from 3 μm to 5 μm and contains AVHRR band 3, whereas the second peak extends from 8 μm to 12 μm and contains AVHRR bands 4 and 5. In the region containing AVHRR band 3, the reflectance varies by 10-15 percent between eruptive episodes, and, for the December 15, 1989, event, the reflectance increases by 20 percent as the distance from the vent increases. In contrast, all of the samples show a broad similarity in reflectance in the region containing AVHRR bands 4 and 5, except for the sample suite from the December 15, 1989, event, where the reflectance increases by 1-2 percent with increasing distance from the vent.

The reflectance spectra of the pumice and the glass and crystal separates are shown in figure 7A-B. All of the coarse-grained samples (fig. 7A) show a reflectance peak at 9 μm . The reflectance at 9 μm is less prominent for the crystal separate and the pumice sample, and the glass separate has a smaller reflectance peak at 11.5 μm . The fine-grained samples (fig. 7B) show a much-diminished reflectance peak at 9 μm for the glass separate and none for the pumice sample and crystal separate. The peak at 11.5 μm is most prominent for the glass sample, but the pumice and crystal separates also have a broad peak in this region. These spectra show that reflectance is influenced more by particle size than by particle composition.

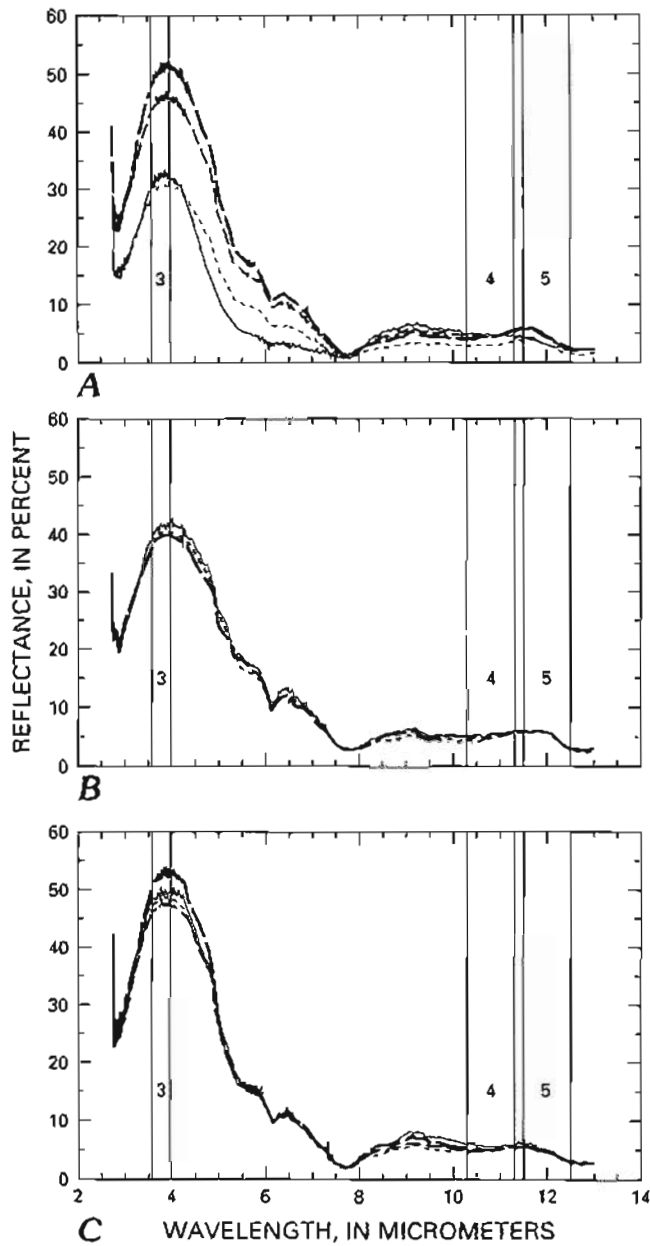


Figure 6. Biconical reflectance plot of ash samples from three eruptions of Redoubt Volcano. The band widths of AVHRR bands 3, 4, and 5 are indicated. Sample locations are shown in figure 1. *A*, Four ash samples from the December 15, 1989, eruption. *B*, Three ash samples from the December 16, 1989, eruption. *C*, Four ash samples from the January 8, 1990, eruption.

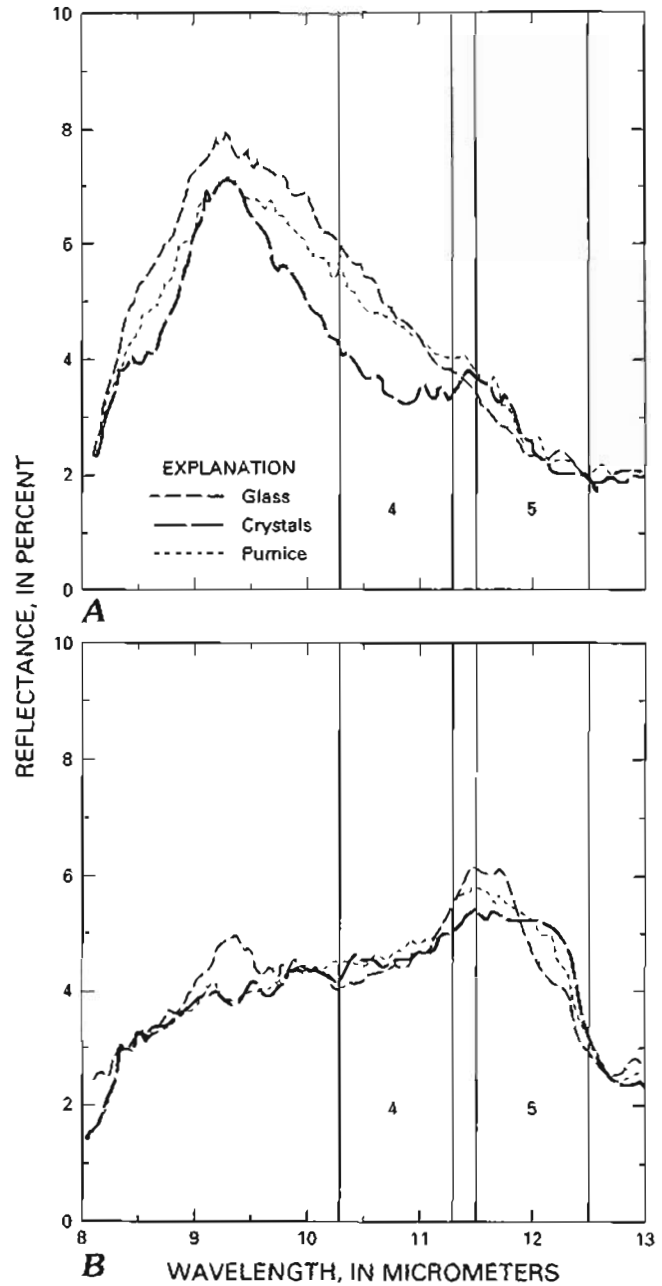


Figure 7. Biconical reflectance plots of pumice, glass, and crystal separates from Redoubt Volcano. *A*, Sieved 0.25–0.88-mm samples. *B*, Sieved > 0.088-mm samples. The band widths of AVHRR bands 4 and 5 are indicated.

DISCUSSION

The spectral discrimination of volcanic clouds is complicated by dynamic processes that occur during the eruption, transport and dispersion of the cloud—these processes may prevent the use of a single image-processing algorithm for use on all volcanic clouds. Previous researchers (Prata, 1989a, 1989b; Holasek and Rose, 1991) have utilized differences and ratios of AVHRR bands 4 and 5 to discriminate volcanic clouds from weather clouds, but these operations were only partially successful at Redoubt. It has been shown that the band-4-minus-band-5 subtraction operation produces positive apparent temperature differences (ΔT) for weather clouds and negative apparent temperature differences for volcanic clouds (Yamanouchi and others, 1987; Prata, 1989b). However, positive apparent ΔT 's can occur for volcanic clouds if the cloud contains a large amount of water or if the particle size is large (Prata, 1989b).

The early eruptions of the Redoubt series (type-1 clouds) more closely resemble the kinds of ash clouds that are likely to be of most concern to aviation safety than do the later ones. Two important features of these early clouds are the success of the discrimination algorithm based on apparent ΔT determined from bands 4 and 5 and the indication that, for success of the algorithm, the cloud must have aged (dispersed freely in the atmosphere) for 1 hour or more. Several observations point to the role of fine silicate particles in explaining these phenomena. Biconical reflectance data suggest that fine particle size may enhance the 4-minus-5 effect, and magmatic explosions resulting from explosive vesiculation may be more likely to produce fine ash than dome collapse. Aging of a volcanic cloud will result in decreasing the grain size of suspended ash because fallout will remove larger particles, and it will also tend to reduce the water or ice in the cloud, thereby enhancing the relative importance of the fine ash particles. Because the largest and most broadly hazardous ash clouds are magmatic (and are likely to generate drifting ash clouds that contain significant concentrations of fine ash) these observations are likely to be of general applicability.

The band-4-minus-band-5 operation produced positive ΔT 's for both volcanic and weather clouds in images of type-2 volcanic clouds from Redoubt, which were collected within 30 minutes of the start of the eruption. These volcanic clouds probably contained large amounts of water, due to the entrainment of moist air from the lower atmosphere, and were identified in band-4 thermal images by their proximity to Redoubt, their circular morphology, and cold temperature (fig. 4A–C). Volcanic clouds of this type could be confused with convective weather clouds, but this is unlikely in winter Arctic images. In two of the images (fig. 3A–B) of type-1 clouds, the band-4-minus-band-5 operation produced positive ΔT 's for the proximal portion of the cloud and negative ΔT 's for distal portions of the cloud. The region of negative ΔT is shown in red in figure 3A–B. We attribute the change

in the spectral signature of this volcanic cloud to a decrease in particle size and water content during transport. Analysis of wind-speed data for this eruption indicates that the transition from positive to negative difference values in the volcanic cloud took about 1 hour.

Type-3 volcanic clouds were difficult to discriminate, perhaps due to their relatively small volume and the dispersion and sedimentation of ash that occurred before they were imaged. Whereas many volcanic clouds can be discriminated using the band-4-minus-band-5 operation, the concentration of ash required to produce a detectable signal is unknown. Another factor that affects the subtraction operation is particle size. The type-3 clouds may have contained fewer fine particles than the type-1 clouds because they were produced as part of a dome collapse, rather than from a purely explosive, volatile, effervescent mechanism, thus reducing the ash signal.

The band-3-minus-band-4 operation was useful in enhancing type-3 clouds, but it did not discriminate them from weather clouds. This operation was more successful during the daytime hours, when band-3 backscatter is important, than at night, when this band has a larger thermal component. Although this is a useful operation, it is difficult to make general observations regarding its success because the reflectance is dependent on a number of factors, including particle size, shape and abundance, sun azimuth and elevation, and the location of the cloud and the satellite relative to the sun. However, this operation, used in conjunction with observations of cloud morphology, can be used to interpret the extent of probable volcanic clouds.

The use of ash fallout reflectance measurements as "ground truth" for interpreting satellite imagery has several shortcomings. One fundamental problem is that the reflectance measurements were made on ash fallout, which by definition is not what is in the volcanic cloud. Very fine particles are probably the most important, yet their collection is difficult because their fallout may be too light to be distinguished on the ground, and the particles fall out long distances from the vent over very broad areas. Another problem lies in relating the reflectance measurements to the emittance recorded by the sensor. Volcanic clouds are heterogeneous assemblages of particles and gases; therefore, subtracting the reflectance measurements from a black body of the appropriate temperature is a poor approximation. Additional work needs to be done to determine the most effective way of using reflectance measurements of ash fallout as "ground truth" for image interpretation.

In spite of these difficulties, the mineral separate spectra show that reflectance is controlled more by particle size than by the particle composition. In a volcanic cloud, this would imply that the discrimination of distal clouds would be controlled more by the reduction in the size distribution of the particle with transport than by the increase in the proportions of volcanic glass in the cloud due to eolian fractionation. Although the exact relationship of reflectance to

emittance is unknown, the effects of particle size, particle shape, and particle composition would probably be enhanced for suspended particles. In this case, the complex shape of glass particles compared to crystals may have an important effect on the emittance of volcanic clouds.

This study has shown that the discrimination of volcanic clouds using AVHRR imagery is more complex than previously thought and has identified several parameters that contribute to this complexity. These include cloud water content and particle size, concentration, and composition. Additional factors not included in this study include the role of acid aerosols (Prata, 1989a) and sensor viewing geometry. The relative importance of each of these parameters can be investigated in laboratory experiments utilizing an imaging radiometer to observe simulated volcanic clouds. Images can be collected at the same wavelength intervals as the AVHRR sensor, and image-processing operations similar to the ones described in this paper can be conducted. Results of the laboratory studies can be used to guide future work on thermal imaging and particle and gas sampling of actual volcanic clouds.

CONCLUSIONS

Volcanic clouds of a variety of types and scales were observed and mapped by AVHRR images during the Redoubt eruptions of 1989–90. These examples broaden the experience on volcanic cloud tracking and discrimination using multispectral image-processing techniques and provide insight on additional work that needs to be conducted.

A major conclusion of this paper is that volcanic clouds have natural variability that is reflected in satellite images and that affects the methods used to discriminate and map their dispersion. This variability is magnified for activity like that of Redoubt Volcano, which changed eruptive mechanism during its period of activity. Most ash-producing eruptions from other volcanoes, particularly the larger ones, are more likely to resemble the early (type-1) clouds of Redoubt. This is encouraging because the simple method of discrimination of volcanic clouds using apparent temperature differences between AVHRR bands 4 and 5 works well on type-1 clouds; therefore, the simplest methodology is likely to be useful in many of the most serious cases. Discrimination of volcanic clouds using the band-4-minus-band-5 operation is difficult or impossible for very young clouds with high water content and (or) a large particle size, but it is very useful for drifting volcanic clouds. A major uncertainty of this method is the particle concentration required to produce a measurable signal.

Ash reflectance is controlled more by particle size than by particle composition. The fractionation of glass and crystals in a volcanic cloud are not likely to produce reflectance and emittance differences on their own, but fractionation will operate in conjunction with the proportional increase of

fine particles as the cloud disperses. Laboratory reflectance measurements are inadequate to explain the spectral variability observed in the imagery of the Redoubt volcanic clouds. Emittance measurements need to be made of simulated volcanic clouds in the laboratory and in situ measurements and particle sampling need to be conducted on actual volcanic clouds to provide "ground truth" for interpretation of satellite imagery.

ACKNOWLEDGMENTS

We would like to thank the following people and organizations for their cooperation and support for this study. Mike Matson of NOAA/NESDIS provided most of the AVHRR data, and Ken Dean of the University of Alaska's Geophysical Institute provided several AVHRR scenes. Joy Crisp of the Jet Propulsion Lab made the ash reflectance measurements, and the Alaska Volcano Observatory furnished field support. This study was funded in part by NSF Grant 91-17726 and NASA Grant 1442-VC1P-011-91.

REFERENCES CITED

- Bartholomew, M.J., Kahle, A.B., and Hoover, G., 1989, Infrared spectroscopy (2.3–20 μm) for the geological interpretation of remotely sensed multispectral infrared data: *International Journal of Remote Sensing*, v. 10, p. 529–544.
- Brantley, S.R., ed., 1990, The eruption of Redoubt Volcano, Alaska, December 14, 1989–August 31, 1990: U.S. Geological Survey Circular 1061, 33 p.
- Casadevall, T.J., 1990, The 1989–90 eruption of Redoubt Volcano, Alaska, impacts on aircraft operations in the vicinity of Anchorage [abs.]: *Eos, Transactions, American Geophysical Union*, v. 71, p. 1701.
- Glaze, L.S., Francis, P.W., Self, S., and Rothery, D.A., 1989, The 16 September 1986 eruption of Lascar Volcano, north Chile, satellite investigations: *Bulletin of Volcanology*, v. 51, p. 911–923.
- Hanstrum, B.N., and Watson, A.S., 1983, A case study of two eruptions of Mount Galunggung and an investigation of volcanic cloud characteristics using remote sensing techniques: *Australian Meteorological Magazine*, v. 31, p. 171–177.
- Holasek, R.E., and Rose, W.I., 1991, Anatomy of 1986 Augustine Volcano eruptions as revealed by digital AVHRR satellite imagery: *Bulletin of Volcanology*, v. 53, p. 420–435.
- Kidwell, K.B., ed., 1991, National Oceanic and Atmospheric Administration Polar Orbiter Data Users Guide: Washington, D.C., National Oceanic and Atmospheric Administration/National Environmental Satellite Data and Information Service, 294 p.
- Kienle, J., and Shaw, G.E., 1979, Plume dynamics, thermal energy and long-distance transport of Vulcanian eruption clouds from Augustine Volcano, Alaska: *Journal of Volcanology and Geothermal Research*, v. 6, p. 139–164.

- Krueger, A.J., 1983, Sighting of the El Chichón sulfur dioxide clouds with the NIMBUS 7 total ozone mapping spectrometer: *Science*, v. 220, p. 1377–1379.
- Malingreau, J.P., and Kaswanda, 1986, Monitoring volcanic eruptions in Indonesia using weather satellite data: The Colo eruption of July 28, 1983: *Journal of Volcanology and Geothermal Research*, v. 27, p. 179–194.
- Matson, M., 1984, The 1982 El Chichón Volcano eruptions—A satellite perspective: *Journal of Volcanology and Geothermal Research*, v. 23, p. 1–10.
- Prata, A.J., 1989a, Observations of volcanic ash clouds in the 10–12 μm window using AVHRR/2 data: *International Journal of Remote Sensing*, v. 10, p. 751–761.
- 1989b, Infrared radiative transfer calculations for volcanic ash clouds: *Geophysical Research Letters*, v. 16, p. 1293–1296.
- Rose, W.I., 1987, Interaction of aircraft and explosive eruption clouds: A volcanologist's perspective: *American Institute of Aeronautics and Astronautics Journal*, v. 25, p. 52–58.
- Steenblik, J.W., 1990, Volcanic ash: A rain of terra: *Air Line Pilot*, v. 59, p. 9–15, p. 56.
- Salisbury, J.W., and Walter, L.S., 1989, Thermal infrared (2.5–13.5 μm) spectroscopic remote sensing of igneous rock types on particulate planetary surfaces: *Journal of Geophysical Research*, v. 94, p. 9192–9202.
- Scott, W.E., and McGimsey, R.G., in press, Character, mass, distribution, and origin of tephra-fall deposits of the 1989–90 eruption of Redoubt Volcano, south-central Alaska: *Journal of Volcanology and Geothermal Research*.
- Yamanouchi, T., Suzuki, K., and Kawaguchi, S., 1987, Detection of clouds in Antarctica from infrared multispectral data of AVHRR: *Journal of the Meteorological Society of Japan*, v. 65, p. 949–961.